Modelling approaches for lucerne growth and development under dryland conditions

A thesis

submitted in partial fulfilment

of the requirement for the Degree of

Masters of Agricultural Science

at Lincoln University

by

Jian Liu

Lincoln University

2021

Abstract of a Thesis submitted in partial fulfilment of the requirement for the Degree of Masters of Agricultural Science

Modelling approaches for lucerne growth and development under dryland conditions

By

Jian Liu

Lucerne is an ideal plant for east coast sheep and beef farmers to integrate on-farm to cope with a dry and drying climate. Expanded use of lucerne on-farm leads to on-farm questions around feed supply, environmental impacts and farm resilience. Many of these questions can only be answered with process-based models. These have been helping researchers, policy makers and farmers to make informed decisions about farm practices worldwide. However, the current lucerne model in the Agricultural production system simulator next generation (APSIMX) is not designed for simulating lucerne responses to dryland conditions. Hence, this study aimed to incorporate previous knowledge obtained from dryland experiments from Lincoln University into the APSIMX-Lucerne mode. New equations were introduced to the model to constraint the growth and development processes including leaf area expansion rate, radiation use efficiency and phyllochron under water-limited conditions. Secondly, this study investigated an alternative approach for increasing the efficiency and reliabilities of model parameter estimation. The reproducibility of the study was addressed as the third objective by adapting data science concepts and state-of-art tools. A literature review of lucerne responding to water stress (water deficiencies) laid out the physiological knowledge to design the mechanism of the APSIMX-Lucerne model. The thesis initially documents previous experiments, the APSIMX framework and data science tools. The conventional approach for APSIMX model development was conducted to gain experience and understanding of the structure and

operation of the APSIMX-Lucerne model, verify the implementation of the lucerne model in the APSIMX framework and identify major issues with current model implementation to guide subsequent improvements. An alternative approach was applied via the R programme and a workflow manager to implement an optimisation procedure for estimating nine water-related parameters in a simple APSIMX water balance model. The optimised parameter values were later transferred into the APSIMX-Lucerne model to evaluate the model performance compared with the conventional approach. Negligible improvement (1% normalised root mean square error reduction) was gained in profile soil water content prediction for dryland trial by the alternative approach although it achieved full reproducibility and quantifiable resource expenses. These results might be caused by multiple contributors. First, both approaches demonstrated that the demand-related parameters in the model were inadequate to impose the correct waster stress effects on lucerne. More specifically, the model failed to constrain above ground variables at water supply limited conditions while the model extracted inadequate water from soil at water demand limited conditions. Furthermore, the model had no mechanism to represent water stress effects on lucerne height. More investigation is necessary to implement the relationship between water stress levels and lucerne height since it is lacking in the current model. Moreover, root distribution patterns differ in different soil types, whereas this study assumed an exponential decay distribution for both stony and non-stony soils, which may not represent reality in deep soils. Lastly, lucerne showed different phenological development in the supply limited conditions in comparison with temperature-driven development under non-limiting conditions. Therefore, in-silico approaches, such as Bayesian inference or specialised root structure mechanistic models, might be required to assist the understanding in the full picture of lucerne growth and development under dryland conditions.

Keywords: dryland conditions, water stress, lucerne model, APSIMX model development, data science, workflow management, reproducibility, soil water balance, surface soil evaporation, transpiration demand, water extraction pattern, soil characteristics.

ACKNOWLEDGEMENTS

It has been a great journey for me to complete the master study. I'd like to address my sincere appreciation to the people that held my hand to help me complete the journey.

Prof. Derrick Moot is my life changer and a marvellous mentor. The enthusiasm and passion that Derrick emits daily deeply influences my views about the world and the way I do science. He guides me to discover myself and teaches me the principles in both life and science. I won't be anywhere near to my present self without his wise words. Words of thanks become far from enough to express my gratefulness to Derrick. Only keeping practising the principles he taught may partially acknowledge Derrick's contribution to my life.

I'd like to offer my special thanks to Dr Hamish Brown, Dr Linley Jesson and Dr Henry Chau. As my science advisors and co-supervisors, they provide me with invaluable knowledge in their domains. Dr Brown generously shared his extensive knowledge in plant physiology and crop modelling. His patience and kindness made me finally understand the pathway from in-field experiments to mechanistic models and vice versa. Dr Jesson pointed me in the direction where I needed empathy to solve the underlying problems. She kindly shared her visions and encouraged me to take on challenges. Dr Chau provided me with extensive knowledge about soil physics on the Ashley Dene farm.

I owe a very important debt to Dr Richard Sim, Dr Rogerio Cichota, Dr Rodelyn Jaksons, Dr Edmar Teixeira, Dr Joanna Sharp, Dr Paul Johnstone, Dr Wei Hu and Dr Xiumei Yang. Without Dr Sim's hard work on collecting the dryland datasets and excellent publications, this master study would be impossible. Dr Cichota taught me a considerable amount of knowledge about soil characteristics and their implementation in the APSIMX framework. Dr Jaksons shared her in-depth statistical knowledge with me and offered practical solutions to solve my problems. Dr Teixeria generously explained to me his understanding of lucerne. Dr Sharp and Dr Johnstone helped me shape the master project to obtain Plant and Food Ltd research support. Dr Hu and Dr Yang inspired me by sharing their stories about their research journeys. Additionally, my special thanks to Dr Lindsay Bell for his permission in using his picture of lucerne morphology.

I want to thank the sustainable production portfolio in Plant and Food research, which kindly supported my study by allocating 300 hours each year for two financial years. This support allowed me to balance work, study and life.

Funding for this project and preparation of the thesis was provided by Beef + Lamb New Zealand, MBIE, Seed Force New Zealand and PGG Wrightson Seeds under the “Hill Country Futures” research programme (BLNZT1701).

Lastly, I express my deepest appreciation to my dearest wife and daughter. They are the purpose and motivation that encourage me to chase my dream, take new challenges and overcome barriers. I would be an incomplete person without their understanding and sacrifices.

TABLE OF CONTENTS

LIST OF TABLES

LIST OF FIGURES

List of Abbreviations

Abbreviation	Description
APSIMX	Agricultural production simulator next generation
AWC	Available water capacity
CLL	Crop lower limit
Cona	Stage II evaporation rate
DAS	Day after sown
DM	Dry matter
DUL	Drainage upper limit
E	Soil surface evaporation
E_o	Potential evaporation rate
ET	Actual evapotranspiration
FRGR	stress factor or relative growth rate for canopy
g_{smax}	Maximum stomatal conductance
k	Extinction coefficient
K	Soil hydraulic conductivity
KL	Water extraction rate (Upper case abbreviation is a convention in APSIMX)
L	Root length density
LAI	Leaf area index
LAER	Leaf area expansion rate
LL15	Lower limit at 15Bar
NP	Neutron probe
nRMSE	The normalised root mean square error
NSE	Nash-Sutcliff efficiency
PAR	Photosynthetic active radiation
PAW	Plant available water
PAWC	Plant available water capacity
Pp_{crit}	Critical photoperiod hours
p_{root}	Percentage of DM partitioned to roots
PWP	Permanent wilting point
R_a	The PAR intercepted by a single leaf
R_{50}	The PAR when g_s is half of its maximum value
RD	Rooting depth
RFV	Root front velocity
RMSE	Root mean square error
RUE	Radiation use efficiency
SWC	Soil water content
SWD	Soil water deficit
SW_D	Soil water demand
$SW_{initial}$	Initial soil water content

SW_S	Soil water supply
T	Actual plant transpiration
T_b	Base temperature
T_D	Transpiration demand
TDR	Time domain reflectometry
T_{max}	Maximum temperature for crop development
T_{opt}	The optimal temperature for crop development
Tt	Thermal time
U	Stage I cumulative evaporation
VPD	Vapour pressure deficit
Θ_T	Canopy conductance
$f_{stress}/f_{optimal}$	Shoot RUE under water deficit relative to the ones under optimal water conditions

LIST OF APPENDICES

1 INTRODUCTION

Climate projections in New Zealand predict less precipitation during summer for the east coast regions of New Zealand from North Otago to Gisborne (Ministry for the Environment 2018). This area of ~3 M ha is categorised as summer dry because evapotranspiration in summer usually exceeds precipitation and prevents pasture growth for 2-4 months (Moot 2012). In this environment, the most commonly sown species in New Zealand, perennial ryegrass (*Lolium perenne* L.) and white clover (*Trifolium repens* L.), fail to persist under rainfed conditions (Mills et al. 2015a). Therefore, alternative pasture species are required. These need to be tolerant of summer dry and water stress conditions and then rapidly recover when rain falls, to assist sheep and beef farms to sustain their farming system now and into a drier future.

Lucerne (*Medicago sativa* L.) is one of the oldest forage crops in human history and is grown on more than 32 M ha globally (Bouton 2012). In New Zealand, it has been recommended for summer dry regions for over 100 years (Douglas 1986). Lucerne has three main advantages over perennial ryegrass in these environments. First, it produces high-quality feed in spring at the time of maximum feed demand (Avery et al. 2008) and therefore has high water use efficiency in spring (Moot et al. 2008). Second, it survives and grows for longer in summer dry conditions than grasses due to its deep tap root (Brown & Moot 2003). Therefore it provides high-quality feed for longer in late spring and summer to support greater live-weight gains than grass-based pastures (Mills et al. 2015b). Finally, it has the potential to solve pressing environmental issues such as mitigating nitrogen leaching (Russelle et al. 2007) and sequestering carbon (Mortenson et al. 2004; Zahid 2009). These distinct characteristics and refined grazing management for New Zealand (Moot. 2003; Moot et al. 2016) have enabled lucerne to be successfully incorporated into current summer dry farm systems (Avery et al. 2008) and has provided resilience to the dryland farming systems (Moot 2014). There is now growing evidence of farmers who have successfully integrated lucerne into their farming systems, to steadily increase their profits and sustainability even under our driest (<400 mm rainfall) rainfall conditions (Moot et al. 2019).

Lucerne was also identified as the most tolerant pasture for deficit irrigation among 15 perennial pasture species examined, due to its deep taproot (Neal et al. 2009). This finding creates new application opportunities for integrating lucerne into the dairy industry. This is particularly relevant given the species fixes its nitrogen and therefore does not require high nitrogen inputs which have recently been legislated to <190 kg/ha. This level is inadequate to maximize production from grass dominant pastures (Mills et al. 2006; Black et al. 2017). Lucerne offers the opportunity to reduce irrigation frequency on dairy farms which would decrease the energy cost and carbon footprint of irrigation and reduce the risk of nitrate leaching from over-irrigation. Furthermore, climate projections predict winter precipitation increases in the regions of Nelson, Otago and Southland (Ministry for the Environment 2018), which increases risks of drainage and nitrogen losses. In southwest Western Australia, lucerne has been used to eliminate excessive drainage during winter and reduce the issue of secondary salinisation (Ridley et al. 2001). In New Zealand, this option has not been explored but lucerne offers the opportunity to drain the soil profile to mitigate leaching risks (Russelle et al. 2007).

However, the integration of lucerne into farm systems can be a time consuming and risky process for farmers without expert guidance. Moreover, it remains unclear how lucerne crops respond to abiotic stresses in different soil types, especially under water stress, across a range of environments in New Zealand. Because lucerne fixes N, water shortage is the major limiting factor to its yield potential in dryland environments (Luo et al. 2020). There is an urgent need for decision-making tools that can simulate lucerne performance in contrasting environments for farmers and policymakers to have the confidence to recommend its use as a tool to reduce production and environmental risks associated with current grass-based pasture systems.

Scientists, policymakers and farmers have successfully applied process-based models as decision-making tools in many aspects of the agricultural industry. Typical applications include yield prediction, disease forecasting, assisting breeding programmes, risk assessment for policy creation and management (Jones et al. 2017). The agricultural production system simulator next generation (APSIMX) is one of the system modelling tools that has been used worldwide to predict crop performance under different scenarios (Holzworth et al. 2015; Holzworth et al. 2018). Compared with other process-based

models, such as DSSAT and STICS, APSIMX has a calibrated lucerne model available for non-limited conditions in New Zealand, which makes it the most suitable tool for this study (Moot et al. 2015). APSIMX has three key features that improve the efficiency of model development and improvement as scientific software (Holzworth et al. 2018). The modulated model structure and well-developed user interface (UI) allow researchers to focus on the model process rather than software development. The reusability of its core codes reduces the chance of users having to "reinvent the wheel". However, the current model lacks of the mechanism to simulate lucerne growth and development for low water holding capacity soils under rain-fed conditions.

To incorporate water stress functions into the current APSIMX lucerne model, the critical challenges are a) the quantification of plant responses to water stress, b) the quantification of water extraction patterns of lucerne in different soil types and c) the representation of different soil types and the physiological mechanism of lucerne under stresses in software scripts. Previously, experiments by Sim (2014) explored the physiological interaction between lucerne and two soil types under water stress. Subsequent efforts have been put into clarifying the effect of water stress on lucerne performance and characterising the soils for model parameterisation (Sim 2014).

Therefore, this study aims to achieve three objectives.

Objective 1 – calibrate the APSIMX model to simulate lucerne growth and development responses to water stress simulations on a spatial and temporal scale

Further analyses of the existing datasets are required to characterise the soil concerning sowing dates. The objective of the analysis is to describe the initial soil conditions as measured and reduce temporal variations. The analysis results will define parameter values for re-establishing a base APSIMX model; therefore, the model performance could be evaluated. A review was needed to clarify the mechanism of water stress on lucerne and how these mechanisms could be implemented in the APSIMX-Lucerne model. Thus, the first objective aims to gain knowledge in the following four aspects:

1. Gain experience and understanding in the structure and operation of the model
2. Gain confidence in the simulation configurations and observed data

3. Verify the implementation of the lucerne model in the APSIMX framework.
4. Appreciate the major issues with current model implementation to guide subsequent improvements.

Objective 2 – introduce waster deficit responses and automate parameterisation

One issue with sophisticated agricultural models like APSIMX is that many parameters are involved during their development and calibration. However, it is rare to obtain a comprehensive dataset that can inform all parameters in models. For instance, root water extraction rate is difficult to measure directly with current technology. It is doubtful that researchers can calibrate all plant traits even if such datasets exist due to the limitations of the manual processes involved. A survey has shown that <10 parameters are estimated in 66% of model calibration practices in the biophysical modelling community (Seidel et al. 2018). Furthermore, manual parameterisation will increase the possibility of equifinality where the modifications of parameters cancel each other and this results in the same model performance after the investment of a considerable time expense.

Well-established optimisation algorithms exist in the R software ecosystem (Cortez 2014). Therefore, In Objective 2 I develop the procedure in R to optimise APSIMX parameters, to achieve automatic parameterisation efficiently and objectively.

Objective 3 – standardisation of a reproducible approach that ingests observed data into automated parameterisation protocols

The conventional approach of parameterisation for APSIMX models is a trial and error approach, which generally consists of three steps: 1) the derivation of parameters from observed (measured) data via linear regressions, 2) the manual modification of parameters in sub-models via the APSIMX user interface or the base scripts in computer languages and 3) the evaluation of the modified model performance (Brown et al. 2018; Harrison et al. 2019). This approach is time-consuming and can be problematic when newly observed data are introduced to improve the comprehensibility of the model, especially if these data come from different sources. The manual process of model calibration could result in poor model performance and potentially increase the models' uncertainty. In contrast,

agricultural models are expected to be validated by as much data as possible from different environments to simulate a wide range of scenarios.

A standardised workflow of model calibration would improve the efficiency of introducing new data to an existing model. Hence, Objective 3 was to establish a workflow to a) standardise the observed data blending process, b) evaluate model performance programmatically, c) document the thinking and logic for APSIMX-Lucerne model calibration.

1.1 Structure of the thesis

Figure 1.1 shows the structure of the thesis. Chapter 1 gives a brief overview of the role of lucerne in New Zealand under the climate change context. Chapter 2 reviews the previous lucerne research in dryland conditions about the physiological mechanisms of water stress on lucerne growth and development. Chapter 3 describes the dataset, modelling framework and data science tools used to fulfil Objective 3. Chapter 4 documents the implementation of the known mechanism of water stress on lucerne. Therefore, the baseline APSIMX-Lucerne model can be established based on currently published results. Objective 1 is the main focus of Chapter 4 and Objective 3 is partially addressed. Chapter 5 deals with Objective 2 and further develops Objective 3. Chapter 5 also introduces the optimisation approach to estimate model parameters systematically. Chapter 6 provides a general discussion of the results from Chapters 4 and 5 and describes a path for future research directions.

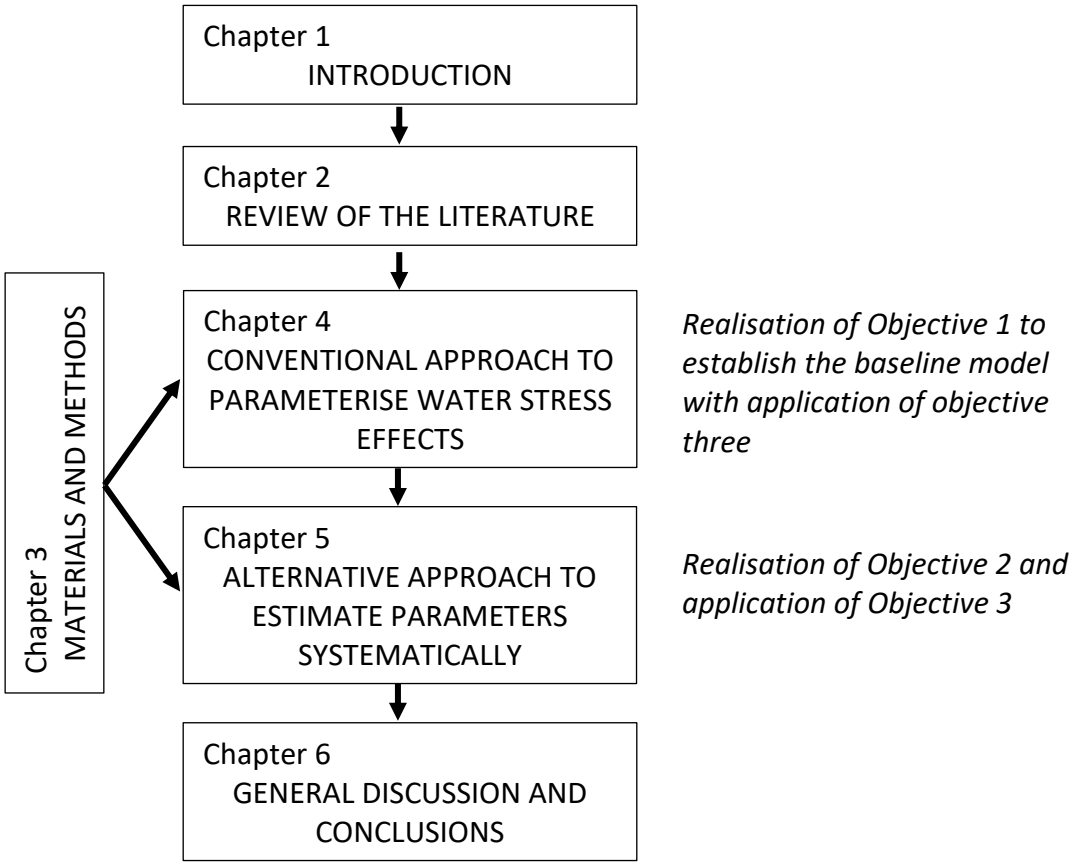

Figure 1.1 Thesis structure diagram

2 REVIEW OF THE LITERATURE

This review of literature provides an introduction to the underlying crop physiological responses to water stress. Water stress can be caused by a water surplus or deficiency. This thesis addresses water stress solely as water deficiency for dryland conditions. The effects of water stress on lucerne are described for growth and development. Modelling lucerne growth consists of three main aspects that affect light capture and utilisation. These are; 1) leaf area expansion rate (LAER), 2) canopy height and 3) radiation use efficiency (RUE). The major use of lucerne in New Zealand is as a forage plant, by either direct grazing or cut and carrying (lucerne is cut by farmers and feed to livestock). Therefore, forage is usually removed before or shortly after the crop reaches flowering so growth and development beyond flower initiation are not considered in this thesis. The phyllochron (interval between leaf appearances) and time to flowering are the focus of lucerne development.

Quantification of the lucerne response to water deficit often calculates the ratio of actual and transpiration demand (ET and T_D). Water stress may occur when $ET < T_D$. This enables the effects of water stress to be examined on each plant component by relating the component performance under water stress to its performance under adequate water conditions. Methods of quantifying ET and T_D will be discussed.

2.1 Crop responses to water stress

Crop responses to water stress consist of genetic, morphological and physiological changes that alter plant growth and development (Bell et al. 2007; Brown et al. 2009; Zahid 2009; Pang et al. 2011; Sim 2014; Luo et al. 2020). Leaves maintain a water potential lower than soil water potential to ensure water extraction from the soil occurs (Hay & Porter 2006a). Plant leaves dynamically lower water potential to accommodate the soil water depletion during a drying cycle (Bell et al. 2007). Without soil water recharge, plants extract the plant available water (PAW) to a point where plants cannot depress their leaf water potential any further because water loss from cells results in leaf turgor reduction and stomatal closure. This point is commonly known as the wilting point (WP).

Leaf turgor progressively declines when plant water loss from transpiration exceeds PAW (Hay & Porter 2006a). Consequently, cell elongation and expansion are limited. Plant

growth rate, therefore, is suboptimal. At the organ level, stem elongation and leaf expansion are affected by water stress. As the canopy is unable to develop at its maximum rate, water-stressed plants often possess a smaller leaf area index (LAI) which intercepts less photosynthetic active radiation (PAR) to assimilate carbon dioxide (CO_2) in comparison with unstressed plants. Yield reduction is, therefore, is likely to occur in the presence of water stress.

Stomata closure is a self-defence mechanism that plants use as water stress increases, to enable them to preserve water. Consequently, canopy temperature may rise because the canopy still intercepts solar radiation but plants lack the cooling mechanism attributed to transpiration. The accumulation of this additional energy may manifest as a more rapid accumulation of thermal time (Tt) that drives plant development, such as time to flowering, and the rate of leaf senescence.

The root: shoot ratio usually increases for plants that experience water stress conditions (Pang et al. 2011; Xu et al. 2015; Luo et al. 2020). This behaviour shows plants adapt to water stress by increasing dry matter (carbon and nitrogen) partitioning to the root system, to search for available water, while reducing canopy expansion that reduces transpiration.

Lucerne may share similar physiological responses to water stress as other plants. However, its deep root system (> 1.6 m) allows it to explore a greater depth of soils than shallower rooted pasture species such as white clover or ryegrass. Under dryland conditions, this trait offers lucerne a relatively large value of PAW, compared with other species. Furthermore, the deep tap root contributes to water preservation. Lucerne stands are less likely to suffer permanent damage during severe water stress conditions and recover more quickly once water is available (Carter & Sheaffer 1983; Orloff et al. 2015).

2.2 The effects of water stress

2.2.1 Canopy

The leaf is the first response organ when lucerne experiences water stress (Brown et al. 2009; Erice et al. 2010; Luo et al. 2020). Lucerne leaf area per plant consists of two main factors; leaf size (area) and leaf number. The former is quantified by the leaf area expansion

rate (LAER) which has a maximum leaf size, and the latter depends on the phyllochron which is regulated by temperature and photoperiod (time unit that plants respond to decreasing daylength) under non-limiting conditions (Brown 2004; Brown et al. 2009; Sim 2014). Both factors can be affected by water stress. Luo et al. (2020) conducted pot experiments and reported that the leaf area of seedling lucerne decreased approximately 60% under severe water stress treatment (45% of saturation) in comparison with the leaf area under their adequate water treatment (85% of saturation). A moderate water stress treatment (65% of saturation) showed a 20% reduction of leaf area. The rapid decline of leaf area under water stress stemmed from a reduction in the total number of leaves (at each node) and individual leaf size. Under severe water stress, the total number of leaves decreased 30% because of fewer branches compared with the sufficient- and moderate-water conditions and leaf size (m^2 $leaf^{-1}$) was reduced by 35%.

In contrast, field experiments showed that the leaf area reduction was mainly caused by suboptimal LAER (smaller leaves) during water stress conditions (Brown et al. 2009, Sim et al. 2017). Brown et al. (2009) found that the relative LAER was reduced to 90% of its maximum rate when the ratio of actual transpiration (T) and transpiration demand (T_D) decreased from 0.97 to 0.2. However, the number of leaves decreased 30% from its optimal value at T/T_D of 0.2. Sim 2014 reported consistent effects of water stress on canopy development under rain-fed conditions. The LAER declined to 0.1 of its optimal rate when T/T_D decreased from 0.9 to 0.5.

The reported effects of water stress on leaf area differ across experiments. These differences are likely to be due to the differences among methodologies, climate and lucerne cultivar. For example, Luo et al. 2020 used pots to grow lucerne under controlled environments and completed data collection on seedling crops before any regrowth cycles. In contrast, Brown et al. (2009) and Sim (2014) conducted field experiments over two growing seasons. Water stress was controlled strictly for seedling lucerne in the controlled environment, while lucerne experienced different water stress levels under field conditions. Nevertheless, both experiments demonstrated that lucerne responses to water stress involved a reduced LAER and fewer leaves.

Crops have different canopy architecture which depends on species (Hay & Porter 2006b). For example, white clover has flat leaves, while cereal crops have erect leaves. This difference is described using the Beer-Lambert's equation (Equation 1) to quantify the relationship between canopy architecture and light interception (Teixeira et al. 2011; Sim et al. 2017)

Equation 1 $$I = I_0 e^{-k \times LAI}$$

where I is the transmitted light after I_0 (total incoming light) is intercepted by the canopy, k is the extinction coefficient which indicates how light penetration decreases through the canopy, and LAI is the leaf area index.

Lucerne seeding and regrowth phases have similar k values under optimal water conditions. For example, Teixeira et al. 2011 found seedling lucerne had a k of 0.96±0.008 while the k of regrowth lucerne was 0.89±0.005. Sim et al. 2017 reported a k of 0.94 ± 0.014 for both seeding and regrowth lucerne in rainfed conditions when grown in deep soil. However, a k of 0.66 ± 0.013 was found in summer regrowth lucerne in stony soils (Sim et al. 2017). This k reduction was likely due to water stress-induced morphological changes in the lucerne canopy. Figure 2.1 shows folded leaflets of lucerne under water stress. The cup shape leaf of lucerne was paralleled with solar radiation, which minimised solar radiation intercepted by the leaves and significantly decreased leaf area.

Figure 2.1 Individual morphology of Lucerne leaflet under water stress conditions (adapted from Bell et al., 2007 with permission).

The agricultural production system simulator next generation (APSIMX) is one of the system modelling framework that has been used worldwide to predict crop performance under different scenarios (Holzworth et al. 2015; Holzworth et al. 2018). APSIMX-Lucerne model uses a simple leaf model to represent the interaction with temperature and photoperiod variations and sink dry matter by intercepting solar radiation (Section 3.5.4). The main concept of simple leaf model is its representation of the entire canopy, which consists of leaf, stem and branches. In the simple leaf model, LAER is the 'central pivot' dominating lucerne growth. This is because LAER initialises LAI accumulation for subsequent photosynthetically active radiation interception. Leaf organ uses Equation 1 and calculates the fractional light interception (I_0/I) based on the LAI and extinction coefficient (k).

Leaf area expansion rate is computed in APSIMX using a linear interpolation with temperature and photoperiod with the consideration of k changes under water stress conditions (Section 3.5.2). Figure 2.2 shows a broken-stick relationship between LAER and air temperature (a) and photoperiod (b, c) (Brown et al. 2005b; Teixeira et al. 2009). It is worth to mention that the figures in the thesis were simplified for modelling purpose. In New Zealand, the base temperature (T_b) of 1°C was found to appropriate for lucerne (Moot et al, 2000). In that scenario, lucerne accumulates thermal time at a slower rate (0.71 °Cd $°C^{-1}$) when the temperature is below inflexion temperature (T_i =15 °C; Figure 2.2 (a)). Thermal time accumulation is at the full rate of 1 °Cd $°C^{-1}$ at mean temperatures from 15 and 30 °C. Effective thermal time was reduced by 2.5 °Cd with every degree of mean temperature above the optimum. Lucerne stops responding to temperature when the maximum temperature (T_m) is reached.

Photoperiod effects on LAER consist of increasing and decreasing phases (Figure 2.2 (b), (c); Teixeira et al. 2009). LAER decreased 0.0014 m^2 m^{-2} °Cd when the photoperiod shortened from 16.5 to 10 h. The reduction rate was doubled (0.0028 m^2 m^{-2} °Cd) once the photoperiod was shorter than 10h. Lucerne would not expand its leaves if the photoperiod was below 8 h. In contrast, LAER increased rapidly from 0 to 0.018 m^2 m^{-2} °Cd when the photoperiod increased from 11.5 to 12 h. Subsequent LAER was 0.0004 m^2 m^{-2} °Cd for every hour photoperiod increased till the longest photoperiod at the location which was 16.5 h.

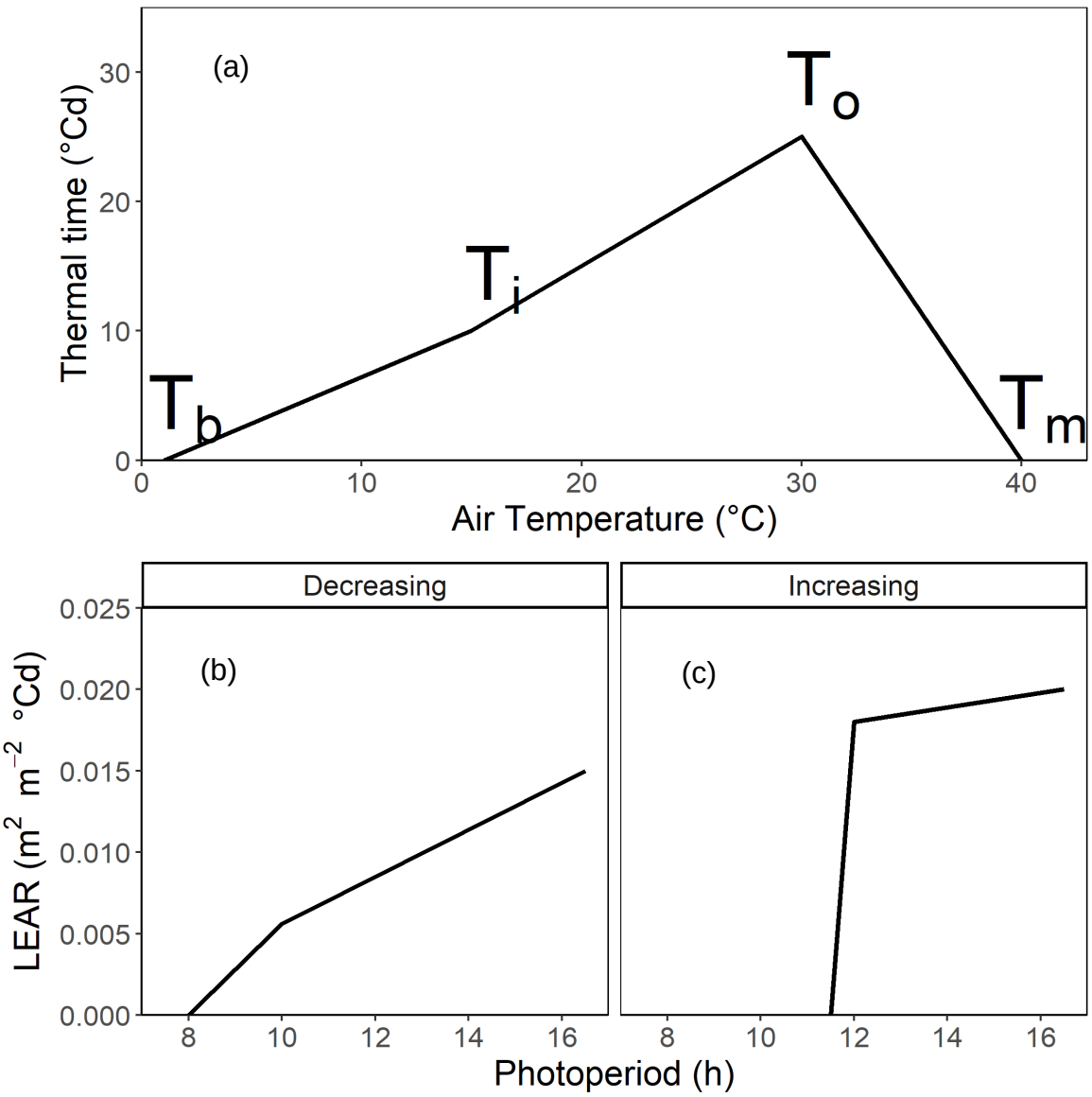

Figure 2.2 The linear interpolation functions for regulating leaf area expansion rate responses to temperature (a; Brown et al. 2005) and decreasing- and increasing photoperiod (b, c; Teixeira et al. 2009). Base, inflexion, optimal and maximum temperature (T_b, T_i, T_o and T_m) equal to 1, 15, 30 and 40 °C, respectively. Grasslands Kaituna was used in both publications. The figure is simplified for modelling purpose.

Regression analysis was the main approach used to obtain the three relationships shown in Figure 2.2 under optimal conditions (Brown et al. 2009; Sim 2014). These three relationships were conservative and hold under dryland conditions (Brown 2004, Sim 2014). Hence, in this study, the effects of water stress were assessed by regressing the underperforming plant trait against that derived when growing at its full potential under

non-limiting conditions. By combining the stress levels and response a relationship can be drawn with the relative effects of the stress factor on each particular trait. Sim et al. 2017 applied this approach and reported the relationship between LAER and water stress levels (Figure 2.3).

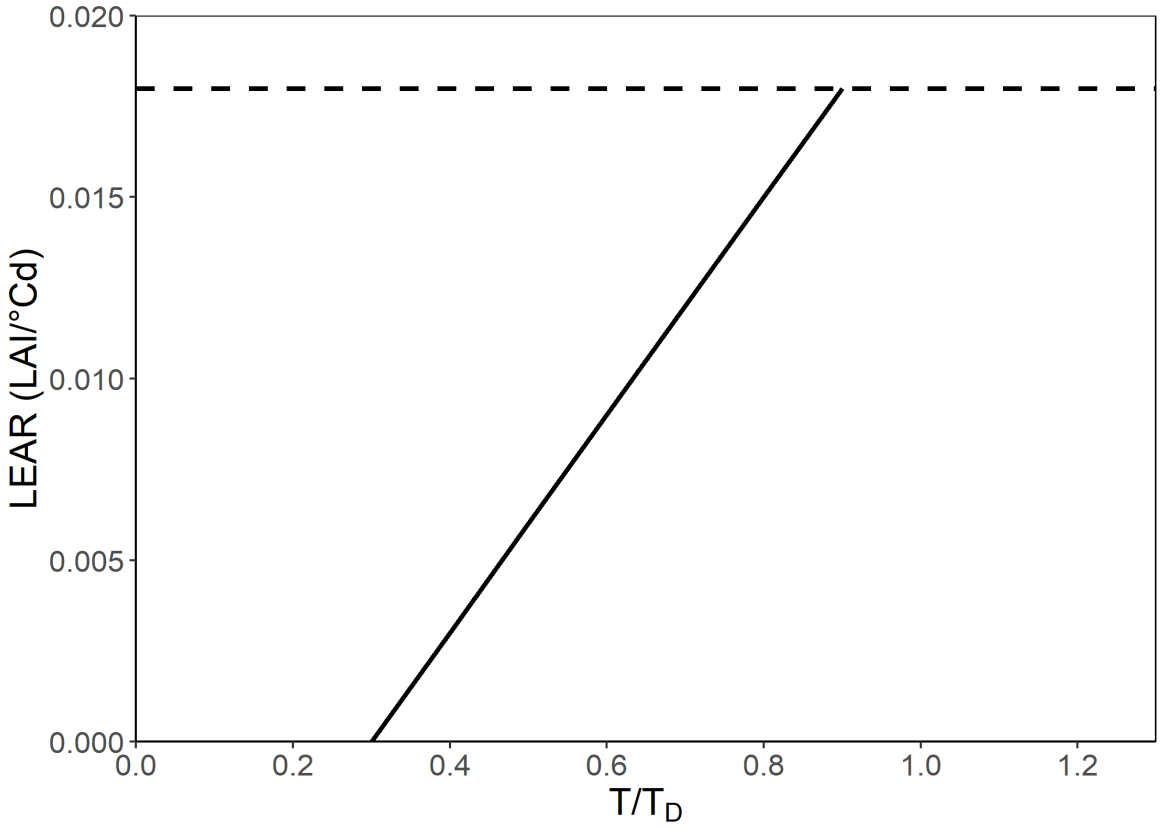

Figure 2.3 Leaf area expansion rate reduction in response to water stress (T/T_D). The linear regression equation is $\boldsymbol{y = 0.03 \times x - 0.009}$. Dash line indicates the optimal LAER (0.018 LAI/°Cd) obtained from fully irrigated conditions. (Adapted from Sim et al. 2017). Grasslands Kaituna was used in the experiment. Figure was simplified for modelling purpose by removing the actual observations.

2.2.2 Canopy height

Canopy height is an essential indicator for farmers to practise grazing management because of its linear relationship with biomass (Mills et al. 2016; Moot et al. 2016). It is a function of stem extension and is susceptible to water stress because it is driven by cell elongation. Stem extension declined 7.8 ± 2.1 mm day^{-1} to 4.5 ± 0.3 mm day^{-1} in the presence of severe water stress during the seedling stage of lucerne (Luo et al. 2020). Luo

et al. 2020 observed a linear relationship between lucerne height and growth stage under severe water stress treatments. In contrast, the well-watered treatment showed a gradual decrease of stem extension from seedling (7.8 ± 2.1 mm day^{-1}) to flowering (5.9 ± 0.5 mm day^{-1}) stages. Furthermore, reduction in height under severe water stress treatment (irrigated to 50% transpiration demand) ranged from 13% to 23% and was reported for all five cultivars, in comparison with a well-watered treatment (Mouradi et al. 2018). Similar results (10% to 23% height reduction) were observed for three varieties in a chemical induced-water stress (water potential -2 MP) experiment, although the water stress only lasted seven days (Zhang et al. 2018).

In field experiments, lucerne height and stem dry matter (DM) were significantly lower under water deficit than in well-watered treatments (Brown & Tanner 1983; Carter & Sheaffer 1983; Hanson et al. 2007; Sim 2014; Mills et al. 2016). Hanson et al. (2007) reported that the maximum height of lucerne failed to exceed 300 mm during deficit irrigation practices while lucerne height ranged between 450 and 580 mm before harvest on the fully irrigated paddock. Sim (2014) observed similar height results under rain-fed conditions under two contrasting soil types. The maximum lucerne height was 310 mm before harvest from the very stony site where it was considered to be water-stressed because of low plant-available water holding capacity (PAWC - 131 mm). In contrast, the values were between 410 and 520 mm at the same time on the deep stone-free soil. Furthermore, results show that lucerne partitioned more dry matter (DM) to leaves than to stems under severe and long water stress (59 days) conditions (Carter & Sheaffer 1983). The leaf-stem weight ratio (LSWR) increased 41% of its value under irrigation compared with the plant under water stress (Carter & Sheaffer 1983). (McCallum 1998) observed lucerne doubled LSWR (from 0.9 – 1.6 to 2.6 – 3.2) in the Wimmera, Victoria, Australia when lucerne experienced summer water stress. The changes in LSWR during water deficiency suggests the lucerne stem was more sensitive to water stress than leaves (Zahid 2009).

Under optimal conditions, the change in lucerne height over time is linearly related to thermal time accumulation (Yang 2020). Yang reported R^2 ranged from 0.91 to 0.99 when height was regressed against accumulated thermal time for regrowth lucerne. However,

the linear regressions showed a seasonal effect from summer to autumn over the four years analysed. Hence, Yang (2020) concluded that the lucerne height response was affected by changes in the photoperiod, which was affecting carbon partitioning. Figure 2.4 shows the exponential decay relationship between heightchron and photoperiod. Heightchron is defined as the thermal time requirement for lucerne to elongate 1 mm under irrigated conditions (Yang 2020). Heightchron decreased from approximately 4 to 1°Cd mm^{-1} when the photoperiod increased from 8 to 10 h, followed by a plateau that showed no further response to the photoperiod above ~11 h.

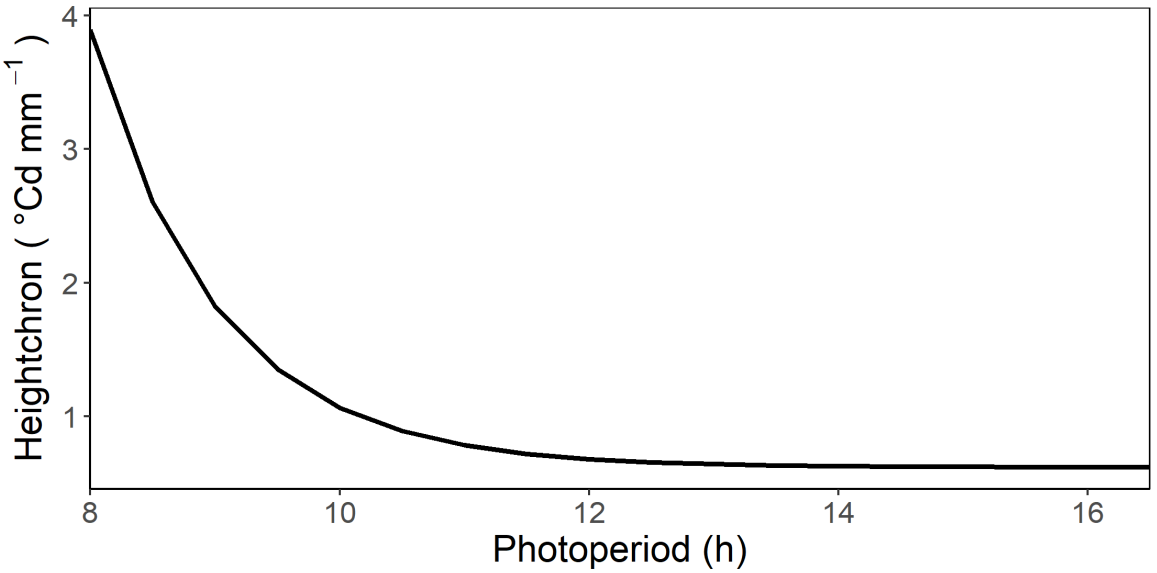

Figure 2.4 The relationship between heightchron and photoperiod changes. This relationship follows a function of $\boldsymbol{y = 0.62 + 9766 \times e^{-x}}$ (R^2 = 0.83) where y is the heightchron and x is the photoperiod. Adapted from Yang (2020). Three different fall dormancy cultivars (FD2, 5 and 10) were used. Figure was simplified for modelling purpose by removing the actual observations.

Heightchron will be affected by water stress. This is because cell elongation drives the process, which is susceptible to water shortage. Water stress effects on LAER (Figure 2.3) could also be an indicator of water stress effects on height due to the correlation between stem and shoot weight (Yang 2020). However, lucerne height data were insufficient to develop the relationship between water stress levels and height reduction.

2.2.3 Roots

Water stress also changes the partitioning of assimilates with more directed to roots, which results in increases in the ratio of root to shoot (Zahid 2009; Erice et al. 2010; Sim 2014; Luo et al. 2020). For example, lucerne seedlings maintained a similar root dry matter accumulation under moderate water stress than under non-water stress conditions, but significantly reduced their assimilate distribution to above-ground biomass under server water stress (Luo et al. 2020). More specifically, plants under moderate water stress had a root DM 16% greater, while plants in severe water stress had a root DM 10% less than that with the well-watered treatment. At the same time, the overall root-shoot ratio increased from 0.38 to 0.54 from well-watered to severe- water stress treatments. The same pattern was reported by Zahid (2009) in field experiments over two seasons. Lucerne root and shoot ratio reached a value of 1.53 without irrigation in southern Australia, which was more than triple that when the crop grew with irrigation. This adaption, or water stress avoidance strategy, has also been observed in rice (Xu et al. 2015). This response allows lucerne to reduce its canopy, and consequently contribute less to transpiration while prioritising the root system to explore more soil (Erice et al. 2010).

Lucerne root growth has a seasonal characteristic (Moot. 2003; Teixeira et al. 2007; Teixeira et al. 2008, 2009; Zahid 2009; Sim 2014), which has been linked to photoperiod under irrigated conditions. Teixeira et al. (2008) reported that the percentage of DM partitioned to roots (p_{root}) increased as photoperiod decreased in autumn as shown by changes in shoot and total radiation use efficiency (RUE) under a 42-day defoliation frequency. Specifically, p_{root} increased linearly ($R^2 = 0.93$) from ~0.05 at a 10.5 h to 0.45 at a 16.5 h photoperiod. The value of p_{root} then remained constant (0.45) during the decreasing photoperiod.

However, the root growth seasonality appeared to be overridden by water stress (Sim 2014). The p_{root} of lucerne DM stayed constant (~0.53) in the very stony soil with a PAWC of 113 mm regardless of photoperiod changes or differences in ontogeny. In contrast, lucerne DM p_{root} was altered by photoperiod and ontogeny in stone-free soil with a PAWC of 336 mm. During the seedling stage (first rotation), p_{root} of DM increased from 0.32 to 0.50 with the increased photoperiod and then remained constant as the photoperiod decreased. During the regrowth stage, lucerne DM p_{root} had a similar trend as seedling

lucerne with photoperiod increasing while p_{root} decreased from 0.3 to 0 when photoperiod declined to 12 h (Sim 2014).

The majority of root biomass was observed in the top 30 or 60 cm of the soil profile and the root distribution generally decays exponentially with soil depth (Luo et al. 1995; Bai & Li 2003; Teixeira 2006; Zahid 2009; Pang et al. 2011). For example, more than 90% of root biomass was found in the top 60 cm of duplex soils regardless of irrigation treatment, and the value declined to single digits (1 to 8% of total estimated root biomass) below 60 cm (Zahid 2009). Bai & Li 2003 reported over 60% of root DM was present in the top 30 cm when excavating lucerne roots at 10 cm intervals across all growth stages. Equally, Teixeira (2006) assumed that the top 30 cm of soil contained 80% of root biomass.

2.2.4 Phyllochron

Phyllochron is the thermal time (Tt) requirement for a plant to develop one main-stem node or leaf (Hay & Porter 2006b). The phyllochron is calculated by regressing the number of leaves against accumulated thermal time. The calculation of accumulated Tt consists of three temperature values that define each species cardinal temperatures. Cardinal temperatures are the base temperature (T_b, below which development ceases), the optimum temperature (T_{opt}, plant development at the maximum rate) and the maximum temperature (T_{max}, above which development ceases because of protein inactivation) (Moot et al. 2000). Plants accumulate Tt once the mean temperature is within the range of T_b and T_{max}. (Fick et al. 1988) reported lucerne cardinal temperatures were 5, 30 and 40 °C. T_b of 5 °C was found to be too high in a cool temperate environment, such as New Zealand. Therefore the lucerne T_b, was adjusted to 1 °C (Moot et al. 2000). Bonhomme (2000) found a non-linear relationship between Tt and mean temperature when the temperature was low which is consistent with a broken-stick relationship, where Tt is accumulated at a rate of 0.7 °Cd/°C till 15 °C, 1 °Cd/°C between 15 and 30 °C, 2.5 °Cd/°C between 30 and 40 °C (Figure 2.1; Moot et al. 2000, 2001).

Lucerne phyllochron is also regulated by photoperiod and water stress (Moot et al. 2001, Brown et al. 2005, Sim 2014). Values of lucerne phyllochron show seasonality that are consistent with the seasonal changes in partitioning preferentially to roots (Section 2.2.3).

For example, phyllochron was 35 °Cd in spring and summer while it increased to 51 °Cd in the autumn (Moot et al. 2001). Brown et al. (2005) quantified the relationship between phyllochron and photoperiod for regrowth lucerne under irrigation. Specifically, phyllochron increased from 37±7 °Cd to 60 °Cd as photoperiod decreased from 15.7 h to 11.4 h in autumn but was constant at 37 °Cd in an increasing photoperiod. The phyllochron was quantified as 34 °Cd across different defoliation treatments at a photoperiod of ≥ 12.5 h (Teixeira et al. 2007). Nevertheless, phyllochron ranged from 40 to 65 °Cd depending on the defoliation frequency once the photoperiod was shorter than 12.5 h. Teixeira et al. (2011) confirmed that seedling lucerne had a longer phyllochron (47±2.3 °Cd) than the regrowth crops (35±1.8 °Cd). Similar results were found via a sowing date experiment. Sim (2014) reported that seeding lucerne sown in October had a phyllochron of 37 °Cd while late summer-sown (February) lucerne had a phyllochron of 58 °Cd. Regrowth lucerne in the stone-free soils of high water holding capacity showed a nearly identical phyllochron as that outlined by previous studies (Sim 2014).

The APSIMX-Lucerne model structure consists of three phases in the lucerne life cycle; juvenile, vegetative and reproductive. Figure 2.5 represents the implementation of photoperiod effects on phyllochron. Phyllochron is constant during the juvenile stage (Teixeira et al. 2011). Lucerne responds to the photoperiod once it enters the regrowth phase. Phyllochron increased from 35 to 49 °Cd when the photoperiod decreased from 16.5 to 10 hours. In contrast, lucerne decreased its thermal time requirement sharply from 49 to 31 °Cd when the photoperiod increased from 10 to 12 hours and showed no responses to further photoperiod increases. The reproductive phase currently has no response of phyllochron to environmental factors because this has not been measured due to the focus predominantly being on forage production (Yang et al. 2020).

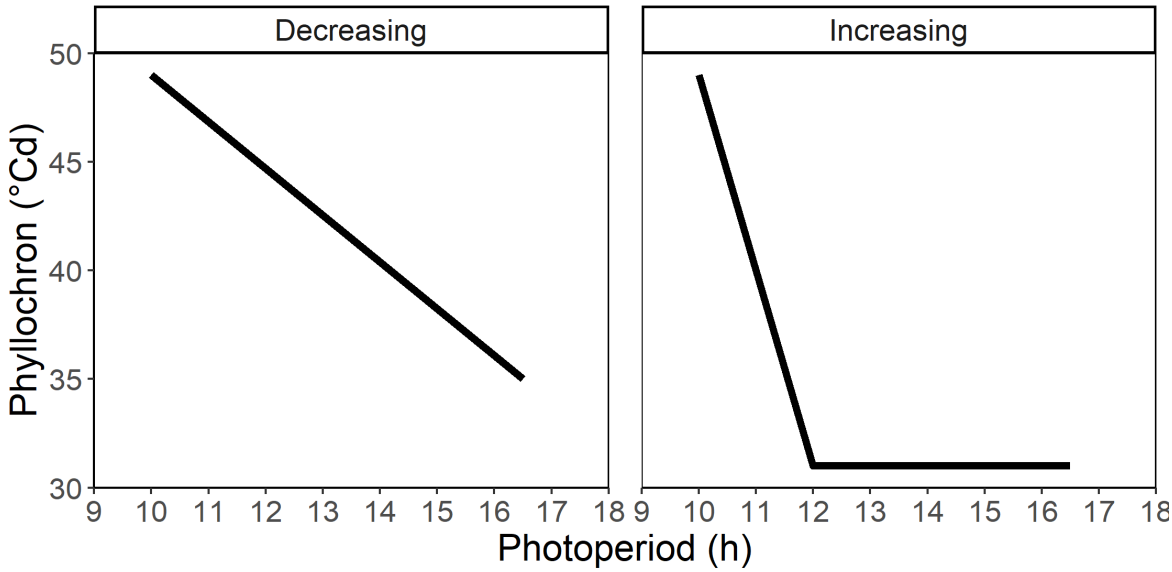

Figure 2.5 The relationship between phyllochron and photoperiod for lucerne. Lucerne increased thermal unit (°Cd) requirements to produce the main stem node when photoperiod decreased while thermal unit requirement dropped during increased photoperiod (Adapted from Teixeira, et al. 2007 & 2011). Grasslands Kaituna was used in the experiment. Figure was simplified for modelling purpose by removing the actual observations.

In contrast, lucerne grown in stony soil had a phyllochron 1.5 to 2 times longer than the stone-free soils (Sim 2014). This result implies that water stress had a significant impact on node appearance. Phyllochron was 54, and 44 °Cd for seedling and regrowth lucerne grown under low PAWC (131 mm) conditions, and there was no apparent pattern to show it responded to photoperiod. Meanwhile, lucerne grown under high PAWC (362 mm) conditions demonstrated the same seasonal pattern of phyllochron concerning photoperiod changes. For instance, spring-sown lucerne had a phyllochron of 37 °Cd and this increased to 50 °Cd in late summer. The comparison of lucerne growing in high and low PAWC soil types suggests that severe water stress could override photoperiod effects on lucerne node appearance.

Furthermore, Sim (2014) regressed relative phyllochron (values in dryland concerning optimal values obtained in irrigated conditions) against a T/T_D and fitted a logistic model (Figure 2.6). The strong relationship (R^2 = 0.88) showed that lucerne phyllochron was insensitive to water stress until T/T_D was below 0.7. It increased abruptly as T/T_D decreased

from 0.7 to 0.5, more specifically, the value doubled and remained at that rate irrespective of photoperiod.

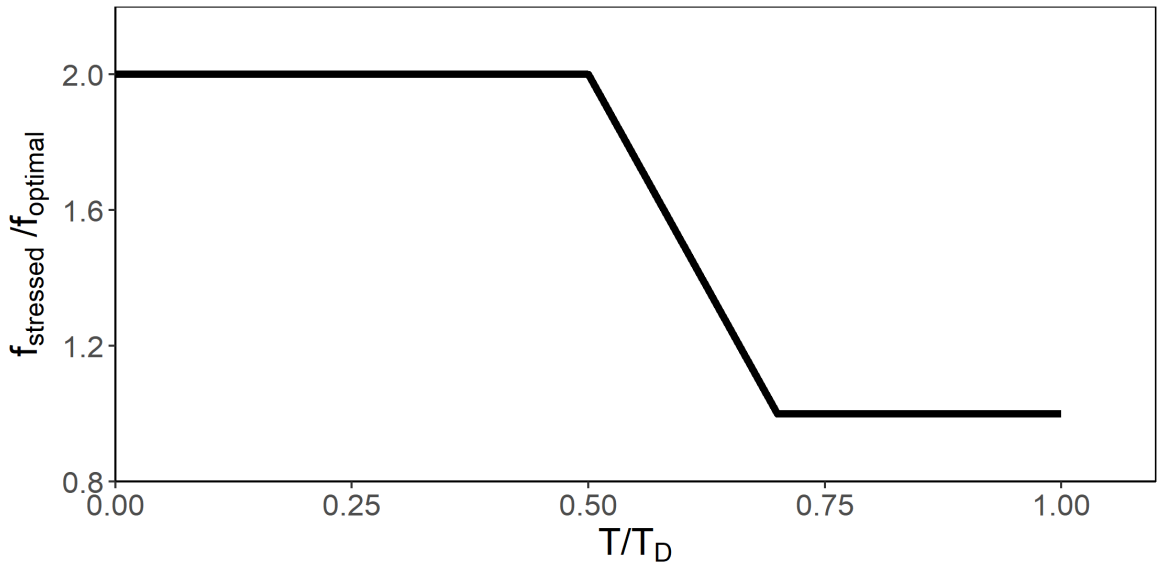

Figure 2.6 The relationship between water stress effects on phyllochron ($f_{stressed}/f_{optimal}$) and the water stress level (T/T_D). The graph was redrawn based on data presented in (Sim 2014). Grasslands Kaituna was used in the experiment. Figure was simplified for modelling purpose by removing the actual observations.

2.2.5 Flowering

Flowering is the time when a plant switches from vegetative to reproductive priority. It was common to use lucerne flowering in decision-making for grazing or cutting management worldwide (Moot. 2003; Teixeira et al. 2011; Rimi et al. 2012; Pecetti et al. 2017). Lucerne reproduction initiates from bud development and is influenced by ontogeny, temperature and photoperiod under optimal conditions (Zahid 2009, Teixeira et al. 2011, Sim 2014). During bud initiation and open flowers, lucerne responds only to temperature (Teixeira et al. 2011). More specifically, seedling lucerne required more accumulated Tt (exact number depends on photoperiod) to reach 50% of bud visible than regrowth lucerne. The period for lucerne to gain the extra Tt requirement was termed as the 'juvenile' period (Pearson & Hunt 1972; Teixeira et al. 2011). However, this 'juvenile' period is invalid once the photoperiod is more than 18 h (Pp_{crit}). In other words, seeding lucerne has no extra Tt

requirement for reproduction. Teixeira et al. (2011) reported that 530 °Cd was the minimum Tt required for lucerne to initiate flower development regardless of cultivar.

Effects of water stress on lucerne flowering depend on the stress severity. Moderate water stress may accelerate the accumulation of thermal time due to a warmer canopy temperature and thus result in earlier lucerne flowering (Zahid 2009). Severe water stress delays flowering or even induces plant dormancy (Orloff et al. 2015). For example, seasonal soil water deficits (SWD) of ~330 mm bought flowering time earlier by approximately 1.5 days compared with SWDs of zero in northern Italy (Pecetti et al. 2017). This difference in flowering time had limited relevance in practice, although was significant statistically.

In contrast, Sim (2014) reported a systematic delay of lucerne flowering time (defoliated when 50% bud visible) in a severe water stress site (PAWC was 223 mm less than the unstressed site with other conditions identical) for three spring-summer sown lucerne plots. Consequently, defoliation times were always later in the water-stressed than well-watered site. In summer, lucerne in the severe water stress failed to flower with leaves senescing rapidly (Sim 2014). This phenomenon was probably due to water stress-induced dormancy, which allows lucerne to recover once soil water is available (Orloff et al. 2015). The cause of delayed flowering is likely due to a longer phyllochron caused by water stress, resulting in a prolonged period for the minimum thermal time requirement for lucerne to accumulate before the switch from vegetative to reproductive development (Figure 2.6). Nevertheless, more investigation is necessary to identify the effects of water stress on the lucerne time of flowering.

2.2.6 Radiation use efficiency

Radiation use efficiency (RUE) is the amount of dry matter production per unit of intercepted solar radiation by the canopy (Hay & Porter 2006b). Plants only utilize solar radiation in the wavelengths between 400 to 700 nm, known as the photosynthetically active radiation (PAR), which is approximately half of total solar radiation. Both total solar radiation and PAR are used to calculate RUE in the literature (Hay & Porter 2006a, Sim 2014). However, in this study, RUE will be expressed based on total solar radiation.

Radiation use efficiency provides a prediction tool for researchers to study yield gaps that result from biotic and abiotic factors by calculating the optimal yields of crops based on the incoming solar radiation in different regions of the planet. For example, 100 g of cereal grain requires about 16.7 h of radiation to shine on 1 m^2 of green wheat leaf area under optimal environmental conditions (Hay & Porter 2006a). Thus, the effects of limiting factors, such as water stress, can be evaluated in a quantifiable approach, and alternative agronomic practices may be introduced to reduce their impact.

Lucerne RUE under non-limiting conditions has been well documented in a temperate climate (Avice et al. 1997; Collino et al. 2005; Brown et al. 2006; Teixeira et al. 2008). Temperature is the main factor that affects lucerne RUE in the field in the absence of other abiotic and biotic stresses. For temperature effects, Brown et al., (2006) reported that total (shoot+root) RUE increased linearly as mean air temperature rose from 6 to 18 °C at a rate of 0.083 g DM/MJ/°C. Teixeira et al. (2008) reported consistent results with total RUE from 0.65 to 1.55 g DM/MJ in relation to temperature. Collino et al. (2005) confirmed a strong relationship (R^2 = 0.713) between RUE and temperature and suggested that RUE was conservative with a slope value of 0.076 g DM/MJ/°C in irrigated conditions in Argentina. The temperature effects are most likely caused by the photosynthetic enzyme response to temperature differences (Hay & Porter 2006a).

Furthermore, management practices may have a role that affects lucerne RUE through depleting carbon and nitrogen reverse in the taproot faster or reducing the photosynthetic capacity of the canopy. Avice et al. (1997) showed the difference in shoot RUE of the cultivar 'Europe' (0.725 g DM/MJ vs 0.935 g DM/MJ) between 30 (362±70 °Cd) and 45 (541 °Cd) days cutting frequencies in spring. Four out of eight observed total RUE values were 0.35 to 0.50 g DM/MJ, less than the predicted total RUE regarding a cutting frequency of 28 days (237±55 °Cd) (Teixeira et al. 2008).

Radiation use efficiency decreases with water stress but is less sensitive than canopy development (Collino et al. 2005, Brown et al. 2009, Zahid 2009, Sim 2014). In most cases, shoot RUE was consistently lower in water-stressed conditions than well-irrigated lucerne with a considerable amount of variation in duplex soils which resulted in no apparent

pattern (Zahid 2009). However, the application of T/T_D to quantify the effect on shoot RUE on lucerne has been used successfully in Canterbury, New Zealand. This compared shoot RUE under water stress relative to those under optimal water conditions ($f_{stress/optimal}$). A moderately strong linear relationship ($R^2 = 0.76$) was identified when T/T_D declined from 1.0 to 0 in a stone free soil (Brown et al., 2009). Sim (2014) demonstrated a broken stick relationship between T/T_D and shoot RUE by applying the same quantification approach to compare lucerne grown in stony versus stone-free soils. More specifically, the value of $f_{stress/optimal}$ gradually declined to 0.75 from 0.9 when T/T_D decreased from 0.9 to 0.8. Then $f_{stress/optimal}$ declined sharply to 0.15 when T/T_D fell from 0.8 to 0.4, and then it remained constant

Reductions in RUE usually result from a lack of carbon dioxide (CO_2) supply caused by stomatal closure (Brown et al. 2009; Brown et al. 2012; Sim et al. 2017). However, Bell et al. (2007) reported that the CO_2 concentration ratio of inside and outside lucerne leaves remained stable until soil water content (SWC) dropped to the value of the lower limit (LL). LL is defined as the soil water potential of -1,500 kPa, below which water extraction ceases. This result indicates that stomatal closure may not cause a reduction in lucerne RUE under water stress conditions. Historical research of photosynthetic mechanisms in soybean and sunflower suggested that low leaf water potentials could inhibit chloroplast activity (Boyer & Bowen 1970; Mohanty & Boyer 1976) that consequently affects photosynthesis. Regardless of the mechanism, there is a need to understand the relationship between water stress and RUE.

APSIMX-Lucerne uses total radiation use efficiency (RUE) to produce DM from intercepted PAR and carbon dioxide. RUE is mainly subject to temperature fluctuations due to enzyme activity in an irrigated environment (Teixeira et al. 2008). Yang (2020) regressed total DM against accumulated intercepted PAR to determine the relationship between RUE and temperature (Figure 2.7). By assuming this relationship is conservative, Sim (2014) related RUE under dryland conditions to its performance under optimal conditions and found that water stress did affect RUE (Figure 2.8). However, the “broken-stick” relationship is likely to shift to a straight line relationship once more data is incorporated.

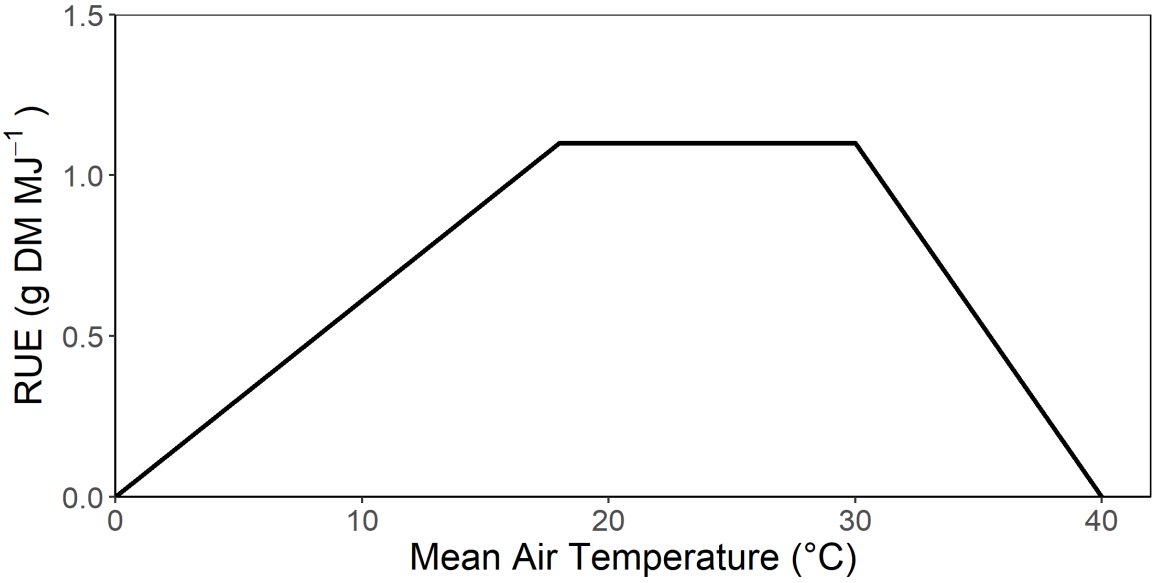

Figure 2.7 Radiation use efficiency (RUE) response to mean air temperature (Brown et al. 2006, Yang 2020). Grasslands Kaituna was used in the experiment. Figure was simplified for modelling purpose by removing the actual observations.

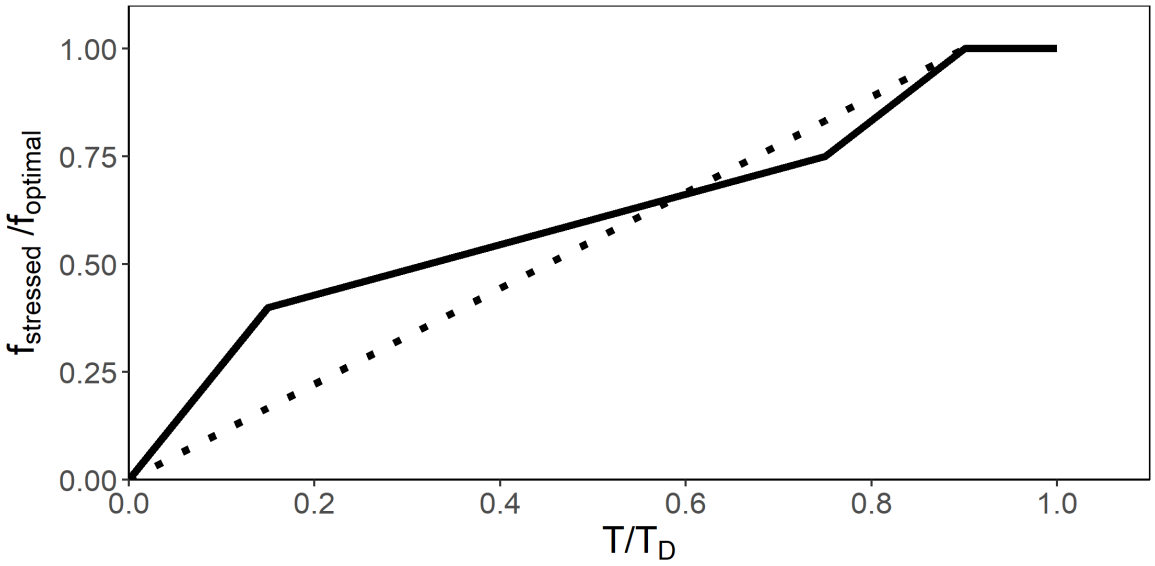

Figure 2.8 The relationship between water stress effects on RUE ($f_{stress}/f_{optimal}$) and the water stress level (T/T_D). The solid line indicates the relationship reported by Sim (2014). The dotted line represents the potential generic relationship. Grasslands Kaituna was used in the experiment. Figure was simplified for modelling purpose by removing the actual observations.

2.3 Quantifying water stress effects

The ratio of actual to transpiration demand is a common approach to quantify the magnitude and effects of water stress on lucerne (Brisson 1998; Robertson et al. 2002; Brisson et al. 2003; Brown et al. 2009; Sim et al. 2017; Jing et al. 2020). A water deficit may affect lucerne growth and development if the ratio is lower than 1; otherwise, water is considered unlimited, and transpiration demand (T_D) equals actual evapotranspiration (ET). Actual evapotranspiration is the minimum of soil water supply (SW_S) and crop transpiration plus soil surface evaporation (soil water demand - SW_D) (Brown et al. 2009). For example, ET is equal to transpiration and evaporation requirements when the soil water supply is sufficient. Otherwise, ET is limited by the available water in the soil. Brown et al. (2009) developed a framework that implemented the concept of using soil water supply and demand with the corresponding yield formation components to quantify water stress effects on lucerne (Equation 2).

Equation 2

$$\begin{cases} f_{ws} = \frac{SW_D}{SW_S}, & t \leq t_x \\ f_{stress/optimal} = f(f_{ws}), & t > t_x \end{cases}$$

where f_{ws} is the water stress factor, SW_D is the plant water uptake and surface evaporation, SW_S is the available soil water to plants, t is the sampling timestamp and t_x is the time that water supply inadequate to meet the demand. Equation 1 provides a reliable approach to examine water stress effects solely through soil water measurements. Sim (2014) applied this approach and successfully quantified water stress effects on lucerne canopy development (Section 2.2.1), radiation use efficiency (Section 2.2.4) and phyllochron (Section 2.2.4). An important component of the relationship was defining SW_D and SW_S.

2.3.1 Quantifying soil water supply

The amount of soil water available is defined by three main parts separated by two essential concepts: drained upper limit (DUL, or field capacity) and the lower limit at -1.5 MPa (LL15, or Wilting point) (McLaren & Cameron 1996). When soil water is above DUL drainage is expected or loss of water as overland flow. In contrast, water below LL15 is considered unavailable to plants. Thus, the difference between DUL and LL15 defines the available water capacity (AWC) for a particular soil based on six main factors (Equation 3).

Equation 3 $$AWC = f\begin{bmatrix} texture, & structure, \\ layering, & depth, \\ organic\ matter, & stones \end{bmatrix}$$

These soil physical properties affect AWC interactively and it is difficult to separate their individual effects. However, general rules have been extracted (McLaren & Cameron 1996). For example, the finer the soil texture, such as clay, the higher the AWC. High organic matter content in soils maintains good soil structure which contributes to more surface area and higher porosity, which results in greater AWC. In contrast, a high stone content reduces the AWC in soils proportionally. Furthermore, it is common in New Zealand that sandy soils have high AWC values due to soils that have a highly compacted layer that stops drainage. Once the AWC is known for soil the depth of each layer, this then determines the soil volume available to hold water in a soil profile.

The PAWC may also be equal to, or less, than the calculated or measured AWC depending on crop species. Thus, PAWC is a combined property of soil and plant while AWC is a soil property. In summer dry conditions, saturation rarely occurs because AWC is defined in laboratories and usually deviates from field conditions. The actual lower limit (LL) in the field can be variable due to plants ability to adjust leaf water potentials and the soil type (Ratliff et al. 1983; Dolling et al. 2005). Therefore, the crop lower limit (CLL) is used to differential the lab-measured LL15 (Dalgliesh & Foale 1998). Lucerne can adjust its osmotic potential to maintain leaf water potentials well below -1.5 MPa (Bell et al. 2007), which means the lucerne CLL could be equal to or lower than the commonly accepted LL15.

Detailed methods to obtain DUL and CLL are discussed below. It has to be noted that SWC measurements determine these variables. SWC measurements are usually obtained via neutron probe (NP) or/and time domain reflectometry (TDR) sensors. A given soil profile is usually divided into multiple arbitrary measuring layers based on data resolution requirements, labour and sensor capabilities. For example, an interval of 10 cm thickness was used by Sim (2014) to measure SWC below the top 20 cm soils. In contrast, Teixeira et al. 2018 used 20 cm intervals to collect SWC below the top 30 cm soils. A common practice

of measuring top layers (top 20/30 cm) is to use TDR sensors due to performance and safety concerns of using NP in the top layers (Brown et al. 2005a; Sim 2014; Teixeira et al. 2018).

2.3.1.1 Initial soil water content

Initial soil water content determines the amount of water available in the soil at the time of sowing. Equation 4 shows the most straightforward approach to calculate $SW_{initial}$.

Equation 4 $$SW_{initial} = mean(SW_i)$$

where $SW_{initial}$ is the soil water content in each measured layer at sowing. However, soil water measurements occasionally align imperfectly with sowing dates due to labour constraints or equipment availability (Brown et al. 2009, Sim 2014). To overcome this, the nearest $SW_{initial}$ measurements were used when the time differences between sowing and soil water measurement were less than one day (Sim 2014). Model fitting procedures were used to adjust $SW_{initial}$ when the time difference was more than one day (Brown et al. 2009).

2.3.1.2 Drained upper limit (DUL)

The drained upper limit (DUL) describes the state when soil water reaches equilibrium. It is probably impossible to measure DUL precisely because it is a dynamic state influenced by soil properties and meteorological factors such as temperature and precipitation (Kirkham 2005). There are two main approaches to obtain DUL values, including laboratory estimation and field measurements (Ratliff et al. 1983). For laboratory estimation, the SWC of intact soil cores are measured at -0.033 MPa and recorded as volumetric water content. Ratliff et al. (1983) reported that the laboratory method significantly overestimated DULs for fine soils such as silt loams and silty clay loams while it underestimated DULs for sandy soil such as sandy loams after they compared 282 paired soil samples of laboratory and field measurements. They concluded field measured DULs were the preferred method for each given soil (Ratliff et al. 1983, Kirkham 2005). In brief, the process of obtaining field measured DULs has three simple steps: 1) wetting up the soil completely to saturation, 2) allowing drainage and 3) monitoring SWCs (Dalgliesh & Foale 1998). In practice, this method could provide suitable estimates for DULs in free-draining soil but may

overestimate DULs in heavy clay soils. This is because drainage occurs slowly over time in heavy soils. However, DULs estimated for heavy soils are still acceptable since slow draining water is available for plants (Dalgliesh & Foale 1998).

Several authors have successfully determined DULs by field measured SWC (Brown 2004, Brown, Moot, & Pollock 2005, Dolling et al. 2005, Brown et al. 2009, Sim et al. 2017, Teixeira et al. 2018). The recommended approach is to determine DUL at the field was using rain-out facilities described by (Dalgliesh & Foale 1997). Nevertheless, SWC data collected from dryland conditions could estimate DULs if data covered the entire drying cycle with a complete soil profile recharged by precipitation before the drying cycle. For example, (Dolling et al. 2005) used the maximum measured SWC from NP after sufficient rain recharged soil profile and averaged the maximum values over at least two years of data to estimate DUL (Equation 5).

Equation 5 $$DUL = max(mean(SWC))$$

Time domain reflectometry sensors could improve the estimation because researchers could set up automatic logging stations. DUL could be derived once TDR measurements show a plateau after winter rain (Dolling et al. 2005, Sim et al. 2017). In New Zealand, normal winter rainfall usually recharges soil water content back to DUL with the potential for drainage in late winter and early spring. Under these circumstances, an estimate of DUL can be obtained from the fully saturated soil water profile. Equally, at the end of a long dry summer, or water stress period, the AWC will be minimal and this can be used to estimate LL. Repeated measures of soil water over several years, that include wet and dry conditions, can be used to estimate DUL and LL for a given soil. This method is used in this thesis. DUL could range from 0.3 to 0.4 mm^3/mm^3 in a deep Wakanui silt loam soil (*Aquic Haplustept*, USDA Soil Taxonomy) in New Zealand while reduced to approximately 0.1 mm^3/mm^3 in a very stony soil (Sim 2014).

Surface layers require extra attention when measuring SWC to estimate DUL. This is because surface layers actively interact with the atmosphere and soil evaporation has a significant impact on SWC (Section 2.3.3). Thus, previous studies measured SWC at night

(Dolling et al. 2005) or in winter (Sim et al. 2017) when evaporation was negligible to minimise the evaporation effects.

2.3.1.3 Crop lower limit (CLL)

Crop lower limit (CLL) is the SWC value at which crops are unable to extract any further water from the soil. The concept of CLL is based on field measurements and should be treated differently to the permanent wilting point (PWP), especially for lucerne. The classic definition of PWP is the "amount of water in the soil at which plants are permanently wilted" (McLaren 1996) and this is generally considered to be at an SWC of -1.5 MPa (McLaren 1996, Kirkham 2005). However, lucerne has been shown to extract water below PWP and survive 35 days of water stress treatment (soil water potential below PWP) (Bell et al. 2007). Furthermore, Ratliff et al. (1983) concluded that PWP obtained from laboratory measurements differed with soil texture and deviated largely from field measurements. Moreover, Jordan & Miller (1980) found that sorghum failed to extract a substantial amount of water (50 mm) when SWC was greater than PWP despite the water stress. Therefore, CLL derived from field data probably represents soil water status more precisely than PWP for lucerne.

In field conditions, the minimum SWC measured represents the lucerne CLL for a given soil layer during a drying cycle (Equation 6; Dolling et al. 2005, Zahid 2009, Sim 2014). Precipitation exclusion is still the preferred method to obtain CLL, although the cost may be substantial to investigate multiple sites. Under dryland conditions, lucerne could reach CLL for all layers up to the maximum rooting depth during summer (Dolling et al. 2005, Sim 2014). In a New Zealand deep soil, such as Wakanui silt loam, lucerne CLL ranged between 0.1 and 0.3 mm^3 mm^{-3} but was less variable than in the very stony soil (0.05 to 0.1 mm^3 mm^{-3}) (Sim 2014).

Equation 6 $$LL = min(mean(SWC))$$

2.3.2 Quantifying water extraction pattern

Soil water supply, or PAWC, can be considered as a `bucket of water`. The bucket's depletion rate is quantified by a water extraction pattern, consisting of two concepts: Root

front velocity (RFV) and water extraction rate (KL). The former defines the rate at which roots reach a particular soil layer, and the latter defines the rate of water uptake by the root from a given layer. Detailed methods of obtaining RFV and KL will be examined. Similar to DUL and CLL, RFV and KL are only valid in the context of soil layers.

2.3.2.1 Root front velocity (RFV)

Previously researchers derived water's disappearance rate from soil moisture content measurements in specific depths to calculate RFV in field conditions (Dardanelli et al., 1997; Dolling et al., 2005; Sim et al., 2017). The assumption was that the rate of crop root development downwards approximately matches the water disappearance under water-limited environments (Dardanelli et al. 1997). RFV is expressed as mm per day; therefore, it could be derived from dividing the depth by the days after sowing (DAS) of SWC descending at an arbitrary threshold. Dolling et al. (2005) applied a descending threshold of 2% to calculate RFVs for lucerne over nine Western Australia sites. RFVs ranged from 1.7 to 9.2 mm day^{-1}. The results were lower than the observation (11.2 to 14 mm day^{-1}) reported by Meyers et al. 1996, who directly measured root elongation. The cause of low RFV values was likely due to the soil physical and chemical properties which hindered lucerne root development (Dolling et al. 2005).

In New Zealand, Sim (2014) manually identified SWC decreases through visualising changes in SWC data for the entire drying cycle over different layers and regressed the maximum depths over time. Seedling lucerne had an RFV of 12.9±1.02 mm day^{-1} in deep soil and 15.1±2.45 mm day^{-1} in very stony soil, which was comparable with results from (Meyers et al. 1996). However, regrowth lucerne in the subsequent seasons had RFVs of 14.2±1.06 and 32.6±1.19 mm day^{-1} in deep and very stony soils, respectively. Dolling et al. (2005) reported a similar observation in which the soil with the lowest PAWC had the highest RFVs for regrowth lucerne. This suggests that the presence of the root systems within the profile allows lucerne to empty “the bucket” more rapidly than for an establishing root system. The phenomenon indicates that a single RFV may be invalid to represent the actual rate of soil water extraction for regrowth lucerne crops.

Figure 2.9 demonstrates a theoretical exemplar of soil water changes over time with plant up-taking water. Soil water content (θ, $mm^3\ mm^{-3}$) remains constant until t_c (Stage A) when the root front arrives at this soil layer. θ declines afterwards because of water extraction. RFV can be calculated by substituting the depth and DAS_{t_c} with soil layer data and t_c in Equation 7. DAS_{t_c} is the critical value to obtain RFV. Previously, the values were extracted by visualising summarised θ over time and manually identifying the decreased trends (Dolling et al. 2005, Sim 2014).

Equation 7 $$RFV = \frac{Depth}{DAS_{t_c}}$$

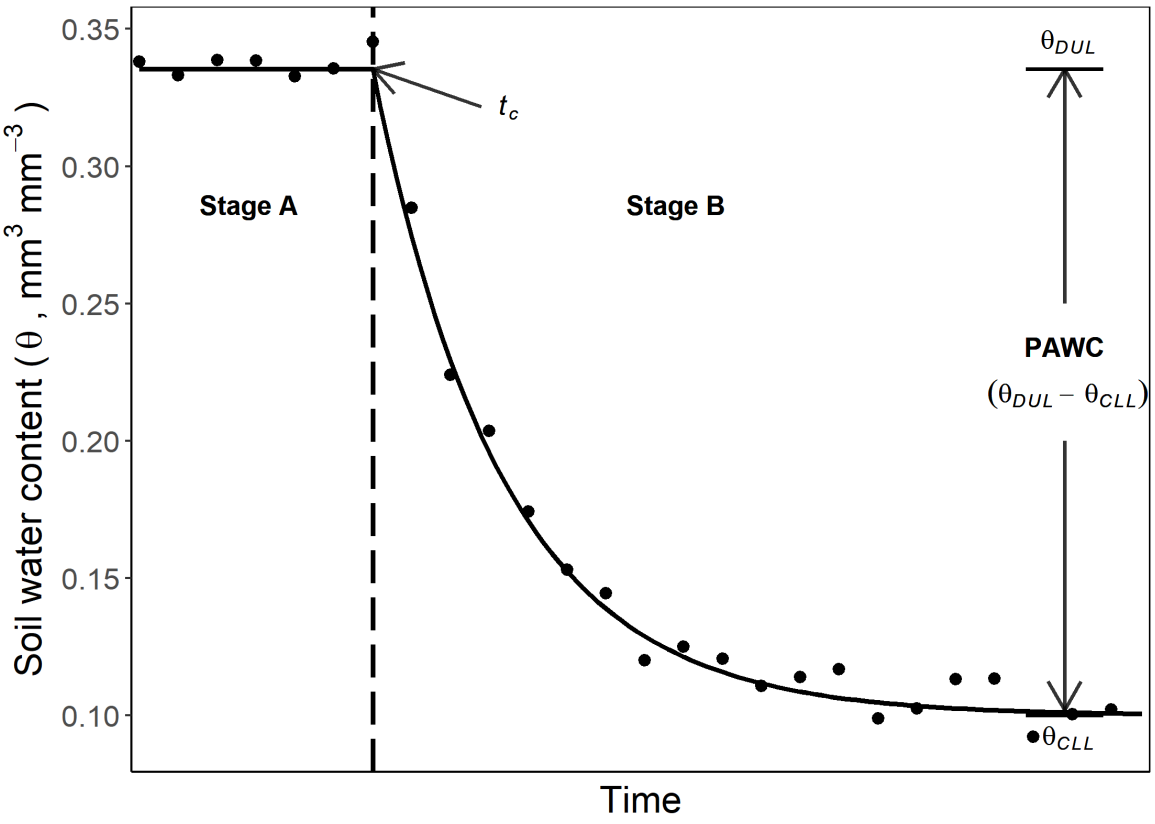

Figure 2.9 A theoretical example of soil water content (SWC) change in a single layer of soil over time. Stage A represents that SWC remains stable at its maximum value (θ_{DUL}) until the change point (t_c). Water extraction occurs at t_c, after which Stage B begins. SWC changes in Stage B can be fitted with an exponential decay function in theory. Root extracts SWC to its minimum value (θ_{CLL}). The value between θ_{DUL} and θ_{CLL} is termed as plant available water capacity (PAWC). Adapted from Brown (2004).

2.3.2.2 Water extraction rate

Water extraction rate combines two concepts that influence root water uptake. These are soil hydraulic conductivity (K, $mm^2\ day^{-1}$) and root length density (L, $mm\ mm^{-3}$) (Dardanelli et al. 1997, 2004). The former describes the rate that water molecules travel through soil aggregates, while the latter describes the length of root present in a given volume of soil. Several models have been developed to estimate plant water extraction based on the assumption of water extraction related to root length density (RLD) (Passioura 1983; Monteith et al. 1986). However, these demand measurements or estimates of RLD, which are difficult to collect. Consequently, uncertainties are introduced to estimates. Furthermore, the assumption of uniform root distribution could be violated in soils with cracks and stones. Direct measurements of water disappearance patterns were considered a more appropriate tool to investigate soil water extraction than RLD based models (McIntyre et al. 1995).

Dardanelli et al. (1997) verified the exponential relationship (Stage B) between soil water depletion over time for five species, including lucerne, by applying rain exclusion techniques. They found no consistent relationship between RLD and kl and concluded that an absolute RLD was unnecessary to represent root water extraction. Later, (Dardanelli et al. 2004) developed an empirical model with a constant value termed KL (0.096) for annual crops such as maize, wheat and soybean to address daily water uptake by roots. This empirical model removed the prediction of root length density (RLD) and solely relied on SWC measurements. The same method was used by Brown et al. (2009) and Sim et al., (2017) to successfully reflect lucerne water uptake.

Water extraction rate (KL) can be estimated based on the second segment in Equation 8 (Dardanelli et al. 1997). This method derives KL values by fitting decreasing exponential models to the observed SWC in each layer after the change point (Figure 2.9).

Equation 8
$$\theta = \begin{cases} \theta_{initial}, & t \leq t_c \\ (\theta_{DUL} - \theta_{CLL}) \times e^{-kl \times (t - t_c)} + \theta_{CLL}, & t > t_c \end{cases}$$

Where θ is the volumetric water content at time t, θ_{DUL} and θ_{CLL} are drained upper limit and crop lower limit in a volumetric unit for a given soil layer, respectively. t is the number of days after sowing and t_c is the DAS when the root arrives at the designated soil layer.

Surface KL of lucerne appears challenging to obtain due to incomplete canopy closure post grazing or cutting and consequent soil evaporation that may violate the exponential decay assumption (Monteith et al. 1986). Also, fields without rainout facilities could be affected by occasional rainfall events, and violate the exponential decline in water depletion over time. To tackle these challenges, Teixeira et al. (2018) developed a biophysical modelling approach to take account of random daily rainfall and incomplete canopy closures for ryegrass and lucerne under irrigated and dryland conditions (Section 3.6.2).

2.3.3 Quantifying soil water demand

Soil water demand contains two aspects: crop transpiration (T) and soil surface evaporation (E) (Ritchie 1972). Crop transpiration is determined either by solar energy (when the soil water supply is sufficient) or by the rate of root water extraction (when water is limited) (Brown et al. 2012). In contrast, E is estimated to globally account for 20% of terrestrial precipitation (Or et al. 2013). Soil surface evaporation may significantly impact the grazed lucerne system and vice versa because the defoliation management regularly exposes the soil surface (Moot et al. 2003, Brown et al. 2009). Both T and E are discussed below regarding their quantifying methods.

2.3.3.1 Plant transpiration

Plant transpiration is driven primarily by climatic factors, such as wind speed, temperature and radiation, coupled with canopy characteristics (Monteith et al. 1986, Brown et al. 2012, Kirkham 2014). With the assumption of unlimited soil water supply, a short green crop and complete ground cover, Penman defined potential transpiration (T_D) to describe soil water demand in 1948 (Monteith et al. 1986). The original definition has been further developed to remove two major constraints 1) a uniform short green crop and 2) complete ground cover, and taking into account limited soil water supply (Monteith et al. 1986). More specifically, Monteith et al. (1986) defined soil water demand as a function of DM

production rate divided by transpiration efficiency (q) which incorporated the work completed by (Tanner & Sinclair 1983).

Tanner and Sinclair (1983) identified that q could be estimated from vapour pressure deficit (VPD) determined by daytime temperatures (Robertson et al. 2002, Brown et al. 2012). Canopy temperature close or equal to air temperature is the essential assumption of their method. However, this assumption might be invalid in cool and humid conditions since canopy temperature could be warmer than the air temperature (Brown et al. 2012). Brown et al. (2012) developed a canopy conductance (Θ_T) approach to predict lucerne transpiration demand. Validation results showed root mean square error (RMSE) was reduced from 126% to 26% of observed mean when the Θ_T approach ($\Theta_T = 0.45\ mm\ MJ^{-1}kPa^{-1}$) was applied in comparison with the transpiration efficiency approach ($\omega = 5\ Mpa$) under dryland and irrigated conditions in Canterbury, New Zealand. Sim et al. (2017) validated that the Θ_T approach was linearly related to radiation interception for seedling and regrowth lucerne crops across three different soil types.

Maximum stomatal conductance (g_{smax}) and R_{50} are two essential parameters in APSIMX to simulate plant transpiration (Section 3.5). Stomata control the water transmission between the leaf internal and the external atmosphere. Stomatal conductance (g_s) measures how efficiently water and gas (CO_2) exchange occurs through the stomata. Maximum stomatal conductance (g_{smax}; m s^{-1}) represents when the leaf is in an optimal environment (adequate water supply, optimal temperature, low vapour pressure deficit and fully expand leaf). (Kelliher et al. 1995) reported that g_s is correlated with photosynthetically active radiation (PAR) but this depends on the leaf position within a canopy and an assumed hyperbolic function (**Equation 9**)

Equation 9 $$g_s = \frac{g_{smax} \times R_a}{R_a + R_{50}}$$

where R_a is the PAR intercepted by a single leaf and R_{50} is the PAR when g_s is half of its maximum value. In APSIMX, these two parameters form single leaf conductance and are

further scaled up to canopy conductance in the MicroClimate module for subsequent T_D calculation (Snow et al. 2004).

Plant species determine g_{smax} values. For example, temperate grassland has field-measured g_{smax} of 0.008±0.004 m s^{-1} while temperate deciduous forest had g_{smax} at 0.0046±0.0017 m s^{-1} (Kelliher et al. 1995). Field measurements of g_{smax} and R_{50} for lucerne are rare and possibly unreliable due to the underlying assumptions that occur rarely in field conditions. Furthermore, porometers often require time to obtain accurate records, which results in fewer measured leaves, which makes it difficult to develop a full representation of an entire field. Thus, an optimisation procedure is often a cost-effective alternative approach to estimate these two parameters (Teixeira et al. 2018).

2.3.3.2 Soil surface evaporation

A two-stage process of E is widely acknowledged and applied in soil physics studies (Or et al. 2013) and agricultural system modelling (Foley & Fainges 2014). Ritchie (1972) suggested that solar energy controlled the first stage of E and soil hydraulic properties contributed to the second stage. The first stage occurs when the soil surface is wet, and water supply is not limiting, whereas the second stage commences once the cumulative evaporation reaches a threshold (Foley & Fainges 2014). Figure 2.10 shows a conceptual diagram of the two-stage process. During stage I, water continually evaporates until the drying front arrives at a threshold (termed as Stage I cumulative evaporation; U) depth around day 7. At Stage I, the evaporation rate is previously reported as linearly related to the potential evaporation rate (Eo; Lehmann et al. 2008; Ritter & Muñoz-Carpena 2013; Foley & Fainges 2014). Soil physical properties constrain the liquid flow for water evaporation from the drying front at an exponential decay rate (termed as Stage II evaporation rate; Cona) since stage II started.

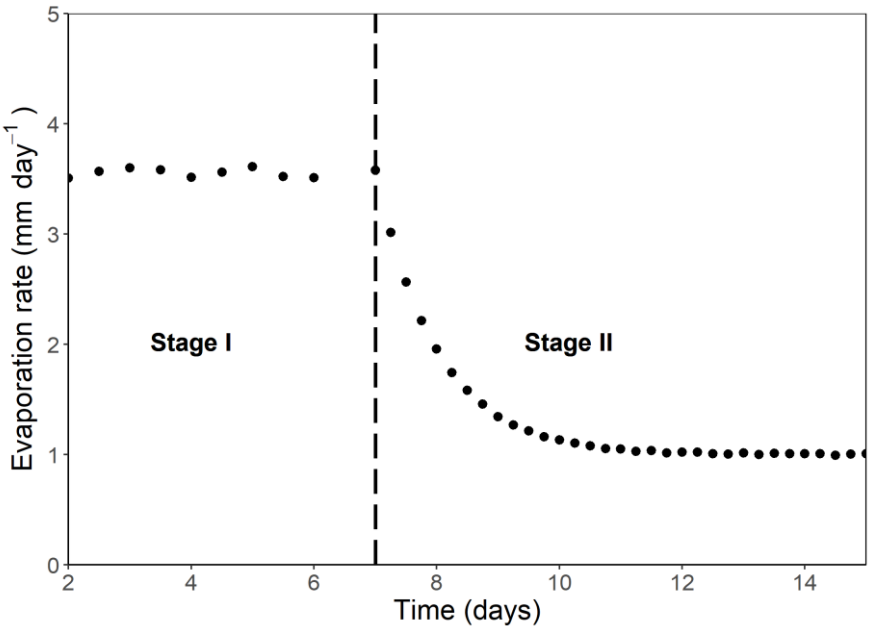

Figure 2.10 Conceptual diagram of two-stage evaporation. During the first stage, the drying rate is constant (potential drying rate =4 mm day^{-1}). Water evaporates from the surface and liquid flows from the drying front to the surface within micro pores that act as "straws". At the end of Stage 1, liquid connections break and the drying rate decreases (falling rate period). (Adapted from Lehmann et al. (2008))

Various U values have been found in different soil types (different hydraulic properties) and climates (Ritchie 1972; Yunusa & Sedgley 1994; Foley & Fainges 2014). Ritchie (1972) found that clay soil tended to have a greater U (12 mm) than sandy (6 mm) soil. Yunusa et al. (1994) investigated the relationship between U and Cona via weighing lysimeters with a fine texture soil in winter and summer in south-western Australia. They found that high U and low Cona values in summer overestimated E, and similar values of U (4.7 mm) and Cona (4.04 mm day$^{-1/2}$) could more accurately predict (lowest sums of squares of deviations) E in both seasons. Thus, they recommended low U values and high Cona values for dryland environments where seasonal evaporation fluctuates. Foley & Fainges (2014) reported a much lower U value of 2 mm and two distinct sets of Cona values for winter (3 ~ 3.7 mm day$^{-1/2}$) and summer (4.6 ~ 5.3 mm day$^{-1/2}$) in south-east Queensland, Australia. The low U values were likely due to low solar energy input because of frequent drizzly rainfall events and overcast conditions. In contrast, Jamieson et al. (1995) used a U of 9 mm and Cona 4.4 mm day$^{-1/2}$ to study evapotranspiration of barley in deep soil at Lincoln University.

APSIMX implemented the two-stage equation to quantify the soil surface evaporation (Section 3.5). U and Cona are hypothetical values that have not been directly measured in the past. By far, the most accurate approach to estimating U and Cona is using weighing lysimeters with rain-out shelters to derive them from the drying cycle (Foley & Fainges 2014). However, soil physical properties and climate significantly influence U and ConA. Consequently, APSIMX has two sets of U and Cona for winter and non-winter seasons. The complex interactions between the soil surface-atmosphere and extensive cost for lysimeter systems make optimisation exercise the most cost-effective approach to obtain U and Cona under dryland conditions (Objective 2).

2.4 Conclusions

Lucerne response to water stress can be defined as:

1. Water stress can change the morphology, and physiology of lucerne based on the severity of stress.
2. Components of lucerne stands will respond to water stress differently regarding growth. For example, canopy components such as leaf size are sensitive to water deficit followed by the stem, and then the root.
3. Water stress is likely to increase the root: shoot ratio of lucerne to reflect lower LAER and greater root system exploration of the soil.
4. Water stress will extend lucerne phyllochron and override the photoperiod effects, and therefore affect lucerne development. Consequently, flowering might be delayed or even fail as water stress intensifies. Or it may accelerate under mild stress due to warmer canopy temperatures.
5. Reductions in radiation use efficiency with water stress may be caused by both reduced light interception from rolled leaves and reduced CO_2 assimilation from stomatal closure.
6. The effects of water stress on lucerne can be quantified by the ratio of soil water supply and demand with corresponding responses of each yield-forming component.

7. Field measurements of SWC are reliable data sources to estimate DUL, LL, RFV, and kl to quantify soil water supply and lucerne water extraction patterns in different soil types.
8. Soil water demand can be partitioned into plant transpiration and soil surface evaporation. Both processes are physics-driven and regulated by either specific lucerne or soil hydraulic constants.

All of these processes need to be considered when developing a model to account for effects on lucerne growth and development at different levels of water stress.

3 MATERIALS AND METHODS

The aim of this chapter was to parameterise and validate the APSIMX model using previous data measured in the field. This chapter consists of eight sections, which lay out the data and methodological foundations to tackle the three objectives. This study is all in silico, using data previously published from two experiments. However, it was necessary to understand each experiment and the constraints concerning environmental conditions and management practices. Therefore, Sections 1-4 outline the datasets with their site specified information, such as climate and soil classification. The soils, weather and management details outlined all become inputs for model development. Sections 5-7 explain the fundamental structure of the APSIMX model and methods to parameterise the key submodules (e.g. soil and plant module) from historical datasets. Section 7 introduces the basis of biophysical model evaluation before Section 8 describes an overall workflow to achieve reproducibility.

3.1 Datasets and source

The study used two datasets. These were collected by Dr Richard Sim during his PhD study and are designated experiments ADM2 and I12. These were critical for model development. Full experimental design and management are reported in previous publications for New Zealand datasets (Table 3.1).

Table 3.1 Two datasets used in this study with essential information for model development. These two datasets were from Sim (2014) PhD experiments that were conducted in two contrasting soil types.

Abbreviations	Description
ADM2	Data obtained from M2 paddock in Ashley Dene research farm
I12	Data obtained from I12 paddock in Iverson research farm on campus

3.2 Meteorology

Rainfall and temperature data were recorded on-site for experiments at Ashley Dene. However, only rainfall was recorded on-site for experiments on the University campus (Iversen12). The other meteorological conditions, such as solar radiation and Penman's

transpiration demand (T_D), were downloaded from Broadfields Meteorological Station (agent number 17603; NIWA, National Institute of Water and Atmosphere Research, New Zealand), which is located 2 km north of the experimental site.

3.2.1 Rainfall

Mean Potential Penman evapotranspiration (T_D) exceeded mean seasonal rainfall in Canterbury over the last 20-year period (2000 to 2020). Seasonal rainfall ranged as low as 407 mm in 2014/2015 to 804 mm in 2012/2013 while seasonal T_D ranged from 741 to 996 mm. Ashley Dene and Iversen12 had different monthly rainfall patterns in 2011/12 (experiment season) although they are only 15 km apart (Figure 3.1). Ashley Dene received greater than 30 mm more rainfall during summer in 2011 but less autumn rain compared with Iversen12. Both sites had a wet summer and autumn when the majority of the rainfall occurred. However, total seasonal rainfall was 30 mm different (639 and 604 mm for Ashley Dene and Iversen12, respectively) for these two sites in the 2011/2012 season.

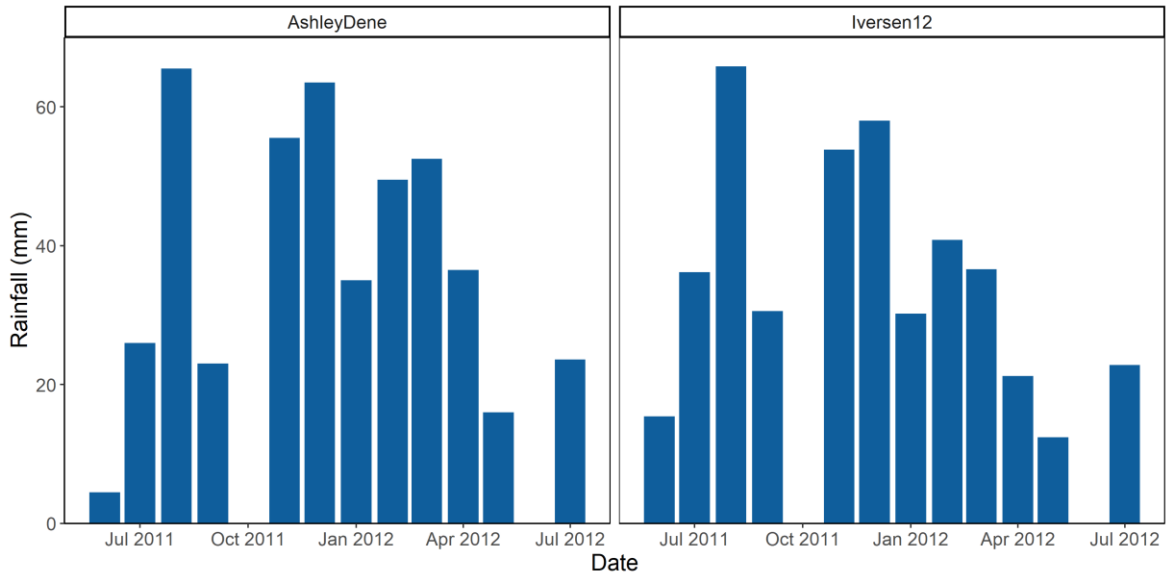

Figure 3.1 Monthly rainfall from 25th June 2011 to 12th July 2012 for Ashley Dene and Iversen12.

3.2.2 Temperature

The daily mean temperature ranged from -3.3 to 20 °C in season 2011/2012 (Figure 3.2). Given the cardinal temperature of lucerne shown in Figure 2.2 (a), the seasonal growing

degree days (GDD) for lucerne in Lincoln was 2650 °Cd from 1st July to 30th June in the next year.

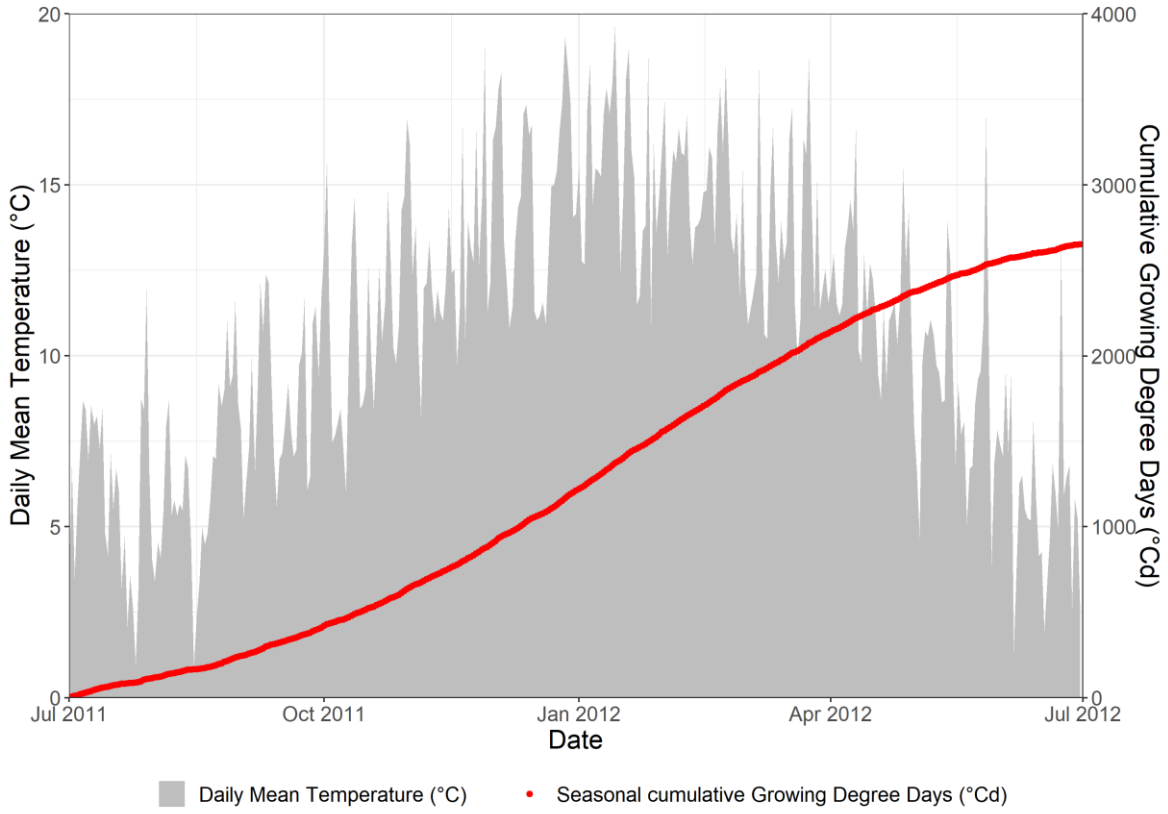

Figure 3.2 Average daily mean temperature and seasonal cumulative growing degree days (GDD) in Lincoln. The data were retrieved from Broadfields Meteorological Station (agent number 17603, NIWA, National Institute of Water and Atmosphere Research, New Zealand). The period was from 1st July 2011 to 1st July 2012. Growing degree days were calculated using the cardinal temperature (Figure 2.2 a) for lucerne grown in New Zealand.

3.2.3 Radiation

Figure 3.3 shows the long-term average global radiation incident in Lincoln. The daily radiation ranged from 0 to 34.6 MJ m^{-2}. The seasonal average cumulative radiation was 5179 MJ m^{-2}.

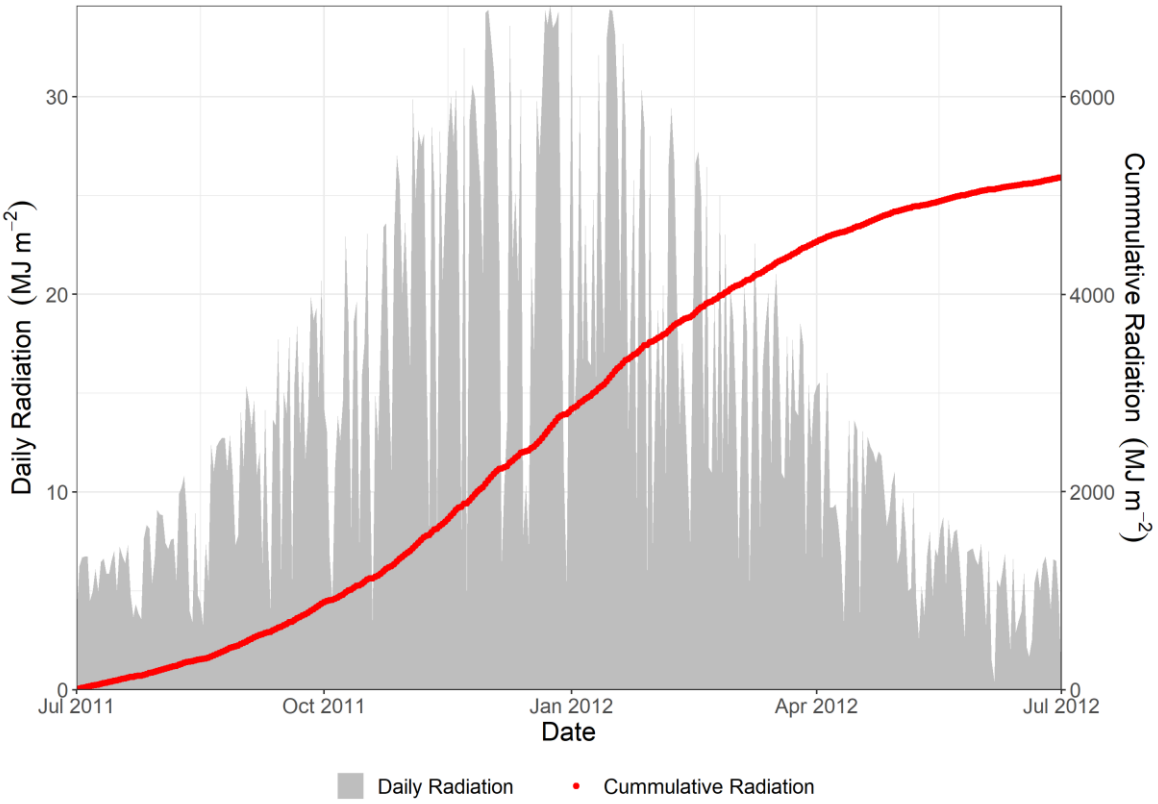

Figure 3.3 Daily global radiation and seasonal radiation accumulation in Lincoln. The data were retrieved from Broadfields Meteorological Station (agent number 17603; NIWA, National Institute of Water and Atmosphere Research, New Zealand). The period was from 1st July 2011 to 30th June 2012.

3.3 Soil description

3.3.1 Ashley dene

Ashley dene is a research farm located 15 km west of the Lincoln University campus (Lucas et al. 2012). The main soil type is a Lismore stony silt loam (*Udic Haplustept* loamy skeletal, USDA Soil Taxonomy) at the paddock M2B at the Ashley Dene farm, where the main dryland dataset (ADM2) was obtained (Lucas et al. 2012, Sim et al. 2017). Figure 3.4 shows the soil profile of a typical Lismore stony soil. This soil type has large gravel deposits because of glacial outwash alluvium. Consequently, the topsoil is generally shallow (15 ~ 20 cm) with a higher than 8% stone content in volume. The total bulk density ranges from 1.38 $\pm$ 0.038 g/cm^3 to 2.42 $\pm$ 0.017 g/cm^3 and depends on the location and depth (Graham et al. 2019). The subsoil has stone contents that range from 44 ± 5% up to 70 ± 2% and also contains a large proportion of sand (23 to 94 %). Therefore, the soil profile is free drained and low in water storage capacity (approximately 140 mm). However, dense gravel pans

occurred at about 1.5 m at the M2B paddock during the installation of neutron probe access tubes. These gravel pans can slow down soil water drainage and create logging issues (Sim 2014).

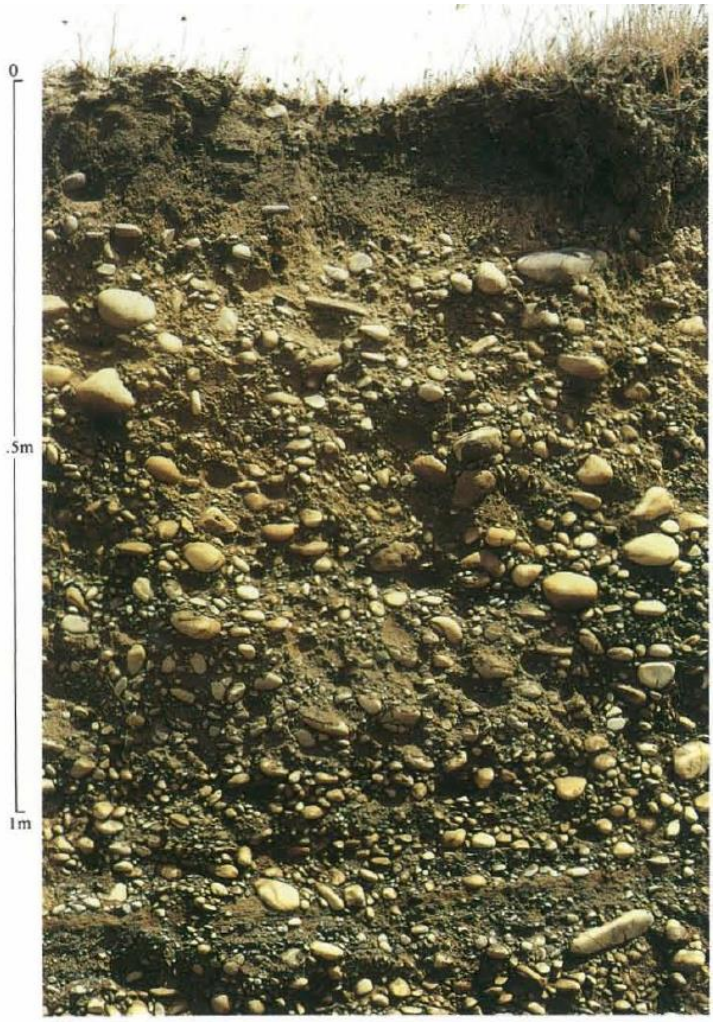

Figure 3.4 Soil profile of Lismore soils. Citied from Molloy (1998).

3.3.2 Iversen 12

Iversen field is a research farm located on the Lincoln University campus. The dataset, I12, was obtained from paddock 12. Paddock 12 is a Wakanui silt loam soil (*Udic Ustochrept*, USDA Soil Taxonomy), or Mottled Immature Pallic soil in New Zealand soil classification

(Hewitt 2010; Sim 2014). This soil type originated from the same parent material as the Lismore soil.

Figure 3.5 illustrates the soil profile in Iversen12. The horizon change often occurs around 30 cm for the topsoil. Silt to loamy sand underlies the fertile topsoil, which has a thickness from 2 to 3 m. This Wakanui soil has approximately 362 mm of PAWC.

Figure 3.5 Soil profile at Iversen 12. From Sim (2014)

These two soil types may represent the two extreme soil conditions in New Zealand. On one hand, the soil profile in Ashley Dene (Figure 3.4) shows the extremely low water holding capacity soils. On the other hand, Iversen12 soil might be the best one for growing crops in the country. Having these two soil types that cover each end of the

spectrum of soil water conditions would serve the principle of biophysical model development – the model is generic enough to cover the majority of conditions.

3.4 Experiment management

Two datasets completed by Sim (2014) were used in this study. Detailed information was documented in the PhD thesis. The follow sections presented brief and essential information.

3.4.1 Agronomic management

Appendix 1 documents the detailed cutting dates to inform model configuration. Fertiliser and agrichemicals were applied to experiments to avoid nutrient deficiency and pest stresses such as weeds. Detailed measurements for seedling and established crops were collected in ADM2 and I12. To differentiate sowing date treatment in two sites, experiments in Ashley Dene and Iversen12 are referred to as ADSD 1 to 10 and I12SD 1 to 10, respectively. Crops in both sites grew under rain-fed conditions.

3.4.2 Soil water measurement

Volumetric soil water content (SWC) was recorded at different depths by a combination of two soil moisture sensors: time domain reflectometers (TDR) and neutron probes for ADM2 and I12 (Table 3.2).

Table 3.2 Datasets have detailed measurements for soil water content.

Dataset	Depth	The thickness of each layer	Interval	Sensor
ADM2 and I12	2.3 m	0.2 m at the surface 0.1 m below 0.2 m	10 ~ 14 days	TDR Neutron probe

For the experiments at Lincoln University, the SWC was measured by TDR (Trace system, Soil Moisture Equipment, Santa Barbara, California, USA) in the top 0.2 m soil and neutron probe (Troxler Electronic Industries Inc, Research Triangle Park, North Carolina, USA) for the depth below 0.2 m. There were 54 and 55 measurement dates for ADM2 and I12 over the two seasons, respectively.

3.4.3 Plant measurements

Biomass was measured at regular intervals for ADM2 and I12. All biomass samples were dried in a forced-air oven to constant weight. I12 has root biomass data which were extracted from the top 0.3 m within a 0.2 m quadrat.

Table 3.3 Growth variables for two datasets used in the study. Lucerne was harvested regularly (7 to 17 days) for shoot biomass and leaf area measurements. The Sunscan sensor collected radiation interception data. Root biomass was collected at the end of the growth cycle in the Iversen12 experiment.

Dataset	Variable	Unit	Interval
ADM2	Shoot biomass	g/0.2 m^2	7 ~ 14 days
	Leaf area	cm^2	
	Radiation interception	percentage	NA
I12	Shoot biomass	g/0.2 m^2	7 ~ 14 days
	Leaf area	cm^2	
	Radiation interception	percentage	NA
	Root biomass	g/0.2 m^2	Growth cycle

Detailed canopy measurement data were available for ADM2 and I12. Destructive leaf area measurements were taken from 20 shoots sub-sampled in each biomass assessment. A leaf area meter (LI-COR 3100, Licor Inc. Lincoln, USA) was used to take the measurements. Also, a Sunscan canopy analyser (Delta-T Devices Ltd, Burwell, Cambridge, England) was used to measure the radiation interception (I/I_0). The Sunscan sensor requires a clear sky to provide accurate measurements, which provided 25 measurements in the second season for Ashley Dene and Iversen 12.

3.4.3.1 Phenological variables

Lucerne was continuously monitored for phenological development (Table 3.4). Development of lucerne was assessed by marking 5 -10 stems per plot during the seedling phase and 5 plants in the regrowth stages at ADM2 and I12.

Table 3.4 Measurement for phenological variables.

Dataset	Variable	Interval
ADM2 and I12	Leaf appearance	3 ~ 7 days
	Visible buds	
	Number of stems	7 ~ 10 days

3.4.4 Defoliation

Defoliation strategies differed in the different experiments due to the purpose of experiments, seasons and abiotic conditions. Phenological stages and height were the two main criteria to determine the defoliation times. For example, seedling lucerne was defoliated when the plant population was at the onset of the reproductive phase (Sim et al. 2015). Defoliation based on the lucerne height of regrowth crops is common for farmers and researchers (Sim 2014). Abiotic factors, such as water stress, may trigger defoliation early because the crop failed to reach pre-determined criteria. Two primary methods were used across experiments: grazing and mechanical defoliation (e.g. lawnmower or crop harvester). Details of the defoliation events are given in Sections 3.4.4.2 and 3.4.4.4.

3.4.4.1 Ashley Dene

The defoliation plan in Ashley dene was influenced by phenology, summer water stress, and the lucerne seasonality. The first defoliation occurred when 50% of the 10 marked lucerne plants had an open flower. The growth period from sowing to this first defoliation is termed the seedling stage (Sim 2014). Subsequent rotations are defined as "regrowth" crops and these were defoliated either when 50% of the marked plants reached the bud visible stage or the plant height reached 35 to 40 cm but before flowering (spring only). The onset of summer dry conditions also triggered defoliation regardless of the plant phenological stages or height.

Lucerne shoot material was mown to a residual 5 cm height by a lawnmower until 27 September 2011. Sheep grazing was introduced after this. There were 100±20 ewes that grazed the experimental area for a period of 7 to 10 days. The stock was removed when stem height was reduced to approximately 50 mm to avoid overgrazing. Post grazing topping was carried out mechanically to ensure no residual leaves were left which would affect measurements in subsequent regrowth cycles. In the establishment season (2010/11), the number of defoliations was 1 to 3 times depending on sowing dates, and five times in the second season (2011/12). In both seasons, an early winter (June) grazing was used to complete the season.

3.4.4.2 Iversen12

The defoliation plan in Iversen 12 was influenced by phenology and the lucerne seasonality. The seeding crop in Iversen12 was defoliated similarly to that at Ashley Dene. The first cut occurred when 50% of the marked plants had open flowers, and regrowth crops were cut when 50% of the marked plants reached bud visible stage or at a height of 35 to 40 cm (spring only). A lawnmower was used to remove the biomass during the experiment except for the final winter grazing. Regardless of treatments, 120 ewes grazed the experimental area for 7 to 10 days in early winter in both seasons. The number of defoliation events was 1 to 4 in the first season, based on the sowing date, and seven times in the second season.

These management factors all need to be captured as inputs for model development.

3.5 Model description

The Agricultural production systems simulator (APSIM) is a framework that consists of more than 80 plant and soil models (Holzworth et al., 2018). The latest version of APSIM is called APSIM next generation (APSIMX), which refines the APSIM classic infrastructure. A modulated design of APSIM allows users to simulate a wide range of scenarios from advising farm practises to climate change studies via assembling desired models (Keating et al. 2003; Holzworth et al. 2018). These models can be grouped into four main modules to represent the biophysical mechanism of agricultural systems. Four modules are plant, soil, manager and climate. The plant module contains crop models that capture the physiological process of crops. The soil module simulates the water and nitrogen movements dynamically. The manager module mimics management practices such as fertiliser application and harvest. The climate module takes care of input climate data and estimates transpiration demand (Snow et al. 2004). All modules operate on daily time steps and are driven by an engine that controls the modules' information flows (Keating et al., 2003).

3.5.1 Soil module

A typical soil module in APSIMX has seven nodes representing soil chemical and physical properties in a given location (Figure 3.6). The module inherits its primary structure (water redistribution) from CERES-maize models (Brown 1987). Adoptions from PERFECT are incorporated into the module to improve the module flexibility in scenarios such as simulating potential soil evaporation when crop residuals cover the ground and/or small

rainfall events occur (APSIMInitiative ; Littleboy et al. 1992). Soil physical properties that are relevant to water movement were studied in this project. These properties are in nodes: Physical, SoilWater and Initial water. These node names are changeable and therefore may differ depending on the APSIMX version.

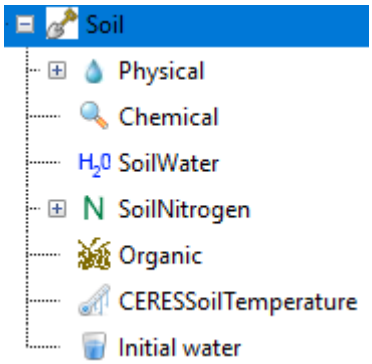

Figure 3.6 A snapshot of APSIMX soil module (version 2020-10-09 5723). The soil module normally contains seven sub-modules to mimic soil physical and chemical properties.

In the Physical node, there are 15 properties users can modify. The essential ones are 'Depth (cm)', 'BD(g/cc)' (Bulk density), 'Crop.LL' (Crop Lower limit), 'DUL' (Drained upper limit) and 'KL' (water extraction rate). These five properties describe the important soil components, to define the amount of water in the soil and the rate of water uptake by plants in each layer. Other properties, such as 'AirDry' (Air-dried soil water content), 'LL15' (Lab measured 1.5 MPa lower limit), 'SAT' (Saturation) and 'XF' (root exploration factor), are necessary components to run a simulation. However, 'AirDry' and 'LL15' can be identical to the 'Crop.LL'. The 'SAT' can be the same as 'DUL'. The 'XF' often has a default value of 1, which indicates that there is no physical restriction on root growth, while a value of 0 means the soil layer is impenetrable by plant roots. The rest of the six properties are optional, but it follows that the more information users provide, the more realistic the soil description for providing water and nutrients.

In the soil water node, soil water balances are controlled by 19 soil physical properties. The default settings are generally applicable for annual plants except that users must modify the 'Depth (cm)', 'Thickness (mm)', and the associated 'SWCON (/d)' values to match the soil layer settings in the soil physical node. Users can determine the 'Depth (cm)' and 'Thickness (mm)' based on the soil water measurement design. The 'SWCON (/d)' is an

estimated value that describes the rate that water drains down to the next layer when the soil water content in a particular layer is greater than DUL but lower than saturation limits (APSIMInitiative). Two other properties, surface evapotranspiration and unsaturated flow might be necessary to consider for this study because defoliation of lucerne exposes soil surfaces. Incomplete ground cover affects water balance calculations and the soil water content in the top layers. Unsaturated flow can occur in both directions (surface and downwards) between two adjacent layers. The soil water model allows users to modify the two parameters 'U' and 'CONA' (Section 2.3.3.2) that define water losses through evaporation and define a diffusivity that describes the rate of water diffusing from one layer to another (APSIMInitiative).

The effects of incomplete canopy cover on surface soil water content can be challenging to parameterise. Therefore, a separate APSIM-Slurp model was used which takes measured canopy covers as input to estimate the critical parameters in the soil module. Section 3.5.4 introduces the Slurp model. Detailed soil module parameterisation was described in Section 2.3.1

User-specified soil water content is the most appropriate method for the dataset with detailed soil water measurements for each layer. Thus, it was used here when datasets have layered soil water measurements. However, initial soil water as a percentage of PAWC is another primary approach used when only soil water profile data are available, and users must decide that the water is either evenly distributed in each layer or filling from top to bottom layers.

3.5.2 Plant module

The Plant module consists of 23 regrowth and 23 developing crop models in APSIMX. Users are advised to select an existing crop model that is most relevant to their requirements and modify the model within the plant modelling framework (PMF) to achieve specific purposes (Brown et al. 2014). The PMF provides a generic plant model template by abstracting plants into three main classes with three sub-classes (Figure 3.7). The three main classes include Plant, Mid-level and Function classes. The plant class is a high-level class that oversees all the other classes and communicates information with soil and climate modules. The Mid-

level classes govern plant growth and development via organ classes (Leaf, Root and others.), process classes (Phenology, Structure and Arbitrator), and sub-classes (Phase class, Cohort class (not shown) and Biomass class). Function classes provide the fundamental mathematical functions to calculate the values for Mid-level classes.

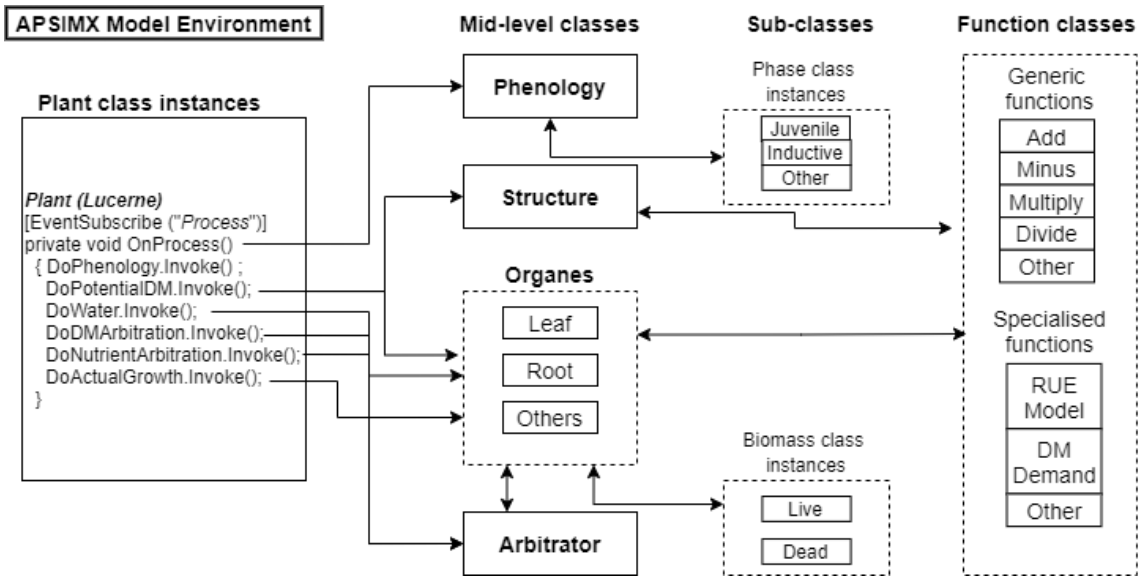

Figure 3.7 Schematic of the plant modelling framework. Redrawn from Brown et al., 2014.

Currently, there is one modified existing APSIMX-Lucerne model which has been developed under non-limiting environmental conditions (Yang et al. 2019). This study aims to extend the model performance under dryland conditions. The detailed lucerne model description was presented in Section 3.5.4. In this study, it was necessary to modify the lucerne module mainly in the 'Leaf' organ class. The effects of water stress on lucerne growth and development can be presented by inserting a 'Multiply' low-level function to a different organ or process class. Therefore, two multipliers consist of 1) rates of growth and/or development without water stress and 2) an array of values that represent water stress responses at different severities.

3.5.3 Manager module

The manager module can mimic real farm management by customising templates in C# or VB.NET scripts (Moore et al. 2014; Brown et al. 2018; Holzworth et al. 2018). This module allows the user to "copy" the management plans from the brain of a human manager, and

establish a virtual plan computed by computers. The general idea or assumption to implement such a concept is that human management is a combination of discrete actions, such as sowing and irrigation. Therefore, each discrete action can be represented in a script, and form the basic rule as management building blocks. When setting up a simulation for experiments, users can source these building blocks in APSIMX and organise them in a sequential order based on the actual management. The management events described in Section 3.4 were inputs to this module.

Figure 3.8 shows the currently available rule templates in custom-built APSIMX version 5723. The management toolbox contains 17 standard management practices, such as sowing the crop and irrigation application. Users can copy any of these templates and paste them into a specific experiment, and construct a management plan in the APSIMX file. To customise a rule template, users can modify values in the interface on the right side window (Figure 3.8 the management "building blocks" in APSIMX. The snapshot was taken on version 2020-10-09 5723.), which will change the irrigation strategies immediately. However, fixed management rules may be inadequate for complex pasture management, primarily when harvesting is assessed by phenological signals or height (Moot et al. 2003; Moot et al. 2016). In this case, users will have to write or modify scripts in C# or VB.NET to define a management plan that can realistically represent the actual management practices (Holzworth et al. 2018). The programming implementation of management practices does create extra burden to users, although the user-defined management rules will be compiled and validated immediately via the .NET framework, and users are warned if there are any incorrect codes. Therefore, existing rule templates were used where possible in this study. Customised manager scripts would be addressed for a unique experiment (Section 4.2.4).

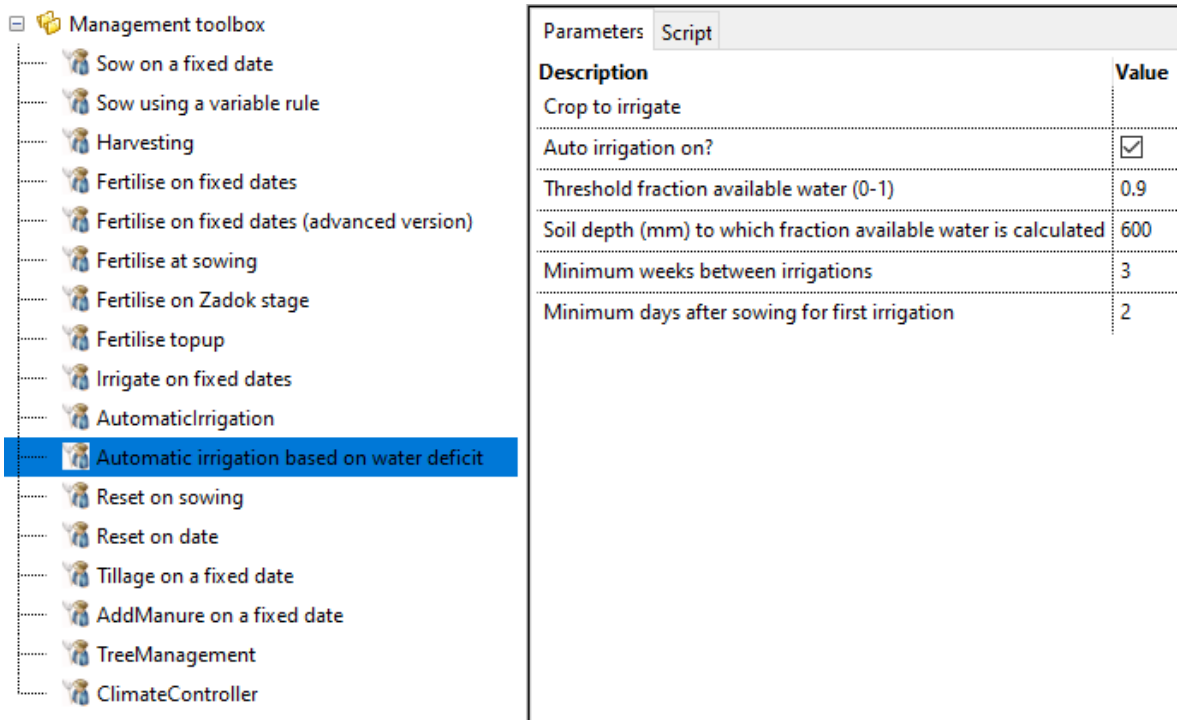

Figure 3.8 the management "building blocks" in APSIMX. The snapshot was taken on version 2020-10-09 5723.

3.5.4 APSIMX-Lucerne model

The APSIM-Legume model was developed in Australia to represent the growth and development of four legume species, including lucerne (Robertson et al., 2002). The generic model is for the underlying physiological process of regrowth lucerne grown under warm and irrigated conditions. (Moot et al. 2001) calibrated the legume model using New Zealand lucerne data to parameterise the model in a temperate environment. The model was further improved by using root biomass data to represent lucerne seasonality, especially the dry matter partitioning between above- and below-ground growth (Moot et al. 2015).

The APSIM next generation (APSIMX) was realised in October 2014, which refined APSIM classic's infrastructure (Holzworth et al., 2018). The lucerne model in APSIMX has been refurbished by adapting the PMF framework (Brown et al., 2014), and developed to a new phase by incorporating genotype responses to the temperate environment (Yang et al., 2019). The lucerne model in APSIMX is well developed to represent non-limited conditions. It is ready to be parameterised for limited conditions such as water stress in dryland environments.

Figure 3.9 illustrates a possible abstract of the lucerne model under dryland conditions. Temperature and solar radiation drive lucerne phenology that is also influenced by photoperiod and management practices such as harvest and sowing. Lucerne water demand is regulated by temperature, radiation and wind speed. Precipitation and soil conditions define the four critical soil parameters being the drained upper limit (DUL), lower limit (LL), initial soil water content ($SW_{initial}$) and root exploration factor (XF). The ratios of water demand and supply (FW) influence the essential growth parameters, including leaf area expansion rate (LAER), extinction coefficient (k) and radiation use efficiency (RUE). APSIMX-Lucerne uses a simple leaf model to represent the entire canopy development. Therefore, node appearance and branching are considered within the canopy, which means parameterisation is optional for these two parameters. However, canopy height might be required to mimic the canopy structure because water stress is likely to decrease stem extension (Luo et al. 2020). The leaf model produces a bulk of dry matter allocated to different organs based on the arbitrator settings with the regulation of photoperiod changes. For instance, the root organ will gain more dry matter when the photoperiod decreases (Teixeira et al. 2008). The leaf and root organs interact with each other daily. More specifically, the water-stressed canopy would provide below potential DM, causing submaximal root growth which will further reduce the plant capability to access water. Consequently, lucerne crops might experience consistent water stress in dryland conditions.

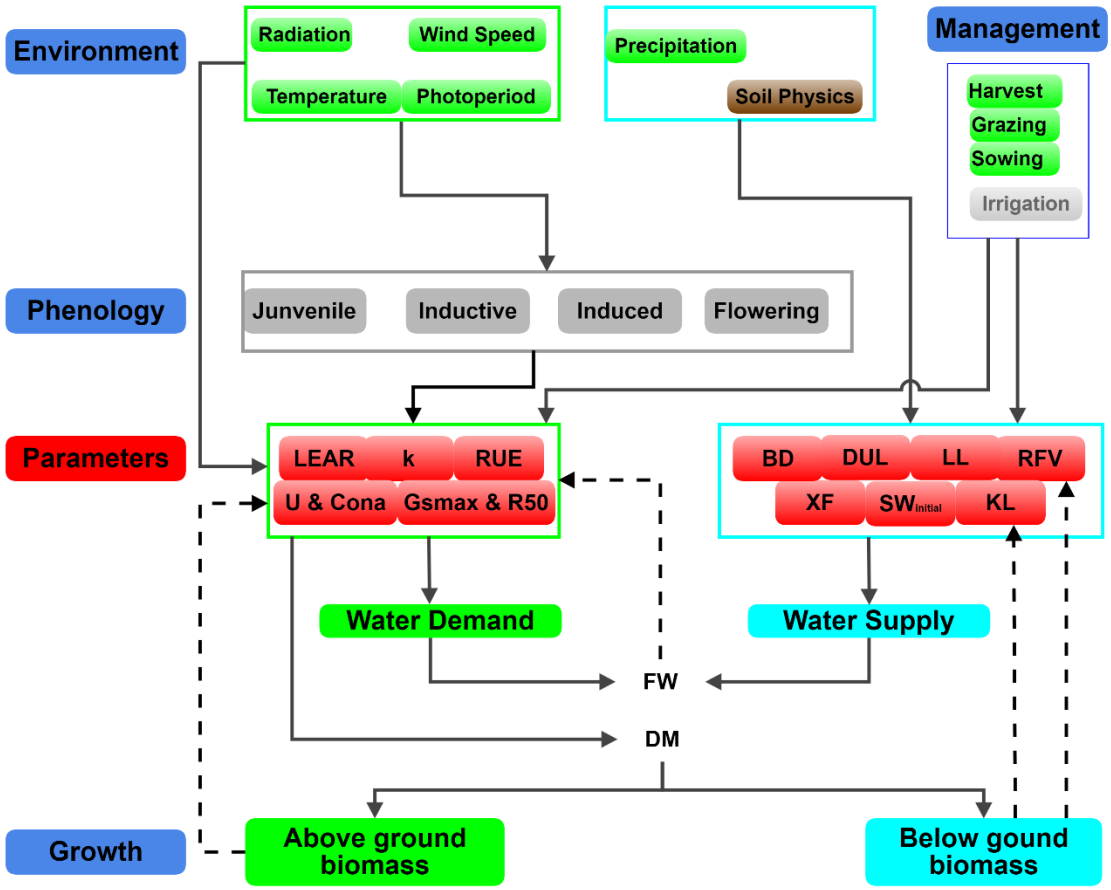

Figure 3.9 Schematic abstract of APSIMX-lucerne model under dryland conditions with essential parameters. Solid and dash lines represent deterministic and feedback effects respectively.

It is difficult to quantify both plant and soil parameters in the full lucerne model under dryland conditions. Due to the dynamic interaction between above- and below-ground organs in the lucerne model, the ratio of water demand and supply is dynamic (FW in Figure 3.9). Under non-water limited conditions, the water demand is purely driven by physical conditions such as radiation, temperature and wind speed, and the demand is always satisfied. The dynamic relationship has the supply as a constant component. Therefore, model developers can solely focus on demand-related parameters that can provide the best goodness of fit values between simulations and observations.

In contrast, soil water-related parameters must be considered under water-limited conditions. This is because supply cannot always meet demand, and soil water parameters

differ in different soils. Both demand and supply differ under water-limited conditions and both sides respond to the changes of the other. For example, a stressed canopy will close its stomata, resulting in less water demand and different water extraction patterns than an un-stressed canopy. APSIMX-Slurp model was used to tackle this challenge.

3.5.5 APSIMX-Slurp model

APSIMX-Slurp is a simplified crop model developed to research water and nitrogen balances in a given agricultural system (Teixeira et al. 2018). It expects daily leaf area and climate data as input to constrain the canopy development, and instruct the climate module to account for surface evaporation from partial coverage of the soil surface. Therefore, researchers can focus on exploring the water and nitrogen uptake via the root system. Consequently, APSIMX-Slurp has only two components, leaf and root. The leaf component controls water demand and light interception by communicating with the climate module. The root component controls the rooting depth and water uptake.

Table 3.5 lists the parameters in the APSIMX-Slurp model. In the leaf organ, the fractional light interception (R_i/R_o) is essential for the model to simulate water and nitrogen uptake. Users can provide daily R_i/R_o values as input with modifications in the manager-script. However, the default settings require a daily leaf area index (LAI) and a constant extinction coefficient (*k*) of a crop. These two values can calculate R_i/R_o as in Equation 10.

Equation 10 $$R_i/R_o = 1 - \exp(-k \times LAI)$$

Table 3.5 Parameters in APSIM-Slurp. Leaf and root organs have six and three parameters, respectively. These parameters define the mechanism of lucerne canopy architecture (Height, leaf area index, extinction coefficient), light interception (R_i/R_o, nitrogen content), transpiration (g_{smax} and R50). Root parameters control the root growth rate, water extraction rate and rooting depth.

Leaf	Root
1. Height (cm) 2. Leaf area index (LAI, m^2 leaf/m^2 soil) 3. Extinction coefficient (*k*, percentage) 4. Fractional light interception (R_i/R_o, percentage) 5. Nitrogen content	1. Root front velocity (cm/d) 2. Extraction depth (cm) 3. Water extraction rate modifier ($kl_{modifier}$, percentage)

6. Parameters quantify the canopy response to shortwave radiation
    a. g_{smax}
    b. R50

Daily LAI measurements are rarely reported in previous studies. However, daily LAI can be interpolated linearly as a function of cumulative thermal time between actual measurements (Teixeira et al. 2018). A customised R function, 'interp_LAI', was used to automate the interpolation process in this study. Lucerne has *k* values that range from 0.64 to 0.94 in different water conditions (Teixeira et al. 2007; Sim et al. 2017). Users can supply a constant *k* value in the APSIMX users interface when the *k* is consistent throughout the experiment. In contrast, a series of daily *k* values as input data is achievable by customising the manager scripts in the Slurp model. In this study, the manager-script was modified to accept inconsistent *k* values based on Sim et al., (2017).

3.6 Model parameterisation

In the APSIMX soil module (Section 3.5.1), a minimum of six essential parameters is necessary to configure a soil to represent soil water supply (Section 2.3.1). These are BD, DUL, KL, LL, RFV and $SW_{initial}$. Parameter BD values were inherited from the previous model. Section 3.5.1, 3.5.4 and 3.5.5 discussed the other five parameters and their interactions with other modules. Conventionally, all five parameters are derived from observed data via Equations 4 to 8. In this study, a conventional approach will be used in Chapter 4. The optimisation approach will also be explored using programme language with state-of-art data science tools in Chapter 4.5.

3.6.1 Streamlining the analysis pipeline

An R package was developed to ensure the reproducibility of calculating DUL and LL (https://github.com/frank0434/autoapsimx). Function '*doDUL_LL'* takes two arguments: mean soil water content in each layer (SW_mean in Figure 3.10) and column names for each layer (value_vars in Figure 3.10). The water node is a tabular dataset that has soil water content for each treatment in each layer over all replicates.

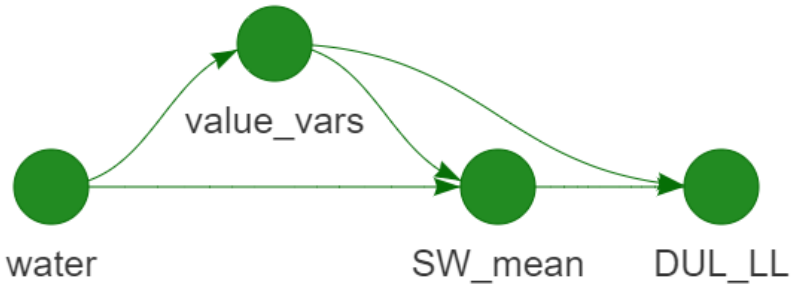

Figure 3.10 Dependency graph of the drained upper limit (DUL) and lower limit (LL) calculations. Labels of nodes represent arbitrary names given to data objects. For example, the node labelled water was the soil moisture measurements data.

3.6.2 Optimisation with APSIMX-Slurp

The APSIMX-Slurp model takes evaporation into account when the soil surface is partially covered (Section 3.5.5 for a more detailed description of the model itself). This feature is useful for pasture systems, which are subject to regular defoliation. The APSIMX-Slurp model assumes a constant hypothetical KL value across the soil profile in the soil module. However, the plant root length density is assumed to decay exponentially from the top to the bottom of the soils. Therefore, a modifier λ_{kl} of KL is used to represent the exponential decay trend (Equation 11).

Equation 11

$$kl_z = \begin{cases} kl_0, & z \leq z_0 \\ kl_0 \times e^{-\lambda_{kl} \times (z - z_0)}, & z > z_0 \end{cases}$$

where kl_z is a kl value for any given soil layer z, kl_0 is the soil surface kl at sowing depth z_0, and λ_{kl} is the decay rate of kl_0 (Teixeira et al. 2018).

APSIMX-Slurp offers a holistic approach to estimate RFV values along with surface KL (kl_0) and kl modifier (λ_{kl}) (Teixeira et al. 2018). Users can define a range of values (extracted from literature or expert advice) for these three parameters. Simulation result analyses can help users select a combination of these values that provide the best goodness of fit statistics (Section 3.7.2). The Slurp approach can be time-consuming if users run a single APSIMX file, including many values for testing. For instance, a proper value coverage with

9 RFV, 20 kl_0 and six λ_{kl} values will create 1080 simulations for one treatment. Therefore, a parallel computing approach will be adapted to reduce the simulation runtime.

3.6.3 Coupled data science tools

Both parameterisation approaches involve multiple ad-hoc processes to estimate parameter values. Thinking logic could be lost or lacking reproducibility in these manual exercises. The R package 'target' is a pipeline toolkit that can orchestrate codes, files, various data sources, and more importantly, document the thinking logic (Landau 2021). This study will utilise three main features of the 'target' package (version 0.3.1) including function-orient programming, caching and parallel computing. The function-orient programming provided an apparent pathway for R package development (Section **Error! Reference source not found.**). The caching feature allows users to do quality checking and only update objects that have modified dependencies. Lastly, the parallel computation feature reduced the computing time considerably (Section 5.3.3). Moreover, the script-based workflow contributes to efficient version control and increases reproducibility.

The application of the workflow concept was to ensure the reproducibility of data integration and analysis, as well as the APSIMX model configuration and simulation result analyses (Objective 3). At the beginning of the study, a conceptual workflow was drafted as in Figure 3.11. Conventionally, one would obtain APSIMX parameter values from field data by using linear regression analyses (Section **Error! Reference source not found.**). These values are then used to configure APSIMX files. Model evaluations would be carried out to examine the appropriations of the model structure and parameters. The application of a calibrated APSIMX model can generate new research directions and invaluable experiments to fill areas that currently lack understanding, for example by (Teixeira et al. 2021).

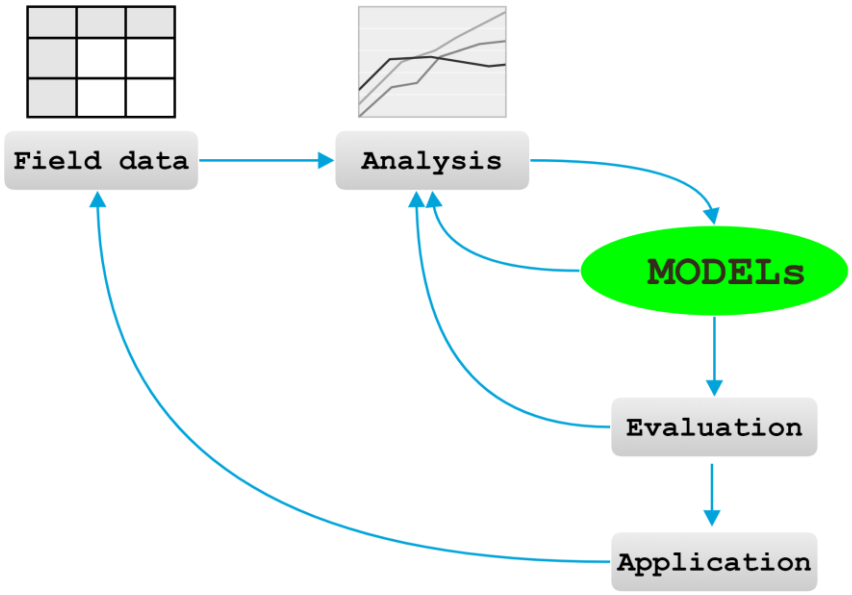

Figure 3.11 A conceptual plan of APSIMX model development.

This study's workflow was managed by a version control software Git (Chacon & Straub 2014) and the R package 'targets'. More specifically, there were two levels of workflow. The first level controls the thesis structure and the second level manages specific tasks to achieve objectives. The branching feature in Git governed the first level workflow. Three branches were set up to contain information for Chapters 1 to 3, 4 and 5, respectively.

3.7 Model evaluation

Model evaluation can be grouped into two steps. The first step focuses on the model structure's sensibility check to evaluate if it provides sensible simulation results for an agricultural system. Mass balances are the critical evaluation mechanism in biophysical models in an agricultural system. The system has climate inputs, such as rainfall and radiation, and management inputs, such as irrigation. Outputs from the system could be profitable materials, such as plants or animals, and environmental impacts, such as leached nitrate. In most cases, the output should be equal to the input within a system. Otherwise, a model structure may be incomplete if, for example, soil water profile results are more significant than the water input. In APSIMX, water, biomass and nitrogen mass balances are three critical balances used to evaluate whether a simulation is valid or requires improvement. Nitrogen balance is out of the scope of this study so water and biomass balances were used (Section 3.7.1).

The second step of model evaluation concentrates on the model performance by regressing predictions against observations (Brown et al., 2018). This step examines the model usefulness and provides a critical path to re-calibrate the model in different environments. Regression statistics can be drawn from the aggregated results to assess the agreement between predicted and observed values. This study used Nash-Sutcliffe efficiency (NSE) and normalised Root mean square error (nRMSE), described in Section 3.7.2.

3.7.1 Balances in water and biomass

The water balance in APSIMX follows Equation 12

Equation 12 $$InputWater = OutputWater + StoredWater$$

where InputWater is from climate or/and irrigation input, OutputWater includes evapotranspiration, drainage, run-off, ponding and lateral flow; StoredWater is the water held by the soil, which can be measured as soil water content. The complexity of the water balance equation depends on the system users attempt to simulate. It consists of all the elements listed above with further unrevealed factors in a high rainfall hill country

environment. However, this study is concerned with a flat dryland environment so Equation 12 can be defined by Equation 13.

Equation 13 $$P = ET + D + SWC$$

where P is precipitation, ET is evapotranspiration, D is drainage, and SWC is soil water content. The equation is evaluated at daily timestamps

The biomass balance shares a similarity with the water balance in APSIMX about evaluating the concept with one exception. Plant biomass has no state property like SWC in the water balance. Table 3.6 shows the primary input and output of the biomass balance. Phenology validation is a relatively straightforward approach to check the plant model structure since it is driven by temperature and modified by photoperiod. The overall biomass requires five elementary inputs, making the checking a challenge when users have limited knowledge of specific crops. Therefore, this approach often requires expert assistance.

Table 3.6 Abstract of biomass balance in APSIMX. Variables were assessed at daily timestamps.

Input	Output
Temperature	Phenology
Radiation	Biomass
Carbon dioxide	
Water	
Nutrient (Mainly N)	
Temperature	

Users can choose their preferred approach to evaluate the mass balances, either via the APSIMX UI or third party software. Visualisation is a critical tool for both approaches. In this study, visualisation of water and biomass balances occurred in R (R core team 2013) and experts asked to validate the model structures.

3.7.2 Statistics

Statistical analyses of simulation results against observations are necessary to assess any models performance. This is because the statistics can quantify model performance in a

reproducible way and objectively (Bellocchi et al. 2010). Coefficient of determination (R^2; Equation 14), Normalised root mean square error (nRMSE; Equation 15) and Nash-Sutcliffe Efficiency (NSE; Equation 16) were applied to evaluate the model performance (Ritter & Muñoz-Carpena 2013; Moot et al. 2015).

Equation 14 $$R^2 = 1 - \frac{RSS}{TSS}$$

where RSS is the sum of squares of residuals and TSS is the total sum of squares.

Equation 15 $$nRMSE = \frac{\sqrt{\frac{1}{n}\sum_{i=1}^{n}(m_i - s_i)^2}}{\overline{m}}$$

where n represents the number of observed data for a variable, m and s are the measured, and simulated values for the ith observed data, respectively, and $\overline{m}$ is the averaged measurements. In theory, nRMSE ranges from 0 to positive infinite. If the predicted values match the observations perfectly nRMSE is equal to 0. Jamieson et al. (1991) categorised the model performance into four categories based on the nRMSE values (Table 3.7).

Equation 16 $$NSE = 1 - \left[\frac{\sum_{i=1}^{n}(m_i - s_i)^2}{\sum_{i=1}^{n}(m_i - \overline{m})^2}\right]$$

where n is the number of measurements, m and s have the same representation in Equation 13 and $\overline{m}$ is the mean of measurements. NSE ranges from negative infinity to 1. The best fit is achieved when NSE = 1. In contrast, a negative NSE value indicates that the model performance is poorer than using the mean of measured values to make predictions. It is acceptable if NSE varies between 0.65 and 1 in hydrology studies (Ritter & Muñoz-Carpena 2013). However, NSE values between 0.5 and 1 have been used as satisfying model performance in the watershed (Moriasi et al. 2007) and lucerne simulations (Table 3.7; He et al. 2017; He et al. 2019, Yang 2020).

Table 3.7 Model performance-rating table refers to Jamieson et al. (1991). Two statistical metrics, normalised root mean square error (nRMSE) and Nash-Sutcliffe efficiency (NSE), are the main tools to evaluate the APSIMX models performance. Four categories of model performance were presented from previous research in non-APSIMX wheat and lucerne model evaluation for $nRMSE$ and NSE, respectively.

Statistical metric name	**Ratings**
Coefficient of determination (R^2)	Excellent: $R^2 = 1$; Good: $0.5 <= R^2 < 1$; Poor: $0 < R^2 < 0.5$
Normalised root mean square error (nRMSE)	Excellent: $nRMSE$ < 10%; Good:10%< $nRMSE$ < 20%; Fair: 20%< $nRMSE$ < 30%; Poor: $nRMSE$ > 30%
Nash-Sutcliffe Efficiency (NSE)	Excellent: NSE = 1.0; Good: 0.50 <= NSE < 1.0; Fair: 0.0 <= NSE < 0.50; Poor: NSE < 0.0

R (R Core Team 2019; version 4.0.2) is the software used to perform the statistical analyses and visualisation.

4 CONVENTIONAL APPROACH TO PARAMETERISE WATER STRESS EFFECTS

4.1 Introduction

The current APSIMX lucerne model performed well under well-watered conditions in New Zealand (Yang et al. 2021). However, it has yet to be tested in water-stressed conditions. Water stress effects can be implemented by re-configuring the soil, plant and management modules. This chapter describes the process of module reconfiguration to allow APSIMX lucerne to simulate lucerne growth and development under dryland conditions. Simulation results are compared with field data to evaluate model performance. Parameter values for the reconfiguration are derived directly from observation data. Empirical or conventional values will be used when data are unavailable to estimate particular parameters. Therefore, this chapter addresses Objective 1.

The results of this chapter are used to demonstrate the conventional method used for model parameterisation, by using existing papers to reproduce results from previous dryland experiments in APSIMX. Poor performance in particular variables is expected because to date the model has only been parameterised for lucerne growing in non-limiting conditions. A list of parameters can be outlined for optimisation or parameterisation after examining the main variables, such as soil water content, LAI and biomass.

4.2 Materials and methods

4.2.1 Experiment sites

Soil water and biomass data from ADM2 and I12 were used to characterise soils from these two sites over 10 sowing dates. Datasets were sourced from Sim (2014). Sections 3.1 to 3.4 described details of these two datasets and experiments. In brief, the two sites are 15 km apart. ADM2 is a very stony soil with low PAWC (131 mm over 2.3 m) while I12 is a stony free draining soil with high PAWC (362 mm over 2.3 m). Both sites had 10 sowing dates as treatments to ascertain model performance in the extremes of soil available water holding capacity. Soil water content measurements were taken using a neutron probe at an interval of 7 to 14 days dependent on the weather conditions. Biomass and phenology assessments were made according to lucerne growth phase, height and season. For example, the first

biomass harvest occurred at the time when 50% of marked plants had an open flower. The period between sowing and 50% flowering was identified as the seedling phase, after which crops were called regrowth crops.

4.2.2 Soil module

This study focuses on soil physical property effects on water content changes. Therefore, only water-related parameters (Table 4.1) are within scope. Section 3.5.1 described the parameter effects and location for these parameters.

Table 4.1 Essential parameters in APSIMX soil module. Parameters are defined by layer basis except for soil surface evaporation parameters (U and Cona). Values labelled `Layered` are presented in Table 4.2**Error! Reference source not found.**

Parameters	Unit	Value	Description
AirDry	mm mm^{-3}	Layered	Volumetric water content in each layer when soils are complete air dried
BD	g cm^{-3}	Layered	Bulk density
Depth	cm	Layered	The thickness of each soil layer
DUL	mm mm^{-3}	Layered	Drained Upper Limit
LL15	mm mm^{-3}	Layered	Lower Limit at 15 Bar
Lucerne LL (CLL)	mm mm^{-3}	Layered	Lucerne Lower Limit
Lucerne KL	fraction d^{-1}	Layered	Lucerne water extraction rate
Lucerne XF	fraction	1	Lucerne root exploration factor
SAT	mm mm^{-3}	Layered	
Summer ConA	mm $day^{-1/2}$	4.4	Drying coefficient for stage 2 soil water evaporation in summer
Summer U	mm	9	Cumulative soil water evaporation to reach the end of stage 1 soil water evaporation in summer
SW	mm mm^{-3}	Layered	Initial Soil Water Content
SWCON	fraction d^{-1}	0.99	Fraction of water drains to next layer each day when soil water is above the DUL for the layer
Thickness	mm	Layered	The thickness of the soil layer
Winter ConA	mm $day^{-1/2}$	2.5	Drying coefficient for stage 2 soil water evaporation in winter
Winter U	mm	5	Cumulative soil water evaporation to reach the end of stage 1 soil water evaporation in winter

Soil water content measurements were reanalysed to obtain $SW_{initial}$, DUL and CLL to accommodate soil status change for 10 different sowing dates over two sites. Sowing date one in the ADM2 experiment was set up by using estimated $SW_{initial}$ because soil water measurements did not occur until 19 days after lucerne was sown on 21 October 2010.

RFV and KL are conservative parameters extracted from an existing publication (Sim et al. 2017). The RFV concept is only valid during root system establishment when roots are first exploring the soil profile (Section 2.3.2.1). This is often discussed along with KL, although RFV is defined in the plant module of APSIMX. The lucerne crop in Ashley Dene and Iversen12 had RFV values of 15.1±2.45 and 12.9±1.02 (mm d^{-1}), respectively. These values are not significantly different from the default value of 15 mm d^{-1}. Thus, the default value of RFV was used.

Table 4.2 lists lucerne KL and bulk density (BD) values for the two sites. Seedling and regrowth lucerne had different lucerne KL values and rooting depth. This is because seeding lucerne develops its root system while extracting water, whereas regrowth lucerne already has a root system present in the entire soil profile and ready for water extraction. Bulk density (BD) is difficult to measure, especially in stony soils, therefore, values are often inherited from similar soil types. Graham et al. (2019) reported BD values down to 1.5 m in a similar soil type as ADM2. In contrast, I12 and profiles below 1.5 m in ADM2 used default values in the current model. Lucerne XF was set to 1, which means no restrictions on root growth, for the entire rooting depth (2.3 m) of regrowth lucerne (Sowing dates 1-5 in site ADM2 and I12). For seedling lucerne (Sowing dates 6-10 in site ADM2 and I12), lucerne XF was equal to 0 below 1.4 m, which represents no root growth at or below that depth to mimic the observation of no water extraction occurring below 1.4 m during the growing season (2011/2012).

Table 4.2 Average total soil bulk density (±standard error when values available) and water extraction rate for Ashley Dene and Iversen 12 over 22 depths. Depth one was surface to 0.2 m and below was at an interval of 0.1 m down to 2.3 m. Bulk density data for Ashley Dene and Iversen 12 were cited from (Graham et al. 2019) and ApsimX default settings. Below surface water extraction rate values

were reported by (Sim et al. 2017). Surface layer (Depth one) water extraction rate for lucerne used the default values in the current APSIMX lucerne model

	Bulk Density (kg cm^{-3})		Water extraction rate (kl; mm d^{-1})			
Depth	AshleyDene	Iversen12	Seedling AshleyDene	Regrowth AshleyDene	Seedling Iversen12	Regrowth Iversen12
1	1.438±0.034	1.260	0.06	0.06	0.06	0.06
2	1.643±0.109	1.260	0.018	0.044	0.039	0.019
3	1.796±0.066	1.260	0.018	0.044	0.039	0.019
4	1.796±0.066	1.440	0.018	0.044	0.039	0.019
5	2.086±0.031	1.440	0.041	0.051	0.043	0.026
6	2.086±0.031	1.440	0.041	0.051	0.043	0.026
7	2.146±0.014	1.570	0.041	0.051	0.043	0.026
8	2.146±0.014	1.570	0.027	0.062	0.04	0.031
9	2.146±0.014	1.570	0.027	0.062	0.04	0.031
10	2.146±0.044	1.580	0.027	0.062	0.04	0.031
11	2.146±0.044	1.580	0.047	0.065	0.03	0.025
12	2.146±0.044	1.580	0.047	0.065	0.03	0.025
13	2.210±0.049	1.580	0.047	0.065	0.03	0.025
14	2.210±0.049	1.590	–	0.046	–	0.035
15	1.950	1.590	–	0.046	–	0.035
16	1.950	1.590	–	0.046	–	0.035
17	1.950	1.590	–	0.054	–	0.021
18	1.950	1.590	–	0.054	–	0.021
19	1.950	1.590	–	0.054	–	0.021
20	1.950	1.581	–	0.022	–	0.019
21	1.950	1.590	–	0.022	–	0.019
22	1.950	1.590	–	0.022	–	0.019

AirDry and LL15 were set equal to CLLs when the default values were invalid. Default AirDry and LL15 values remain intact if they were less than CLLs. SAT must be equal or above DULs; therefore, the opposite logic compared with AirDry and LL15 was applied to SAT values. SWCON, U and Cona for two seasons used the default values as a starting point to establish the baseline model for potential improvement in Chapter 5.

4.2.2.1 Initial soil water content

Initial soil water content was the water status at the sowing date. However, it may be difficult to obtain soil water measurements at the same time as sowing crops in practice. Using SWC at the measurement nearest sowing date is often acceptable for modelling practices.

In a preliminary simulation analysis, it was evident that the original $SW_{initial}$ overestimated the SWC values for SD1. This might have been caused by the combination of plant water uptake and soil surface evaporation. Hence, a manual model-fitting exercise was carried out to estimate the $SW_{initial}$ at crop sowing for SD1. Table 4.3 shows the arbitrary SWC values at the exact sowing date for SD1 to determine $SW_{initial}$after a manual model fitting exercise in APSIMX-Slurp.

Table 4.3 Arbitrary soil water contents (mm) for sowing date one over the top 0.5 m in ADM2. Superscript indicates the measurement intervals in meters. Model fitting was done in the APSIMX Slurp model with fixed canopy values.

Date	SWC $^{0.1}$	SWC $^{0.2}$	SWC $^{0.3}$	SWC $^{0.4}$	SWC $^{0.5}$	SWC $^{0\text{-}0.5}$
21-Oct-10	13	13	12	10	9	57

4.2.2.2 The drained upper limit and crop lower limit

The same logic to define DUL and CLL was used in (Brown et al. 2009, Sim 2014). Briefly, DUL was the maximum SWC when the soil profile completely recharged after a rainfall event while CLL was the minimum SWC when soil moisture deficit (SMD) was at its maximum. However, the preliminary simulation analysis suggested that the maximum SWC, as DULs, constantly overestimated the SWC for the second season simulation in ADM2. Thus, an arbitrary conversation factor (0.95) was multiplied to lower the DULs for all treatments at ADM2.

4.2.2.3 Soil physical properties for each treatment

Soil physical properties differ in spatial dimensions. Spatial variabilities can be captured through mean and standard errors or are negligible when soil type is uniform across the experimental areas. However, soil physical properties can dramatically differ on a spatial scale. Hence, each sowing date treatment had a unique configuration of soil module. The "factors" node in "LucerneValidation.apsimx" file from APSIMX was modified to generate 20 simulations for ADM2 and I12 datasets. More discussion about "factors" is in Section 4.2.4.

4.2.3 Plant module

APSIMX has a fully functional lucerne module based on PMF under irrigated conditions (Section 3.5.2). The relationships reported by (Sim 2014) were used to parameterise the

water stress effects on LAER, RUE and phyllochron. Table 4.4 lists the key change points of water stress effects on three essential parameters in the current APSIMX lucerne model. X represents the ratio of soil water supply and demand while Y represents the effects of water limitations. The XY pairs for the three parameters were incorporated in the plant module via the "LinearInterpolationFunction". This multiplication function uses Y values to reduce parameters' optimal rate based on the corresponding X values.

Table 4.4 Water stress impact on parameter values in APSIMX lucerne model. $X(T/T_D)$ is soil water supply and demand, ranging from 0 to 1. $Y(f_{stress}/f_{optimal})$ represent the relative values to each parameter's potential rate under optimal conditions. Values extracted from Sim (2014)

Parameter	$X(T/T_D)$	$Y(f_{stress}/f_{optimal})$
RUE	0	0
	0.15	0.4
	0.75	0.75
	0.9	1
	1	1
LAER	0	0.1
	0.5	0.1
	0.9	0.9
	1	1
Phyllochron	0	2
	0.5	2
	0.6	1.80
	0.7	1.11
	1	1.00

4.2.4 Manager module

APSIMX uses the manager module to mimic actual agronomic management. Section 3.5.3 discussed the technical details. The essential information for developing the manager module for the lucerne model is provided. In the current lucerne model, three manager scripts have been provided to users to gain control on the diagnosis of intermediate processes and manipulation of agronomic practices. These three manager scripts are DiagnosticsVariables, LucerneSowingRule and Mower. The first script opens channels for users to inspect the internal processes of APSIMX which is normally invisible to users. The second script allows users to define the sowing practices such as sowing date, rate and/or depths. The third script offers users to modify harvest methods, such as "cut and carry" or grazing.

In addition to the three existing manager scripts, a fourth manager, ResetOnDate was added, to reset SWC values on particular dates. This manager reinitialises the SWC based on the field-measured value on 25th June 2011, which was the closest measurement to the starting date of the regrowth period (1st July 2011; Sim et al. 2017). Resetting SWC was to avoid model error accumulation from the previous growing period for SD1 to SD5.

For the ADM2 and I12 datasets, a factorial feature was used to mimic the sowing date treatments (APSIMInitiative NA). The factorial feature allows users to define single or multiple key factors with different levels to run all possible combinations of these factors and levels without having to construct all simulations for all combinations. Figure 4.1 demonstrates the layout of a defined factor called "SowingDate". There are 10 sowing dates as levels for this factor. Within each sowing date level, sowing and harvest dates from ADM2 and I12 were extracted and manually input for each treatment at both sites. Therefore, the simulation sowing dates were identical to the actual sowing dates. Appendix 1 shows the full list of cutting dates for the two sites. The cutting dates also considered the defoliation method and were adjusted to match reality. More specifically, the "mown" method was adjusted one day after the actual harvest date because the cutting function in the model occurs instantly when the clock passes midnight, whereas lucerne crops still accumulate biomass during the harvest process. For example, the cutting date in the model was 29th December 2010 if the actual harvest date was 28th December 2010. In contrast, the "grazed" method took account of the grazing period due to animals consuming the lucerne over time. For example, the cutting date was 21st June 2011 when the grazing started on 15th June 2011.

Field harvest or grazing left approximately 5 cm residual in the paddock. The lucerne model has a default setting of 5% of above-ground DM as residuals after each "cut".

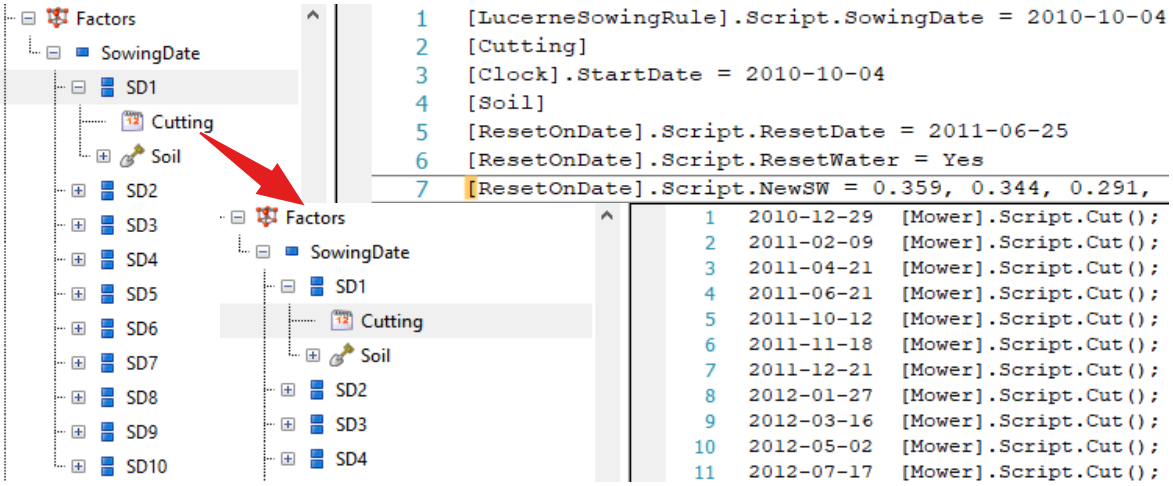

Figure 4.1 Exemplar of using a factorial feature in APSIMX to define sowing dates, cutting regimes, simulation starting date and soil modules. The "Factors" node contains one factor called "SowingDate" with ten levels starting from SD1 to SD10. Within each level, agronomic practises and soil modules were defined. This information will replace the specified model part to generate simulations.

4.2.5 Report module

Key outputs for model performance validations consist of eight variables from the plant module and one variable from the soil module (Table 4.5). Appendix 2 lists another 42 output variables for labelling and model diagnostic purposes.

Variable names followed the conventional names of an existing validation dataset stored in the APSIMX repository. Biomass related variables, such as LeafWt and RootWt, were expressed as kg DM ha^{-1}. This expression differed from the default APSIMX output unit (g m^{-2}). In addition, released APSIMX models, such as Maize and Wheat, use a standard variable name format which is "[Module].Organs/Properties.variables". This approach standardises the variable names and provides definitive metadata for each variable. However, this convention was not adopted to save time in transferring the existing dataset to meet the conventional naming system.

Table 4.5 Description of output variable name for model performance validation.

Module	Variable Name	Unit	Description
Plant	Height	cm	Lucerne main stem height
Plant	LAI	m^2 m^{-2}	Leaf area index
Plant	LeafWt	kg ha^{-1}	Leaf dry matter
Plant	RootWt	kg ha^{-1}	Root dry matter

Plant	StemWt	kg ha^{-1}	Stem dry matter
Plant	ShootWt	kg ha^{-1}	Shoot dry matter
Plant	ShootPopulation	Count	Shoot dry matter
Plant	GrowthStage	NA	Numeric scale to describe lucerne growth stage
Soil	SWCmm	mm	Soil profile water content down to a rooting depth

4.2.6 Validation dataset and analysis

R was the primary analysis tool used to derive parameter values from field-measured data with packages listed in Table 4.6. The existing validation dataset was imported from the APSIMX repository on GitHub. ADM2 and I12 were manipulated and joined with the existing dataset. The details of data manipulation were documented in the "Validation data preparation" R markdown file. Briefly, raw data were aggregated into mean values with standard errors. Key variable names were set to be identical with the existing dataset. An updated Excel file was the final format of this process and read by APSIMX as input.

Table 4.6 R packages used for data analysis.

Package	Version	Purpose
autoapsimx	0.0.0.9000	Deriving key soil physical properties from field-measured soil water content
data.table	1.13.6	Data manipulation and aggregation
DBI	1.1.1	Database interface
ggplot2	3.3.3	Graphing
magrittr	2.0.1	Chaining R code together to form functional chunks
readxl	1.3.1	Importing data from Excel
RSQLite	2.2.2	APSIMX database driver
tabulizer	0.2.2	Extracting data from PDF
targets	0.3.1	Workflow management

APSIMX saves a copy of the validation datasets into the output SQLite database (DB) as an independent table with a name the same as the validation dataset file name. Prediction results were saved in the same DB. A table named PredictedObserved held the pair of prediction and observed data which has identical names and calculates their residuals. In the DB, all three tables share the same foreign key which contains two variables, CheckpointID and SimulationID. The foreign key refers to tables "_Checkpoints" and

"_Simulations". The former controls the version of predication results and the latter stores the actual simulation name in text.

APSIMX has a set of built-in metrics for model performance evaluation. Users can add a regression class under the series node within the Graphing tool. The regression class calculates six metrics including the coefficient of determination (R^2; Equation 14), NSE (Section 3.7.2), mean error (ME), mean absolute error (MAE), root mean square error (RMSD; 3.7.2) and root mean square error to standard deviation ratio (RSR). These metrics will be displayed with a scatter plot of predicted verse observed data. Normalised RMSD, NSE and R^2 were the key metrics in this study to evaluate the model performance (Section 4.3.3).

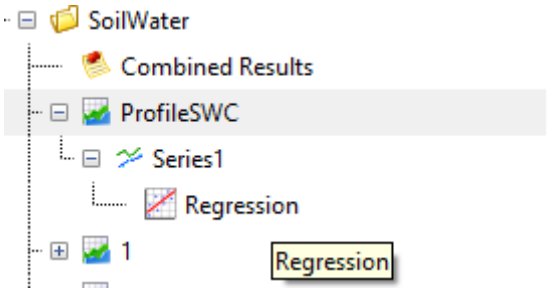

Figure 4.2 Snapshot of adding Regression class into graph node in APSIMX to display model performance evaluation.

4.3 Results

4.3.1 Soil module

4.3.1.1 Initial soil conditions and characteristics

Initial soil water content was below PAWC (136±3 and 387±13 mm in Ashley Dene and Iversen 12, respectively) in lucerne in all treatments (Figure 4.3). $SW_{initial}$ ranged from 9 mm (ADSD10) to 123 mm (ADSD2) in Ashley Dene and from 53.2 mm (I12SD10) to 314 mm (I12SD5) in Iversen 12. Overall, Iversen 12 holds two to three times more water than Ashley Dene soils depending on the sowing dates.

For DUL and CLL, values from Iversen12 exceeded those from Ashley Dene in all sowing dates and depths (Figure 4.3). DUL ranged from 0.083 to 0.300 mm^3 mm^{-3} in Ashley Dene with a trend of decreasing from top to bottom over the 10 sowing dates. In contrast, DUL

was 0.204 to 0.384 mm^3 mm^{-3} in Iversen12 with a fluctuating trend at different depths. CLL showed a similar pattern as DUL since it correlated to DUL. CLL ranged from 0.063 to 0.175 mm^3 mm^{-3} in Ashley Dene and from 0.079 to 0.315 mm^3 mm^{-3} in Iversen Field. The upper limits of CLL in Iversen12 were close to the DULs, which suggests that the layer with high CLL is below the maximum extraction depth.

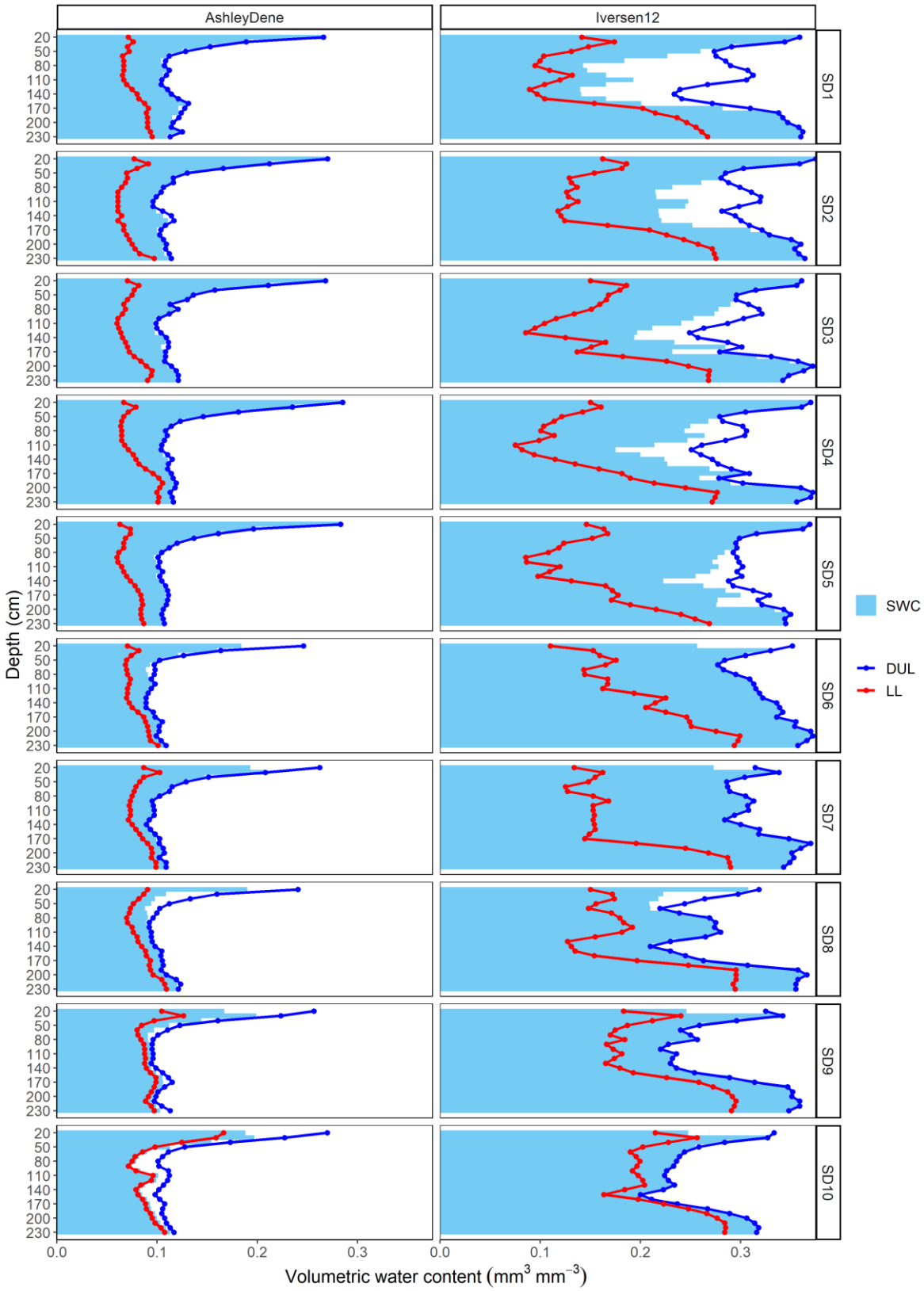

Figure 4.3 Drained upper limit (DUL; Blue), crop low limit (CLL; Red) and initial soil water content (Light Blue area) down to 230 cm for Sowing Dates 1 to 10 in ADM2 and I12 dataset. CLLs are derived from the soil water measurements and differ from the LL15. CLLs get closer to DULs from SD6 to SD10 because later sown seedling crops had not completed a complete drying cycle.

4.3.1.2 Soil water content

The current APSIMX-Lucerne model captured the trend of profile SWC changes in both sites with specified soil physical parameters. In most cases, simulation results follow the temporal pattern of SWC more closely in Ashley Dene than in Iversen12. Predictions in Ashley Dene accurately simulated the spring, summer and early to mid-autumn SWC variations for seedling crops (ADSD6 to ADSD10) and regrowth crops (ADSD1 to ADSD5). For example, treatment ADSD6 was sown on 10th Oct 2010. The profile SWC maintained between 204 to 260 mm until January 2012 when profile SWC dropped sharply to around 210 mm. The autumn rainfall was able to recharge approximately 20 mm of water to the profile SWC but this was extracted quickly by lucerne until the winter clean-up grazing occurred after which rainfall recharged the profile back to DUL. For regrowth lucerne in Ashley Dene, the profile SWC gradually decreased from late winter into spring, which indicates low plant growth. The model successfully simulated the impact of a 60 mm rainfall event on 21st October 2011, which replenished the profile SWC. Regrowth lucerne crops used up soil water during summer and reduced profile SWC to CLLs until the final harvest in June after which winter rainfall slowly recharged the soil.

The model also predicted profile SWC changes in spring and early summer for the Iversen 12 experiment. For example, the seedling crop (I12SD6) started to extract 159 mm of soil water from late December 2011 to late February 2012. Autumn rainfall replenished the SWC by 31 mm but it was exhausted quickly by the lucerne crop. Lucerne used another 20 mm of soil water until the final harvest. However, there were systematic errors present in both seeding (I12SD7 to I12SD10) and regrowth (I12SD1 to I12SD5) crops. The model overestimated the SWC from January 2012 for these treatments. These systematic errors might be caused by two factors. First, the modelled root water extraction might be lower than observed for seedling crops (I12SD7 to I12SD10). Secondly, the modelled canopy might demand less water than the crop actual usage (I12SD1 to I12SD5). Section 4.4.1 discussed in detail.

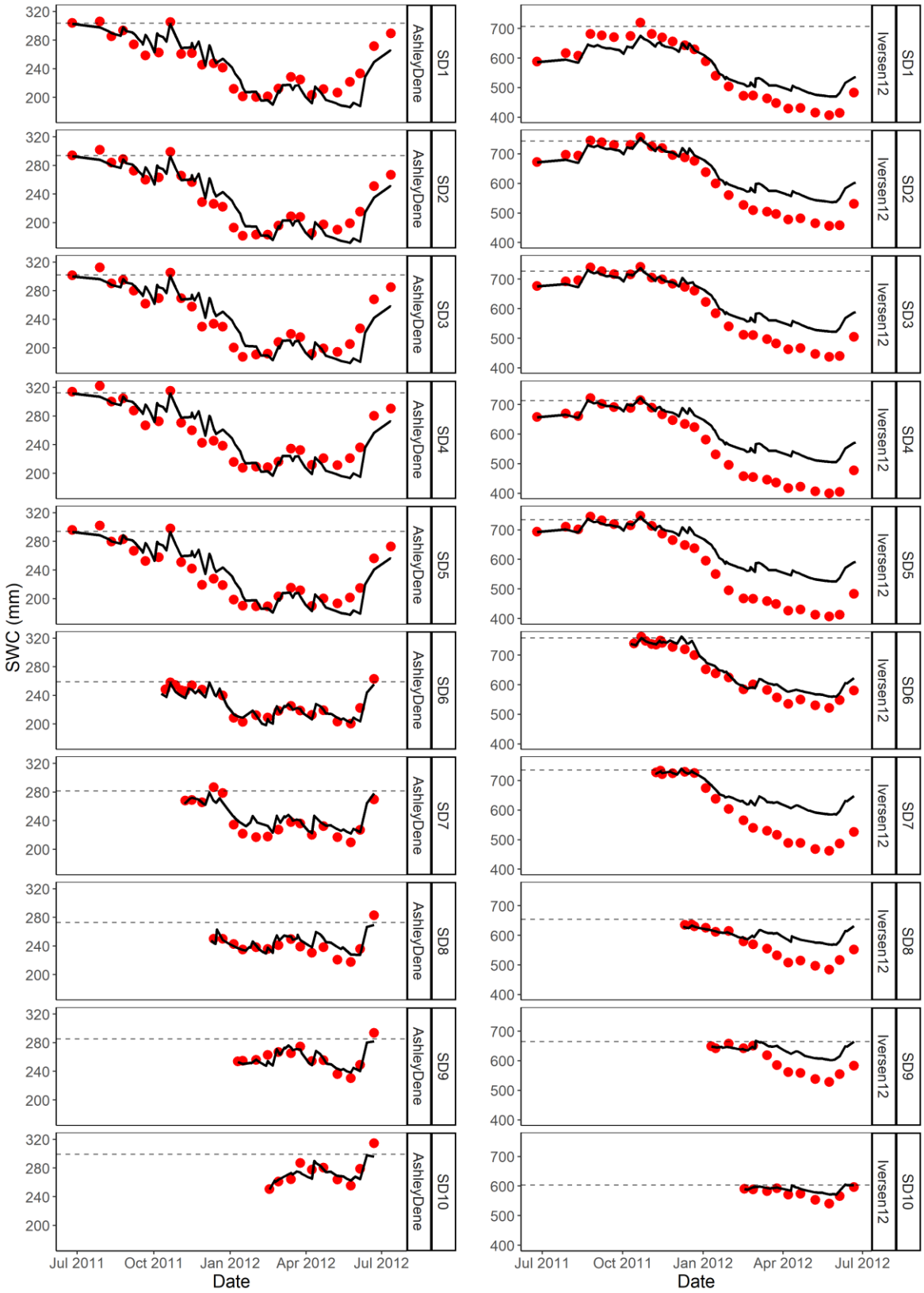

Figure 4.4 Temporal comparison of simulated (—) and observed (●) profile SWC (mm) in two sites for 10 sowing dates. Dash lines represent the drained upper limits for each treatment.

4.3.2 Plant module

4.3.2.1 Phenology

The lucerne model generally captured the major trends of main stem node number (MSNN) over the simulation period (**Error! Reference source not found.**). The model overestimated the maximum MSNN for the first one or two rotations for seedling and regrowth crops at Ashley Dene. Underestimation of MSNN occurred in the last rotation for treatment ADSD1 to ADSD9. The third rotation (late summer and early autumn) of regrowth lucerne (ADSD1 to ADSD5) stopped development in the field whereas the lucerne model showed no sign of development cessation. In contrast, the MSNN simulation in Iversen12 underestimated the maximum observed MSNN with the progress of soil water depletion (Figure 4.4).

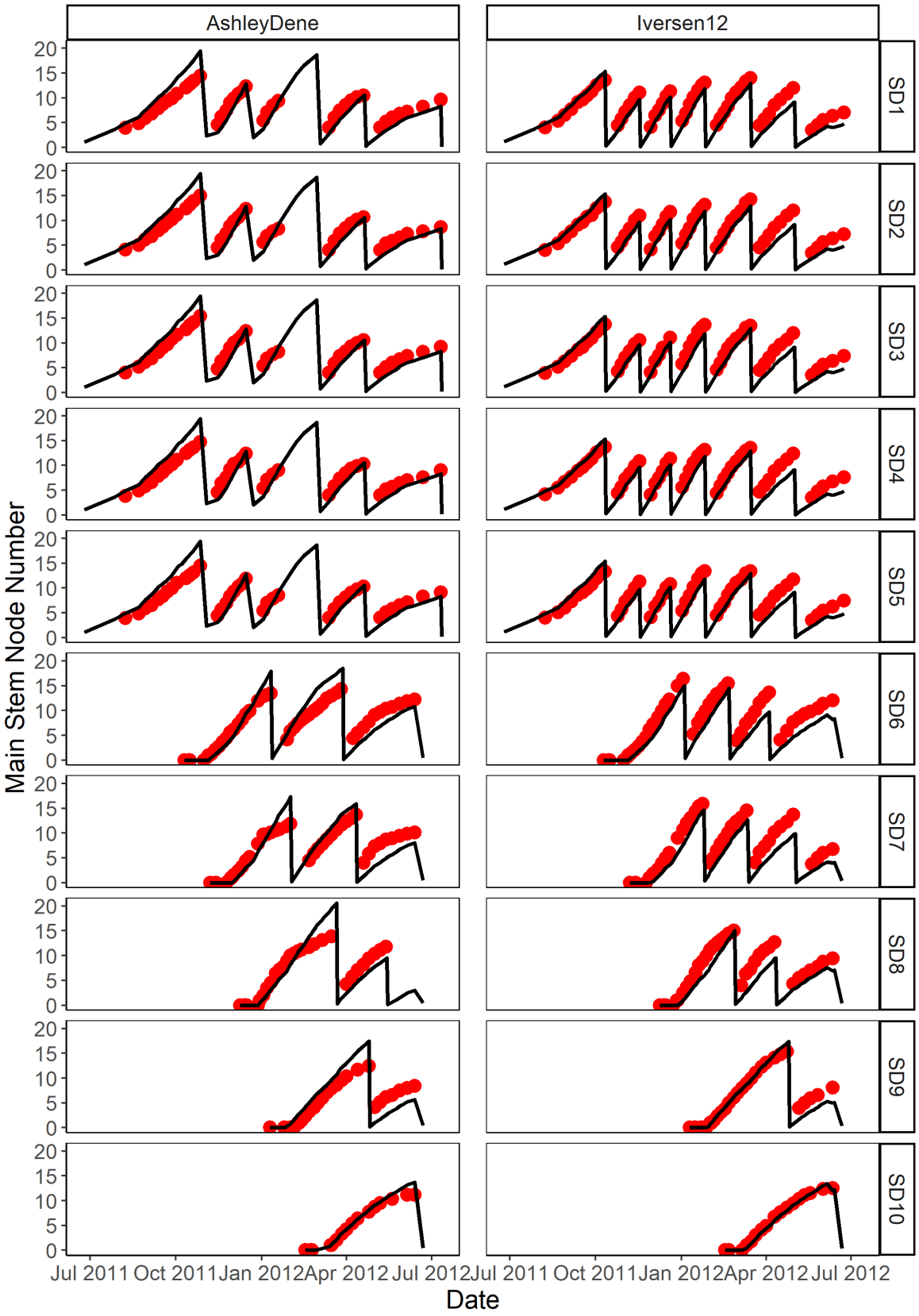

Figure 4.5 Temporal comparison of simulated (—) and observed (●) main stem node number in two sites for 10 sowing dates. Observed data was unavailable for the period of 20th January 2012 to 29th February 2012.

4.3.2.2 Leaf area index

The lucerne model accurately simulated one rotation (Rotation 4) for the first sowing date regrowth lucerne in Ashley Dene (Figure 4.6). In all other rotations, the predicted LAER (LAI) was higher than observed. This suggests that the implemented water stress effects on LAI were insufficient to reflect the actual events that occurred at Ashley Dene. Overestimation of LAI occurred in ADSD6 to ADSD10. However, the maximum simulated LAI was reduced by 50% for ADSD6 to ADSD9. In contrast, the lucerne model accumulated LAI at a rate of 0.12 m^2 m^{-2} day^{-1} for regrowth lucerne in spring (September to October 2011) whereas the field-measured LAI growth rate was only half that at 0.054 m^2 m^{-2} day^{-1}. Rotation 1 of the regrowth lucerne reached an LAI of 6.5 m^2 m^{-2}, which was more than doubled the actual measured value (3.2 m^2 m^{-2}). Overestimation of maximum LAI suggests that the lucerne grew at its full potential with no water stress. Simulations in the second rotation had a maximum LAI close to field measurements but were still higher than observed. Simulations for the third rotation showed the effects of water stress but overestimated the LAI values. Simulated LAI results only aligned with field measurements for regrowth lucerne (ADSD1 to ADSD5) in the fourth rotation.

The model captured the LAI trends of lucerne for all treatments in Iversen12. In seedling crops, the plant module extracted insufficient water to keep up with the demand. Therefore, the lucerne model underestimated LAI for the majority of rotations from I12SD6 to I12SD9 whereas it successfully predicted the maximum LAI for I12SD10. For regrowth lucerne, prediction of LAI aligned with LAI observations for the first five rotations. The sixth rotation had the simulated LAI underestimated for all five regrowth crops (I12SD1 to I12SD5) when observed SWC was adequate to supply the water demand but the lucerne model was unable to extract the water. This inaccurate representation of the water stress effects suggests that the soil water extraction or demand parameters require further parameterisation to represent these lucerne crops in field conditions.

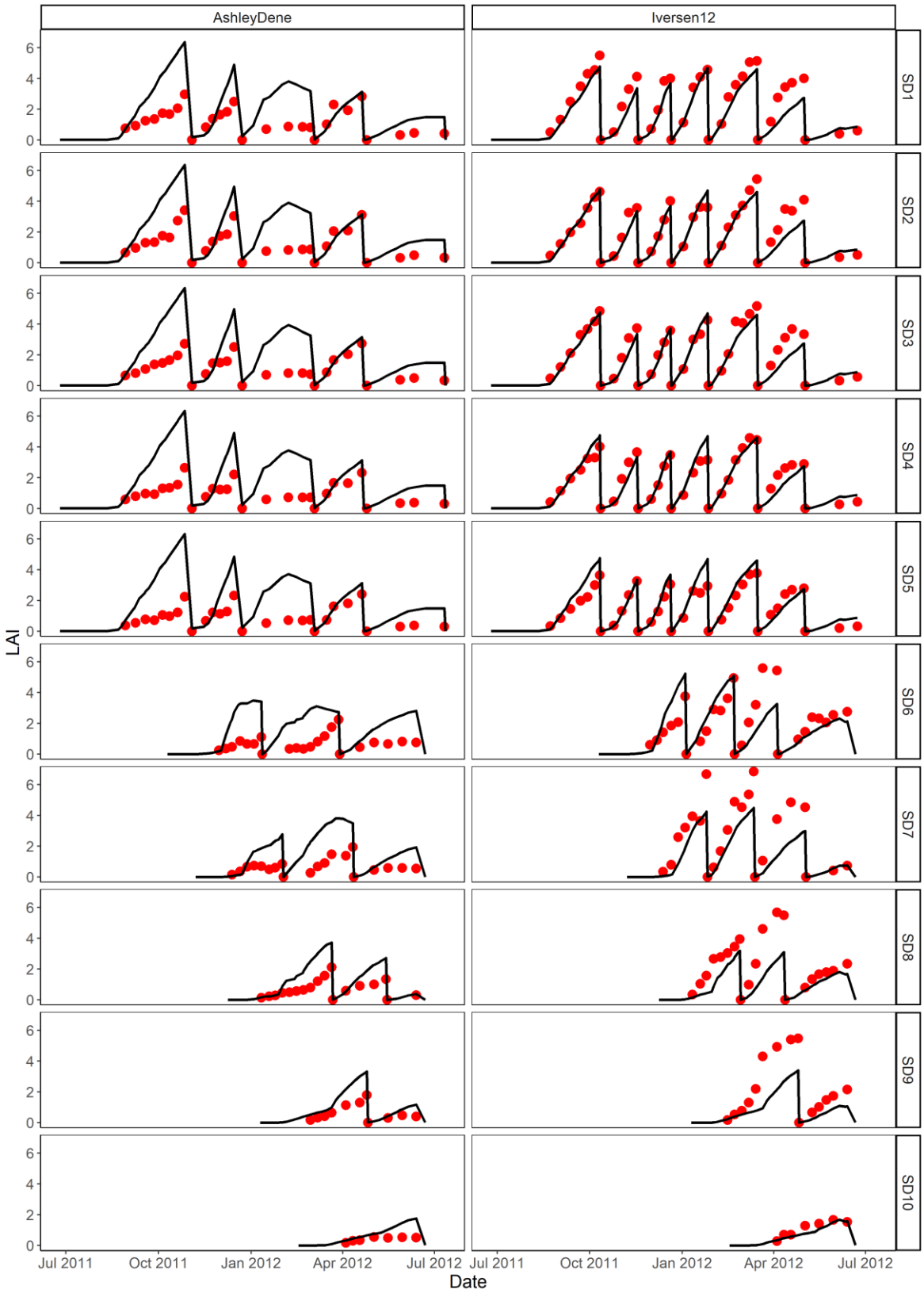

Figure 4.6 Temporal comparison of simulated (—) and observed (●) leaf area index in two sites for 10 sowing dates. SD1 to 5 were the second season regrowth crops while SD6 to 10 were seedling crops. Simulations were for one season.

4.3.2.3 Shoot biomass

Simulation results overestimated Shoot biomass (ShootWt) in Ashley Dene but underestimated it in Iversen12 for both seeding and regrowth crops (Figure 4.7). For treatments in Ashley Dene, field-measured ShootWt ranged from 7621 kg DM ha^{-1} (ADSD1) to 424 kg DM ha^{-1} (ADSD10) with gradual decreases with each delay in sowing date. The model predicted the ShootWt were approximately double those values and ranged from 11355 kg DM ha^{-1} (ADSD1) to 960 kg DM ha^{-1} (ADSD10). For Iversen12, the model simulated ShootWt ranged from 15621 kg DM ha^{-1} (ADSD1) to 962 kg DM ha^{-1} (ADSD10) while the measured ShootWt ranged from 21399 kg DM ha^{-1} (ADSD1) to 1117 kg DM ha^{-1} (ADSD10). This pattern shows that the model supplied surplus water for simulations in Ashley Dene, whereas insufficient water was available for simulations in Iversen12, despite measurements showing there was sufficient water in the soil (Figure 4.4).

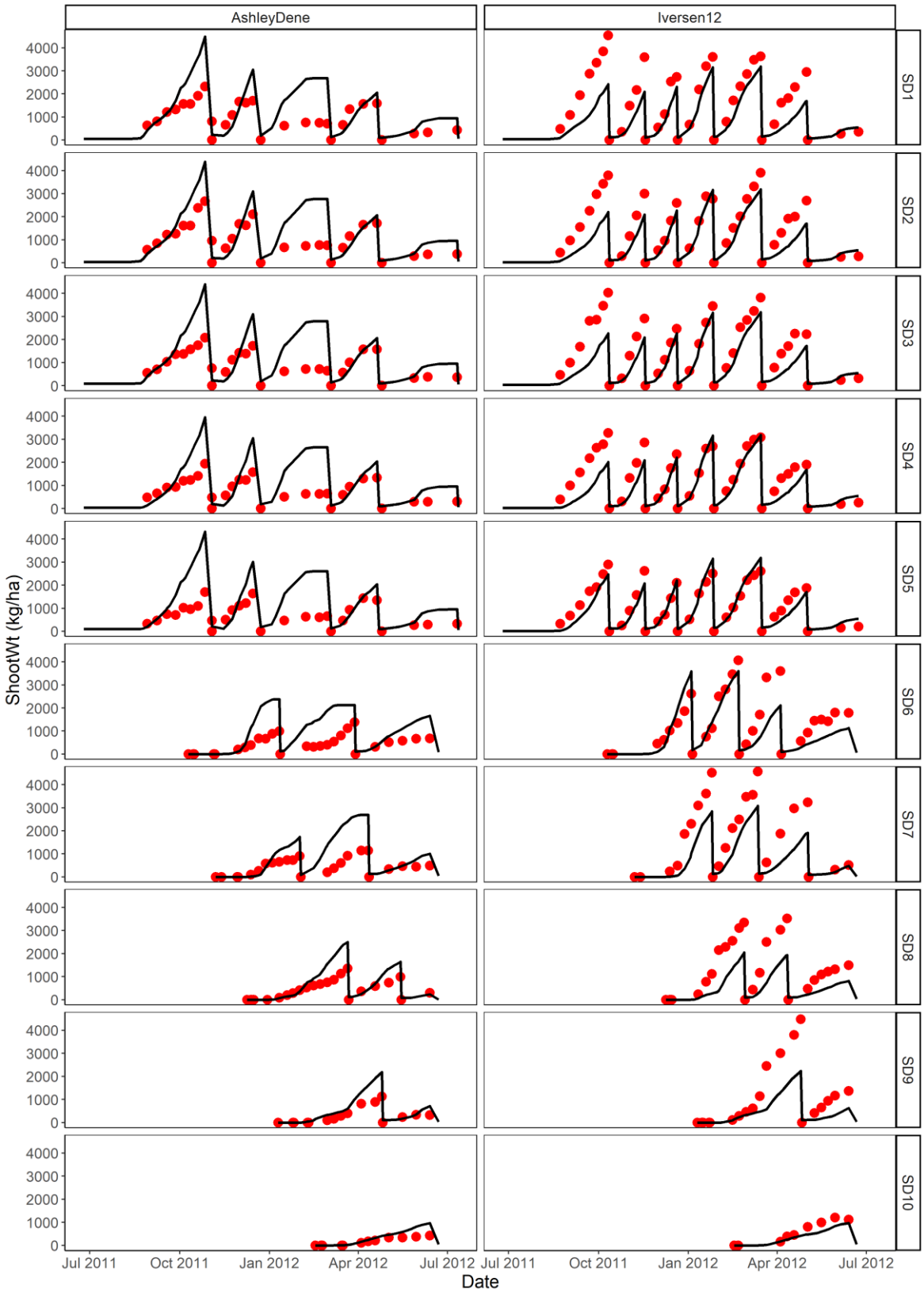

Figure 4.7 Temporal comparison of simulated (—) and observed (●) shoot weight (kg DM/ha) in two sites for 10 sowing dates. SD1 to 5 were the second season regrowth crops while SD6 to 10 were seedling crops. Simulations were for one season.

4.3.2.4 Leaf biomass

Shoot biomass consists of two main contributors; leaf and stem biomass (LeafWt and StemWt). The arbitrator class in the current model controls DM partitioning to these two organs. Figure 4.8 displays the temporal pattern of LeafWt for simulated and field-measured values. Stem biomass was ignored because of a lack of observations. The model simulated the major temporal changes in leaf biomass (kg DM ha^{-1}) for seedling lucerne from mid-summer to early winter and regrowth lucerne from spring to early summer in Ashley Dene. In contrast, simulated leaf biomass (kg DM ha^{-1}) in Iversen 12 was systematically lower than the field-measured values in seedling and regrowth crops. For example, the simulated LeafWt for seedling lucerne (I12SD6 to I12SD9) was approximately a third of the measured biomass. Predictions for regrowth crop I12SD5 produced a maximum leafWt of 7514 kg DM ha^{-1}, which was 66% of the actual LeafWt. This is possible due to the incorrect soil water parameterisation and soil water supply failing to meet the demand.

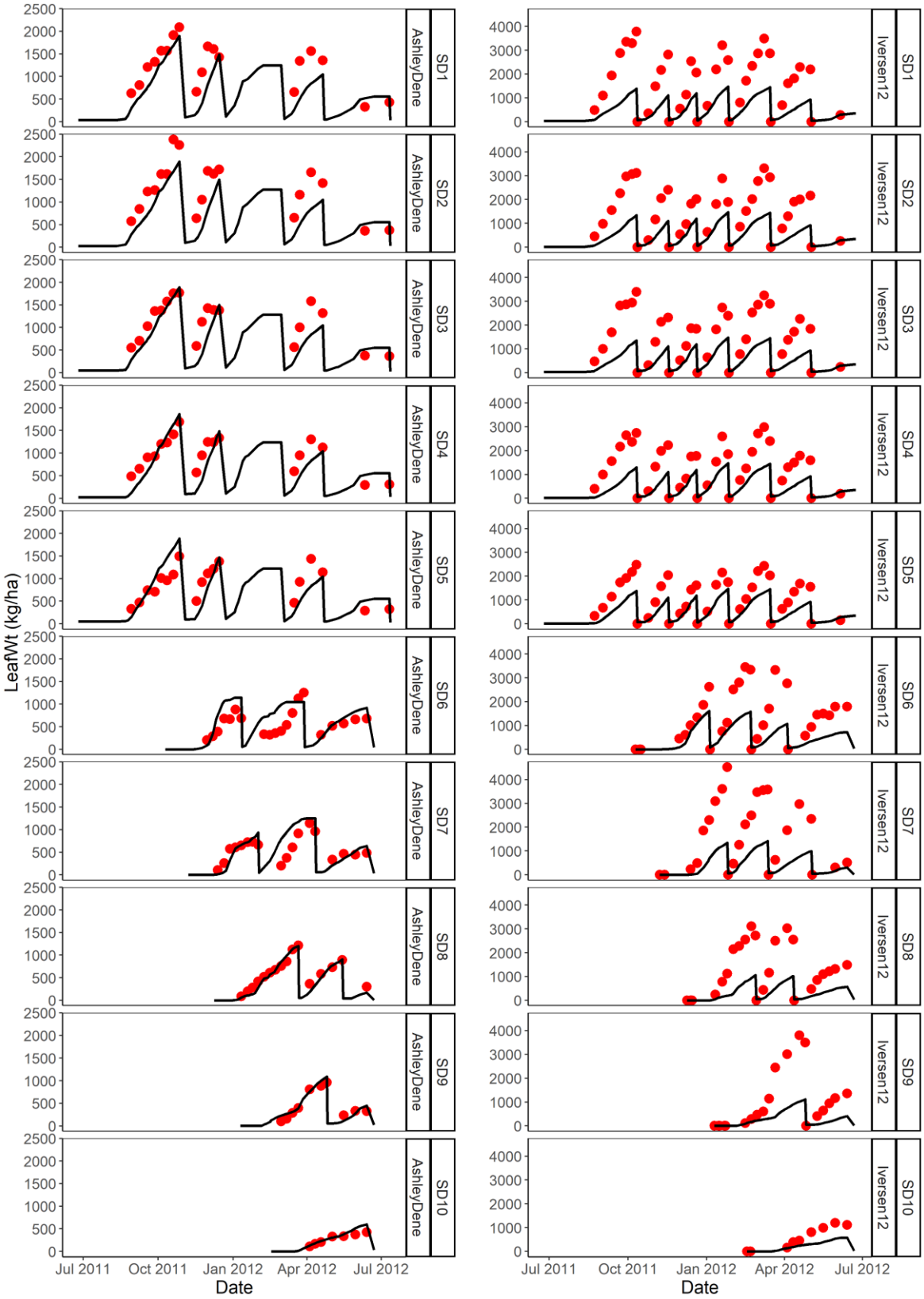

Figure 4.8 Temporal comparison of simulated (—) and observed (●) leaf weight (kg DM/ha) in two sites for 10 sowing dates. SD1 to 5 were the second season regrowth crops while SD6 to 10 were seedling crops. Simulations were for one season.

4.3.2.5 Height

Plant height simulations reflect the temporal pattern of simulated results for StemWt (Figure 4.9). There were no height observations available for seedling lucerne. The model over predicted lucerne height at Ashley Dene for regrowth crops. More specifically, the model predicted a maximum plant height of 89 cm compared with the measured value of 32 cm. However, the model did capture the maximum plant height for the first four rotations of regrowth lucerne in Iversen12 with a predicted height at 45.5±3.9 cm compared with a measured height of 46.4±4.0 cm. Overestimation of lucerne height could be due to the incorrect water stress function that failed to constraint internode elongation when water stress occurred.

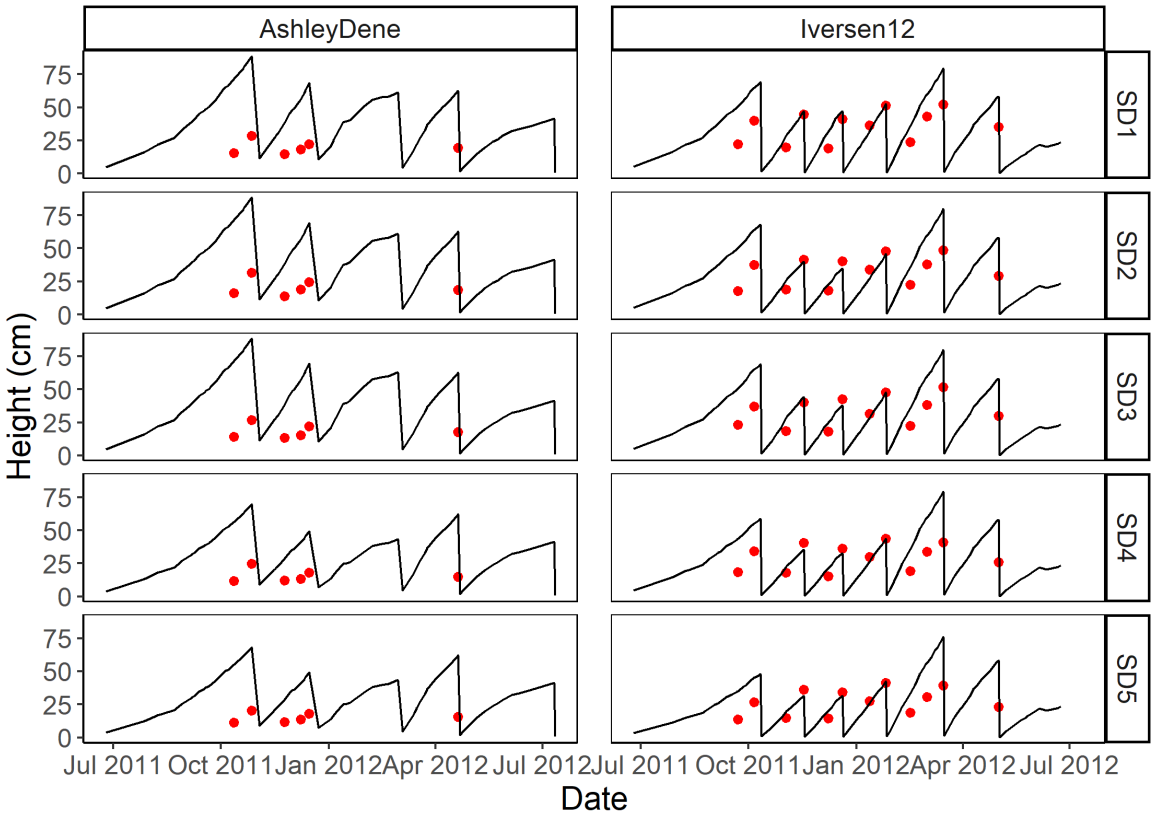

Figure 4.9 Temporal comparison of simulated (—) and observed (●) height (cm) in two sites for five sowing dates in which the plant height was measured.

4.3.3 Model performance

4.3.3.1 Soil water content

Figure 4.10 shows the statistic metric for the lucerne model evaluation. For both sites, R^2 was close to 1 (0.83 and 0.91 for Ashley Dene and Iversen 12 respectively) which indicates that predicted SWC results had tightly correlation to observed SWC. However, the NSE value (0.72) in Iversen12 was lower than in Ashley Dene (0.81) while the nRMSE value in Iversen12 (9%) was ~1.5 times larger than it (6%) in Ashley Dene. The lower nRMSE value suggested that the model predicated SWC changes in Ashley Dene more accurately than in Iversen12. More specifically, the current lucerne model overestimated (blue regression line is above 1:1 line) SWC changes when SWC was close to CLL in Iversen12. The overestimation of SWC gradually decreased when SWC increased to DUL, and resulted in the underestimation of SWC. This trend confirmed the temporal pattern in Figure 4.4. In contrast, model performance was more accurate (greater NSE and smaller nRMSE values) for Ashley Dene over the range of SWC although it underestimated the SWC for regrowth crops (ADSD1 to ADSD5) around CLL. This implies the lucerne extracted more water in the model than it did in the field.

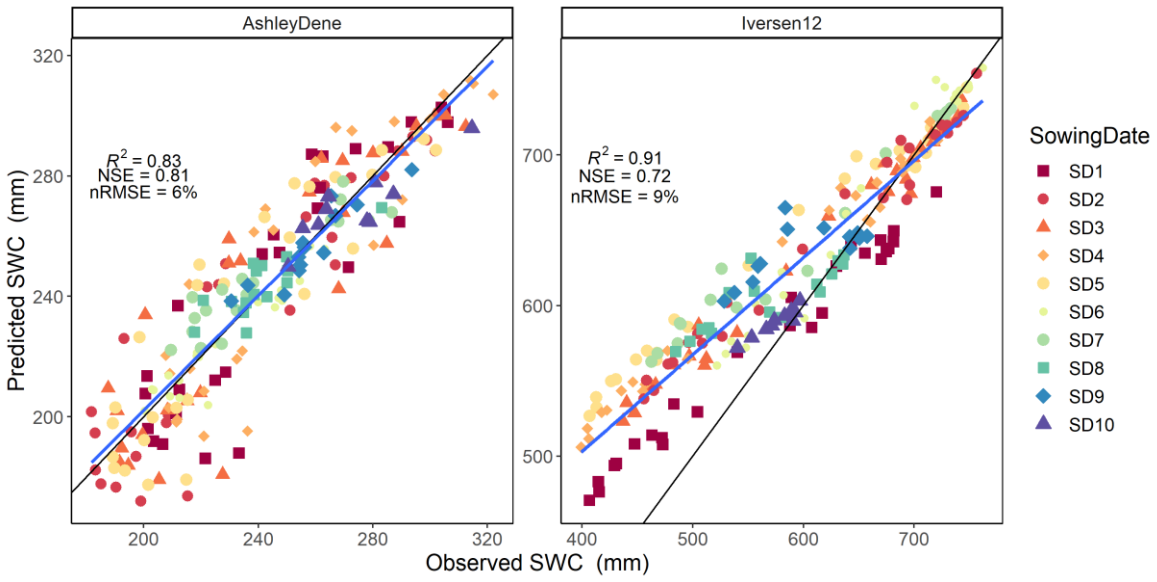

Figure 4.10 Predicted against observed values of soil water content for 10 sowing dates in two sites. All available observations for two sites were included. The black diagonal line is the 1:1 line, the blue line is the regression line and black dots represent the predicted and observed profile soil water content.

4.3.3.2 Leaf area index

Figure 4.11 shows the relationship between predicted and observed LAI for both sites with three key statistical metrics used to evaluate the model performance. The model

performed poorly (NSE < 0) for predicting LAI in low PAWC soil in dryland conditions. For Ashley Dene experiments, the overestimation of LAI dragged the relationship above the 1:1 line. A negative NSE value (-4.14) indicated that the model parameterisation was unacceptable for LAI. Specifically, the model performance was worse than using the measured mean value to predict simulation outcomes. A low R^2 value (0.55) suggested a poor relationship between prediction and observation.

In contrast, results from Iversen 12 had a higher R^2 (0.75) and NSE (0.71) but lower nRMSE (41%) (Figure 4.11). These metrics show three points. First, the relationship between prediction and observation was stronger than it was in Ashley Dene. Second, the model parameterisation reflected part of the biophysical process of canopy development in high PAWC soils without irrigation and was within the good threshold (0.5 < NSE < 1). Third, the four times smaller nRMSE (41%) for Iversent12 compared with Ashley Dene (182%) implied that statistically the model configuration represented canopy development in Iversen12 more closely than it did for Ashley Dene.

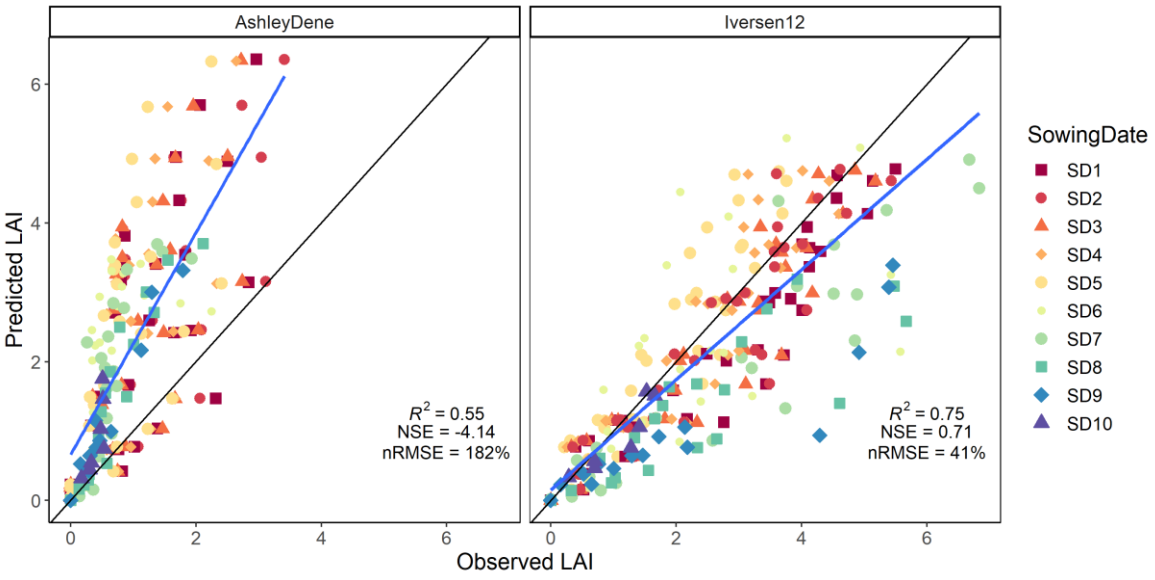

Figure 4.11 Predicted against observed values of leaf area index (LAI) for 10 sowing date treatments over two sites. The black diagonal line is the 1:1 line, the blue line is the regression line and black dots represent the predicted and observed data.

4.3.3.3 Biomass

Figure 4.12 contains the relationships between predicted and observed above-ground biomass (ShootWt) with leaf. Shoot biomass predictions was unacceptable in Ashley Dene due to the low NSE (-1.29) and high nRMSE (132%). Five simulated values (originated from SD1 to 5) overestimated ShootWt by approximately five times, which probably stemmed from the systematic overestimation of plant Height in Ashley Dene (Figure 4.13). This was because evaluation metrics of LeafWt demonstrated good prediction results, and StemWt was the result of LeafWt subtracting from ShootWt.

For Iversen12, the relationship between simulated and actual ShootWt was tighter (R^2 = 0.78) compared with R^2 of 0.63 in Ashley Dene although the model requires improvement because of the clear pattern of underestimation. The failure of LeafWt predictions was apparent in Iversen12, as shown by the NSE (0.05) and high nRMSE (Figure 4.7; 78%).

It has to be noted that the current model had not been configured correctly to represent a constant and correct level of water stress; therefore, predicted outcomes dispersed from the 1:1 line. Furthermore, DM allocation was regulated by the Arbitrator (Figure 3.7). The Arbitrator ranked the DM allocation by each organ's demand concerning other organs (Brown et al., 2014). The default Arbitrator may require re-calibration; however, this task is beyond the current study scope.

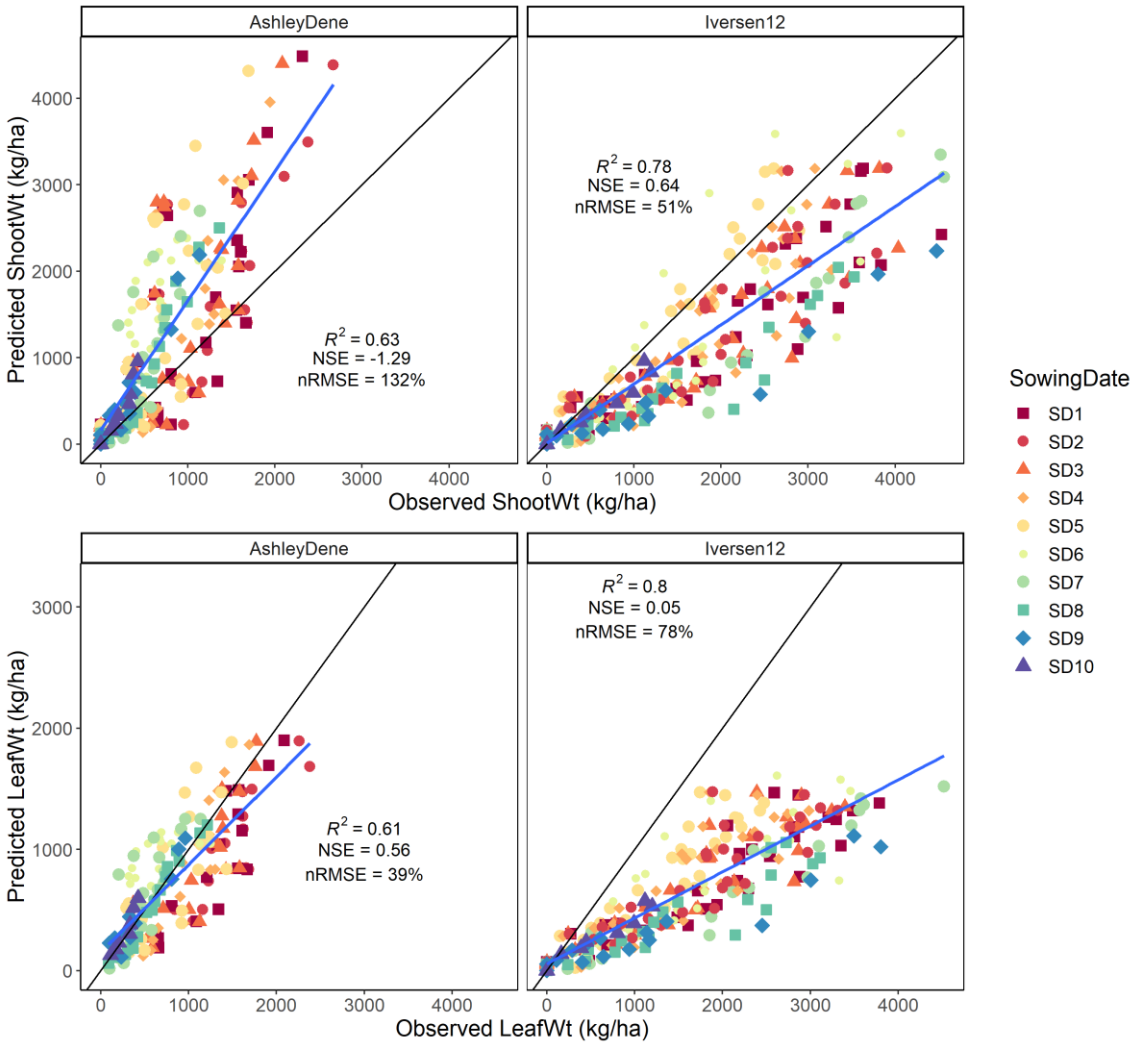

Figure 4.12 Predicted against observed values of shoot biomass and its forming components including leaf and stem biomass. All available observations for two sites were included. The black diagonal line is the 1:1 line, the blue line is the regression line and black dots represent the predicted and observed data.

4.3.3.4 Height

Figure 4.13 shows the relationship between predicted and observed plant height. Systematic overestimation of height occurred and the apparent upper limit clustered in both sites. Statistic metrics also suggested that the model performance for height predictions was worse than using the averaged observed height for both sites. For example, height predictions had the nRMSE value of 240% in Ashley Dene. The height prediction was an exponential function of the photoperiod. The results of this function produced the heightchron (Section 2.2.2) that regulates stem elongation. The current default value indicated that lucerne required less than 1 thermal unit to elongate 1 mm

stem when the photoperiod was over 10 hours (Figure 2.4). The exponential relationship between heighchron and photoperiod might be violated under dry land conditions. Consequently, the model failed to mimic lucerne height for this study.

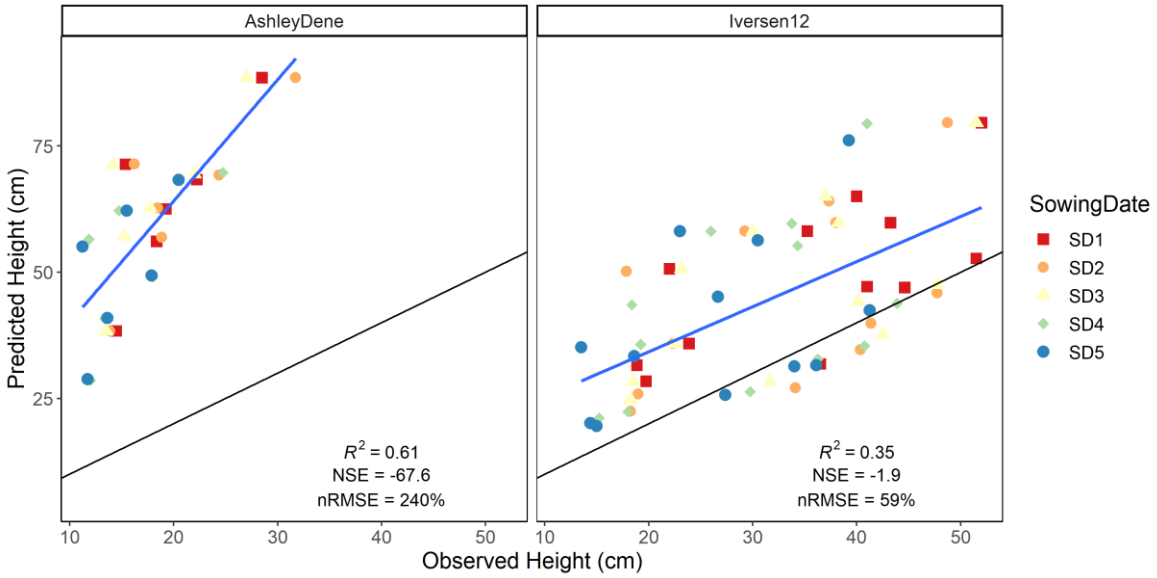

Figure 4.13 Predicted against observed values of plant height. All available observations for two sites were included. The black diagonal line is the 1:1 line, the blue line is the regression line and black dots represent the predicted and observed data.

4.3.3.5 Phenology

There was an overestimation of MSNN in Ashley Dene as crops approached the maximum MSNN while the MSNN predictions for Iversen12 were good. Figure 4.14 shows the results of predicted MSNN against field measurements. The curvilinear tendency in Ashley Dene may reflect the combined effects of water stress and photoperiod changes on phyllochron being less than the actual water stress impacts. More especially, **Error! Reference source not found.** showed that the overestimation of MSNN occurred in spring and autumn rotation where photoperiod increased and decreased, respectively. However, the default values that regulate phyllochron were derived from optimal conditions (Section 2.2.4). Consequently, the default phyllochron was slightly lower (35 °Cd and 49 °Cd at 16.5 and 10 photoperiod hour, respectively) than it was reported in Ashley Dene (37 °Cd and 58 °Cd at 16.5 and 10 photoperiod hour, respectively).

In contrast, the model performance of predicting MSNN was good (NSE = 0.76) in Iversen12. The systematic underestimation was probably due to the overestimation of SWC (Figure 4.4). Therefore, the plant module extraction or soil water demand was inadequate, which resulted in predicted water stress effects on MSNN.

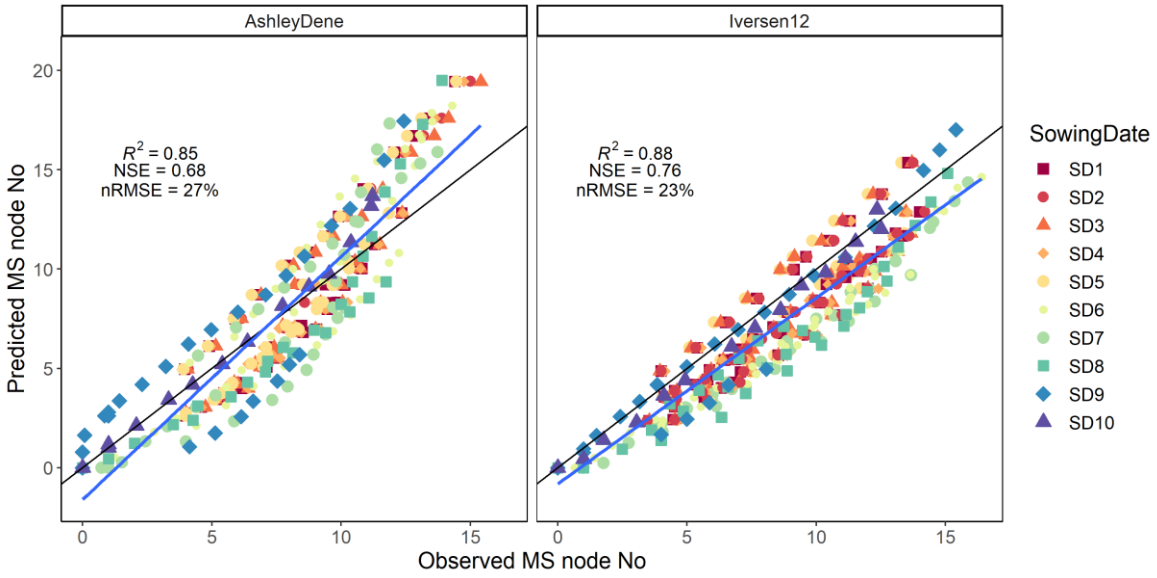

Figure 4.14 Predicted against observed values of the main stem node number. All available observations for two sites were included. The black diagonal line is the 1:1 line, the blue line is the regression line and black dots represent the predicted and observed data

4.3.4 Water supply and demand

The ratio of water supply and demand (Fw) is a multiplier, which controls the actual effects of water stress on organ components of lucerne growth and development (Figure 3.7). Figure 4.15 demonstrated the simulated temporal patterns of Fw for 10 treatments in Ashley Dene and Iversen12. Fw predictions suggested that the regrowth lucerne in Ashley Dene experienced no severe water stress until December 2011. This could explain the overestimation of LAI for regrowth lucerne during the spring and early summer (Figure 4.6). The model possibly used all soil water supply to develop canopies. In contrast, regrowth lucerne in Iversen12 had no water stress effects but water stress presented for I12SD6 to 8 during summer (Figure 4.15).

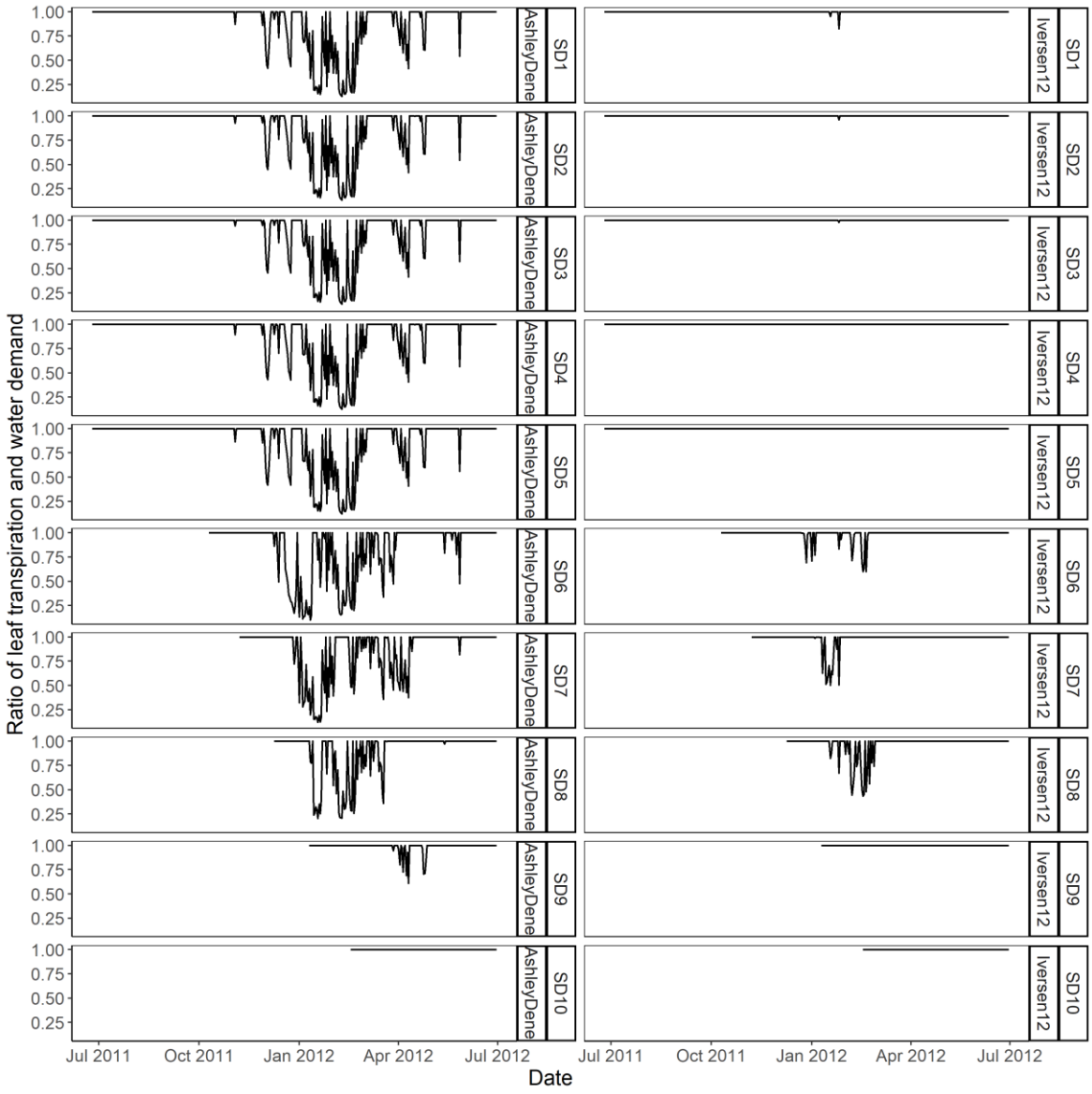

Figure 4.15 Modelled ratio of leaf transpiration and water demand (Fw). Fw ranges from 0 to 1, and is a multiplier to alter leaf growth. A value of 0 represents severe water stress that prevents any growth while 1 means no water stress effects.

4.4 Discussion

Objective 1 was satisfied by this chapter. Water stress effects on LAER, RUE and phyllochron were implemented to the APSIMX-Lucerne model. The updated model was evaluated against observations obtained from dryland experiments. This section discusses the implications of the results and lays out the foundations for the next chapter.

The APSIMX-Lucerne model had been developed in the last two decades under irrigated conditions (Moot et al. 2015; Yang et al. 2021). Previous experiments have studied the

water stress effects on lucerne growth and development (Zahid 2009, Sim 2014), yet the model structure requires improvements to incorporate water stress functions. This chapter used previous studies of lucerne grown in dryland conditions to re-configure the APSIMX-Lucerne model and explore the model performance under dryland conditions. Three existing water stress functions were simplified by Sim et al. (2017). These functions quantified LAI, RUE and phyllochron under different levels of water stresses. Parameters of quantifying soil water supply, DUL, CLL and $SW_{initial}$, were derived from observation data directly for each treatment, while default parameter values were used for soil water demand parameters. BD, kl and RFV also control soil water supply, which was sourced from literature whenever possible.

4.4.1 Profile soil water content

Overall the model gave acceptable fits but there was clear systematic over-prediction during the summer in I12. The re-configured lucerne model provided acceptable predictions of profile SWC (NSE ≥ 0.65) with NSE values of 0.84 and 0.70 for Ashley Dene and Iversen12, respectively. These NSE values were similar to previous benchmarking studies in Australia (Huth et al. 2012). More specifically, predictions of SWC changes followed the real temporal SWC variations in Ashley Dene. The tight temporal pattern between simulation results and observed values suggests that the soil water supply parameters (BD, CLL, DUL, KL, RFV and $SW_{initial}$) successfully represented the field conditions although spatial variability was apparent. It is worth noting that these soil supply parameters were derived from the observed data. Zahid (2009) reported good predictions of profile SWC in rain-fed conditions by using the observed SWC data to configure soil water parameters. However, the time course plots showed an overestimation of SWC in Iversen12 for all treatments over summer (Figure 4.4). These systematic errors indicate re-configuration might be needed for both soil water supply (kl and RFV) and/or demand (g_{smax} and R50) parameters. This is because the modelled seedling lucerne (I12SD6 to I12SD10) developed its root system too slowly (low KL and RFV values) to extract soil water at the rate observed in the field. In contrast, regrowth lucerne with established root systems (I12SD1 to I12SD5) should extract soil water faster to meet demand. The current model failed to do so and created false water stress effects on the leaf (Figure 4.7) and shoot (Figure 4.8) weight for Iversen12 crops. More specific, parameters that modify soil water

extractions require further calibration to represent the water extraction pattern in Iversen 12.

4.4.2 Leaf area index

The systematic overestimation of LAI in Ashley Dene indicated that the simulated lucerne leaf area grew at its full potential with no water stresses expressed in the first rotations (Figure 4.6) for each sowing date. Figure 4.15 confirmed the assumption and shows water stress effects present in the model although mismatched with field conditions. Zahid (2009) reported an nRMSE of 69% and a R^2 of 0.67 in a rainfed field experiment in Australia. The LAI predictions in this chapter had an nRMSE of 182% of the mean observed value, which means the model for predicting LAI is unacceptable.

The poor model performance again suggests an inadequate water stress response. The water stress parameter, Fw, determined the deduction percentage of LAI from its potential values. In short, LAI value = potential LAI × Fw, where Fw $= T_D/SW_s$. Errors might be stemmed from three aspects. Firstly, the response shape could be wrong. Secondly, the soil water supply could be overestimated. Thirdly, the water demand could be underestimated. In general, the Ashley Dene experiment was supply limited while the Iversen12 trial was demand limited because of the difference in PAWC (Section 4.2.1). Increasing demand would be unlikely to affect SWC predictions at Ashley Dene because it was constrained by the limited supply. However, increasing demand would increase the degree of stress and reduce LAI. Increasing demand would likely reduce SWC (to be closer to observed) in Iversen 12 because there was enough water to be extracted. In addition, Fw would likely remain identical since supply can still match the increasing demand; therefore, the performance of predicting plant variables should be intact.

Water demand parameters were represented by the surface soil water evaporation and the canopy conductance. Both parts were quantified in optimal conditions in New Zealand. The current model used a SummerU (first phase) and SummerCona values of 9 mm and 4.4 mm $day^{-1/2}$, which was estimated in a well-drained Templeton silt loam soil (Jamieson et al. 1995). However, U and Cona values differ in different soil types (Foley & Fainges 2014). Hence, the soil evaporation parameter values may be invalid to represent stony soil in

Ashley Dene. To re-calibrate the soil evaporation parameters require a holistic approach due to the correlation between the parameters. Thus, the optimisation approach would be explored in Chapter 5.

Canopy conductance is the concept that APSIM uses to quantify plant canopy response to short wave radiation and estimate plant transpiration (Teixeira et al. 2018). Parameter g_{smax} and R50 were 0.006 m s^{-1} and 100.0 W m^{-2} as default values, respectively. Due to difficulties in measuring g_{smax} and R50, these values are often estimated from fitting predictions against SWC observations. Teixeira et al. (2018) reported g_{smax} and R50 with values of 0.006 m s^{-1} and 175 W m^{-2} under irrigated conditions in a less stony soil type compared with Ashley Dene soils. A model fitting procedure is necessary to find the best fit g_{smax} and R50 values for both sites.

In contrast, LAI predictions in Iversen12 showed an acceptable result with an NSE of 0.6 and an nRMSE of 41% of averaged observations. However, these results need to be viewed with caution to examine whether the model has achieved the right results for the right or wrong reason. Figure 4.4 shows that predicted extraction was lower than measured in the field. Yet the LAI predictions captured the real LAI temporal patterns for I12SD1 to SD5 and SD10. Therefore, optimisation parameterisation of water extraction would be executed in Chapter 5 to re-calibrate water extraction parameters for two sites.

4.4.3 Above-ground biomass

Biomass is a function of intercepted PAR and RUE in the current model structure (Yang et al. 2021). APSIM-Lucerne calculated intercepted PAR based on LAI and extinction coefficient (k; Equation 10). Water stress imposed an incorrect level of effects in both sites because of the incorrect water extraction parameterisation; therefore, biomass predictions deviated from the measured values. Furthermore, the k value used in the model was 0.81 for both sites. However, Sim et al. (2017) reported that k values ranged varied between 0.66 and 0.94 in Ashley Dene dependent on the severity of water stress, but remained constant as 0.94 in Iversen12. Thus, biomass predictions in Ashley Dene were overestimated but they were underestimated in Iversen12.

Inaccurate predictions of LAI should be a contributor to inaccurate predictions of biomass at both sites. This is because LAER was susceptible to water stress. LAER decreased once the ratio of water supply and demand was below 0.9 (Brown et al. 2009, Sim et al. 2017). Although there was no evidence to show canopy architecture changes with different levels of water stress, lucerne has been observed to show paraheliotropism (orient leaves to parallel to incoming sunlight for solar radiation avoidance) as an adaption mechanism to reduce radiation interception and minimise water losses (McCallum 1998, Bell et al. 2007). It seems likely that changes in k occurred when plants experienced severe water stress (Arndt et al. 2001). Sim et al. (2017) observed a reduction of k during summer in Ashley Dene (Section 2.2.1). Therefore, modification of APSIMX-Lucerne may be necessary to use different k values during simulation.

4.4.4 Height

The current lucerne model has no water stress effects on plant height, and therefore this resulted in a large overestimation for both sites (nRMSE 240% and 59%). Earlier field observations in the US showed that lucerne reduced its stem node number and internode length under water-stressed conditions (Brown & Tanner 1983). It is also evident that lucerne stem extension was more sensitive to water stress than leaf area (McCallum 1998, Zahid 2009). More specifically, the leaf to stem weight ratio reportedly doubled when water stress was present (Section 2.2.2). Thus, water stress effects on lucerne height need to be added into the current model to reflect the internode length reduction. Measured height data were absent at both sites. Using an identical function to that used for water stress effects on LAER could be a reasonable starting point, which would be implemented in the next chapter.

4.4.5 Phenology

Main stem node numbers, as the main representation of lucerne phenological development, were simulated accurately (NSE > 0.5). These results confirmed that MSNN was a relatively conservative property of lucerne, and the existing function of water stress effect on phyllochron was appropriate although the model overestimated MSNN in rotations grew in spring and autumn in Ashley Dene (Figure 4.14). Brown et al. (2009) derived a similar function from lucerne grown in the same soil type as Iversen12. Their

water stress function suggested that lucerne would still develop MSNN even at a water supply value of 0 with a phyllochron doubled from that under non-stressed conditions. In contrast, the function used in this chapter stated that the phyllochron requirements would be doubled once soil water supply was half of the demand. The soil type might cause the difference between the two functions. The deep soil at the Iversen research site may ensure lucerne experiences moderate water stress compared with severe water stress at Ashley Dene.

MSNN simulations in Ashley Dene still showed potential for improvement because of their curved pattern (Figure 4.14). This pattern implied that the current model overestimated the maximum MSNN but underestimated early-stage development. Observations suggested that lucerne crops from SD1 to SD5 in Ashley Dene ceased development in the third rotation, although the model continued to produce nodes (**Error! Reference source not found.**). Lucerne would enter dormancy when severe water stress occurs (Bell et al. 2007, Zahid 2009, Orloff et al. 2015). To mimic water stress-induced dormancy, synthetic data of MSNN can be used in combination with an optimisation procedure to re-fine the water stress effect on phyllochron. Additionally, re-parameterisation would make the MSNN prediction in Ashely Dene fit the observation perfectly. However, tweaking parameters without considering the underlying mechanism probably contributes to overfitting problems and worsen MSNN predictions in Iversen12. Nevertheless, a model improvement on MSNN was beyond the scope of this study due to current model performance in phenology being good (NSE > 0.5) and capturing the main trends. Therefore, only a marginal improvement could be potentially gained.

4.5 Conclusion

This chapter took the conventional approach, which was using expert knowledge to guide APSIMX model parameterisation, to re-parameterise water stress effects on lucerne growth and development. Overall, the model performed well for predicting soil water content but poorly for crop growth at Ashley Dene suggesting water supply was simulated well but water demand was under predicted. In contrast, the model generally acted the opposite way in Iversen12 with poor simulations of soil water content and better

predictions of crop growth further supporting an under prediction of water demand. The known sources of errors would be addressed in the next chapter as follows:

- Soil water supply parameters were inadequately tested at Iversen12 because the under-prediction in demand meant the model failed to mimic the soil water extraction pattern in the field. Thus, parameter KL and RFV would be re-parameterised.
- The poor performance of LAI predictions in Ashley Dene was probably due to the incorrect level of water stress the current function imposed. Therefore, soil water demand parameters require investigations. The soil water demand parameters consist of two groups: plant transpiration (g_{smax} and R50) and soil surface evaporation (U and Cona) parameters.

A manual parameterisation of these parameters would be time-consuming and subjective. Hence, an automated parameterisation approach with a customised optimisation procedure could be the alternative method for parameterising multiple functions in a holistic manner. Details about the automated parameterisation and results were documented in Chapter 5.

The parameters that regulate the following three variables were excluded from the optimisation procedure in the next chapter (reasoning associated with each point).

- Above-ground biomass predictions depend on the LAI predictions. Hence, one assumed that the model performance on above-ground biomass would improve once the correct waster stress effects were applied on LAER in the next chapter. The DM partitioning between leaf and stem would be omitted in the next chapter since this study prioritises the entirety of the above-ground biomass over plant organs.
- The model overestimated lucerne height at both sites because of the lack of a mechanism that captures water stress effects on lucerne height. The interaction between water stress and photoperiod remained unclear due to the insufficient height observation under dryland conditions.

- Predictions of the main stem node number in both sites had the best statistical results compared with other variables. Therefore, this study would not address the related parameters further.

5 ALTERNATIVE APPROACH TO ESTIMATE PARAMETERS SYSTEMATICALLY

5.1 Introduction

Parameterisation of biophysical models for non-measurable variables, such as water extraction rate, is an optimisation problem (Harrison et al. 2019). The main advantages of using optimisation algorithms include 1) objective estimation of parameters, 2) reproducible methodologies, and 3) possibility of automation. This chapter focuses on optimising water-related parameters using APSIMX-Slurp to fit water supply and demand parameters and APSIMX-Lucerne to fit growth response parameters, which addresses Objective 2. Theoretically, both models use the identical soil module. The essential difference between the two models is that APSIMX-Slurp requires user input of parameters for canopy status while APSIMX-Lucerne simulates canopy development based on model configuration (Section 3.5). The requirement of leaf area data as input makes the amount of light interception exact; therefore, APSIMX-Slurp allows users to optimise water-related parameters only.

5.2 Material and method

Experiment ADM2 and I12 were used to experiment with optimisation procedures. Climate and experiment details were described in Chapter 3. This section addresses data preparation for optimisation, the model configuration and the setup of the optimisation procedure.

5.2.1 Data preparation

APSIMX simulations depend on pre-defined parameters and user input files. Daily LAI input data are essential for using the APSIMX-Slurp model. However, field data are often obtained on a weekly or fortnightly basis because of labour costs and weather conditions. Hence, linear interpolation is a typical approach to estimate the daily LAI values in between two sampling dates (Teixeira et al. 2018). The “na.approx” function in the zoo R package (Version 1.8.8) was used for LAI data interpolation (Zeileis & Grothendieck 2005). The function requires a numerical vector with field measurements on the exact sampling dates and missing values (NAs) in between sample dates. The function replaced NAs by assuming LAI increases linearly over time (day). This assumption should hold because lucerne was

managed to stay in the vegetative stage for the simulation period and therefore LAI increased over time. Further, field measurements marked out the overall growth trend for LAI, so daily interpolations were constrained by these measured values.

The changes in canopy architecture shown by the extinction coefficient (k) at Ashley Dene have been documented by Sim et al. (2017). Lucerne k values decreased from 0.94±0.014 to 0.66±0.013 from 30th November 2011 to 1st March 2012, probably in response to water stress. To accommodate these changes, manager scripts (Section 3.5.3) were used in the APSIMX-Slurp model configuration to allow daily k values as input (Details of manager scripts Section 5.2.2). An R function was written to combine daily k and LAI values for each treatment and used as input files for APSIMX-Slurp.

Observation data were prepared in classical format to meet APSIMX requirements. Microsoft Excel was the conventional software used to store observation data for APSIMX. The tabular data structure must be used to arrange observations with two identifier columns named as SimulationName and Clock.Today. Two identifier columns hold information about treatment and dates of observations. It is recommended that the names of the two identifier columns remain intact. Variable names can be named freely, however, they need to match APSIMX output variable names if users want to use certain built-in functionalities. For example, observed and predicted variable names must be identical for joining when users attempt to use post-simulation tools to calculate model-evaluation metrics. In this study, 20 Excel files were generated and each contained 37 columns and corresponding observation rows to its field measurements.

Soil configuration data used the same method as in Section 4.2.2 to derive initial SWC, DUL and LL from field measured SWC. An automatic modification was introduced via the implementation of a workflow manager (R package targets; Section 3.6.3) and APSIMX built-in command-line features. The R package targets orchestrated input data, intermediate processes and outputs to achieve two goals – configuration of APSIMX-Slurp simulation files and supervision of the optimisation process. A series of customised R functions were developed to process tabular field measurements, and transform them to APSIMX parameter values or input files. These R functions were documented and version

controlled on the GitHub repository (https://github.com/frank0434/Master/tree/ch5/02Scripts/R).

Figure 5.1 illustrates a directed acyclic diagram of data preparation for ADSD1 in the experiment ADM2 as an example of data preparation. Experiment design data (nodes on the left), site names and sowing dates are used to establish a workflow that then goes through four layers of intermediate processes and arrives at the extreme right-hand side node. The end node contained APSIMX-Slurp configuration and input data in its required formats. The end node then became the input simulation file for the optimisation pipeline (Figure 5.7). The intermediate processes consisted of importing and transforming (second layer on the left), filtering (third layer), summarising (fourth layer), adjusting (fifth layer) data. Bulk density, plant height, file paths, sowing dates and simulation names could be directly fed into the final node because these data were ready to use. In contrast, LAI and soil water-related parameters required a summarising process to estimate values to represent the field conditions. An arbitrary adjustment was inserted into the workflow due to an apparent overestimation of DUL values derived from the averaged maximum SWC.

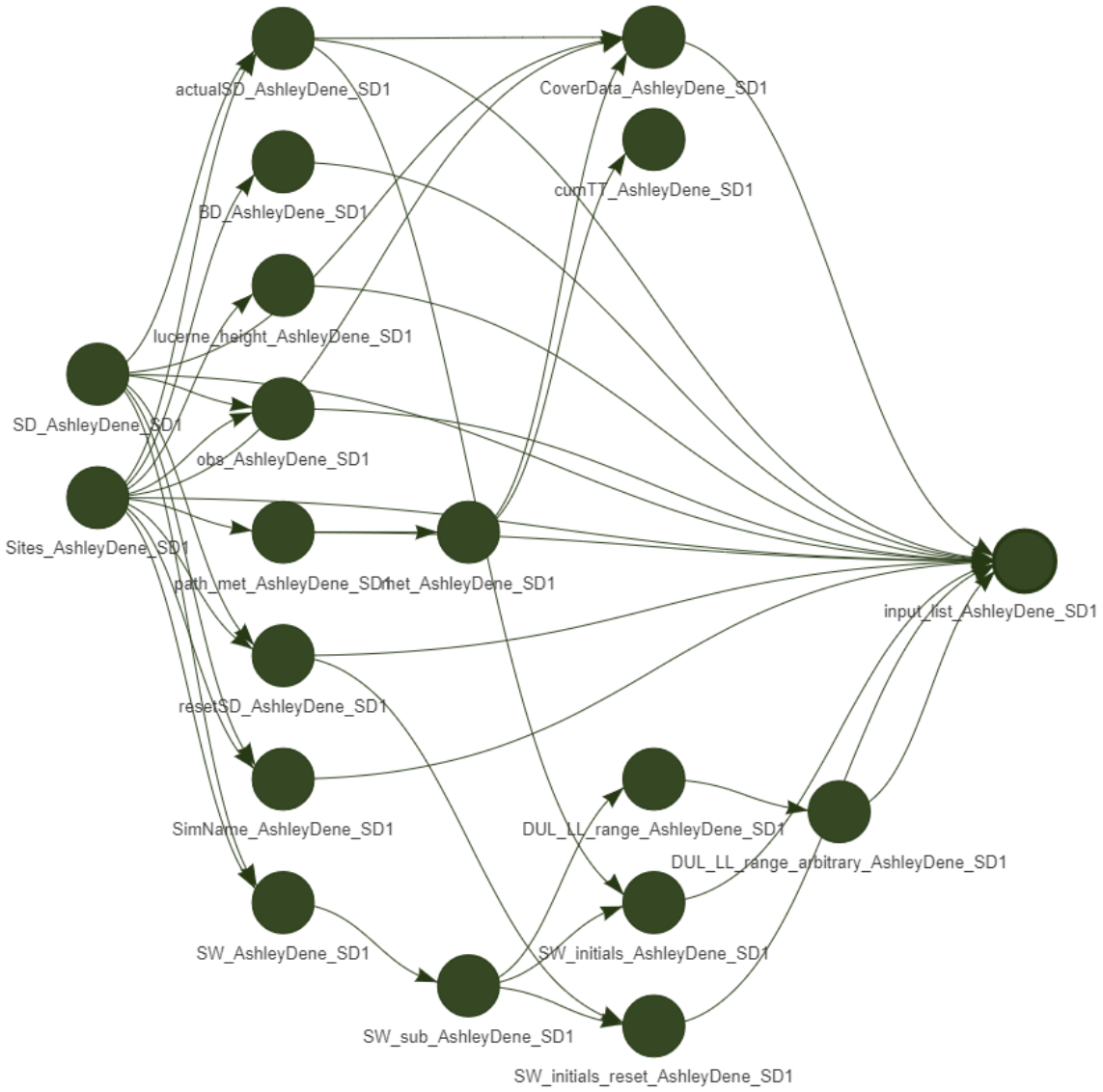

Figure 5.1 A directed acyclic diagram for preparing model inputs and parameter values for sowing date one in Ashley Dene. The graph was generated in R via function `tar_visnetwork" in package targets (Version 0.3.1; Landau 2021)

5.2.2 Model configuration

A single simulation was constructed in the UI (Figure 5.2). This simulation contains minimal components to simulate one treatment in one site. For example, the simulation can be configured to capture ADSD1 in the ADM2 experiment, which includes the exact sowing rules, soil initial conditions and observed data. The hierarchical structure in Figure 5.2 shows the relationships among these essential components. The node "Simulations" is the root. "DataStore" and "Site" are the first level child nodes. The former defines the data input/output (I/O) and the latter determines the mechanism of a given simulation. Two-

second level child nodes were used in the “DataStore” node. “ExcelInput” node declared the file type and path of observed data. The “PredictedObserved” node stated a calculation task for comparing simulated and observed values.

In the “Site” node, five child nodes constituted the simulation process. “Weather” and “Clock” nodes declared the file path of input climate data and simulation period, respectively. “Summary” node provided the feedback functionality to log events during simulation. The “Soil Arbitrator” node determined the depletion mechanism for water and nitrogen in the soil over time based on the plant root system distribution and plant water demand. “Field” node consists of eight child nodes. These nodes defined the soil, plant, management modules, and their interactions with the climate module. For example, “ManagementFolder” provided the interface for users to change internal variables in a report, management, soil, and plant modules. Section 3.5 provided details about these nodes. The vertical order of these nodes does not affect simulations while the horizontal hierarchy can determine whether the simulation completes or fails.

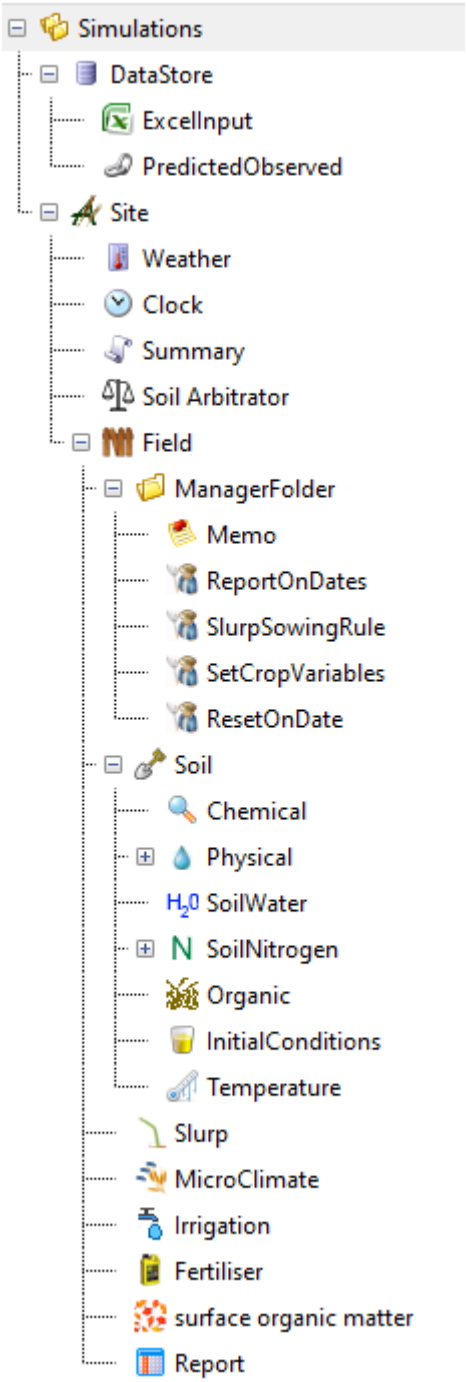

Figure 5.2 Overview of a single simulation file in APSIMX user interface (UI). The simulation file consists of two components: “DataStore” and “Site”. “DataStore” contains the observation of interests with a built-in functionality – “PredictedObserved”. “Site” includes the minimal functional modules to determine the simulation mechanism.

In this study, four management scripts have been used to modify internal variables while the simulation is in progress. Figure 5.3 displays an example script for resetting soil water

content on a particular date. The script was written in C# with APSIMX built-in functions to access and modify internal variables. More specifically, lines 6 to 29 in the script declared the required “Models” and variables. Lines 31 to 45 defined the actual reset command. The command asked the user to input three variables including “ResetDate”, “ResetWater” and “NewSW”, and evaluate the conditions based on user input. The command first checked if the internal clock matched the user-defined reset date. A second evaluation occurred and evaluated if the user wanted to reset SWC when the first evaluation return was true. SWC values in each pre-defined layer were required to update the internal SWC in the soil module once the second evaluation returned true.

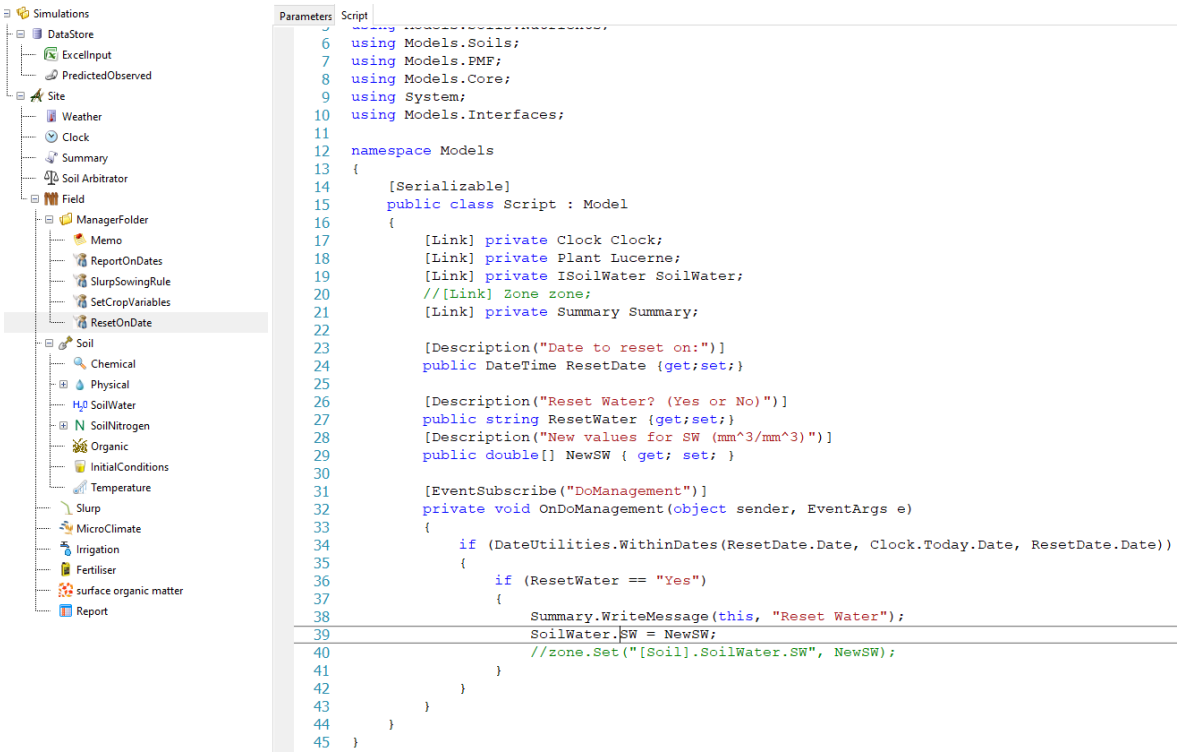

Figure 5.3 An exemplar of APSIMX manager-script. The script allows users to reset soil water content on a particular date.

Table 5.1 lists all four manager scripts and their corresponding functionalities. “ReportOnDates” was disabled in this study because the aim was to estimate parameters rather than diagnose model processes. The reset of three manager scripts was used in conjunction with APSIMX “--edit” flag in the command line to modify simulation configuration automatically. A configuration file is required to provide the modification rules for the APSIMX command “Models.exe”. Figure 5.4 displays a snapshot of such a

configuration file. The file needs to be in plain text format with key and value pairs to instruct APSIMX "Models.exe" where and what to modify. It is worth noting that both relative and absolute paths are acceptable for "Models.exe" to find the variables of interest. The path to the variables must be on the right-hand side of the equal sign, followed by the new values. Relative paths were used in this study to reduce the size of configuration files. For example, "[Site].Name = AshleyDeneSowingDateSD1" means modify the name of node "Site" from its original value to "AshleyDeneSowingDateSD1". Users could obtain the paths to variables of interest via two approaches. Firstly, APSIMX UI provides "Copy path to node" feature, which copies the absolute path to a node into a Window clipboard. However, this approach only provides the user with the path to a node. Users still need to identify the variable name that requires modification. Thus, an alternative approach was developed. In the "Report" node (Figure 5.2), users can type the relative path to a node with a dot to invoke dropdown list selections in APSIMX UI. This approach allows users to identify the path to variables of interest effectively and accurately. This approach was used to construct the configuration file template manually as shown in Figure 5.4.

Table 5.1 detailed functionalities of manager scripts used in the APSIMX-Slurp model.

Manager script	**Functionalities**
ReportOnDates	Report simulation results on particular dates
SlurpSowingRule	Input the agronomic management rules including cultivar, initial sowing depth and sowing date. Declare plant variable parameters including maximum rooting depth, root front velocity, water extraction rate reduction factor and stomatal conductance Define soil surface evaporation parameters including summer and winter U and ConA.
SetCropVariables	Input leaf area index daily, maximum plant height, canopy architecture coefficient.
ResetOnDate	Reset soil water content on a particular date.

```
[Site].Name = AshleyDeneSowingDateSD1
[DataStore].ExcelInput.FileNames =
[SlurpSowingRule].Script.SowingDate = 2010-12-08T00:00:00
[Weather].FileName = C:\Data\Master\01Data\ClimateAndObserved\AshleyDene.met
[SetCropVariables].Script.CoverFile = C:\Data\Master\01Data\ProcessedData\CoverData\LAI_AshleyDene_SD1.csv
[SetCropVariables].Script.MaximumHeight = 390
[Soil].Physical.BD = 1.150,1.150,1.310,1.310,1.950,1.950,1.950,1.950,1.950,1.950,1.950,1.950,1.950,1.950,1.950,1.950,1.950,1.950,1.950,1.950,1.950,1.950
[Soil].InitialConditions.SW = 0.26,0.12,0.1,0.09,0.102,0.098,0.1,0.103,0.101,0.097,0.096,0.1,0.106,0.106,0.114,0.117,0.112,0.109,0.11,0.11,0.114,0.118
[Soil].Physical.DUL = 0.54,0.194,0.158,0.135,0.118,0.114,0.111,0.115,0.115,0.11,0.106,0.116,0.114,0.13,0.138,0.134,0.126,0.128,0.122,0.116,0.128,0.147
[Soil].Physical.SlurpSoil.LL = 0.126,0.08,0.074,0.076,0.069,0.07,0.07,0.07,0.069,0.07,0.073,0.079,0.084,0.086,0.092,0.096,0.094,0.095,0.095,0.095,0.098,0.1
[Soil].Physical.SAT = 0.54,0.194,0.158,0.135,0.118,0.114,0.111,0.115,0.115,0.11,0.106,0.116,0.114,0.13,0.138,0.134,0.126,0.128,0.122,0.116,0.128,0.147
[Soil].Physical.AirDry = 0.126,0.08,0.074,0.076,0.069,0.07,0.07,0.07,0.069,0.07,0.073,0.079,0.084,0.086,0.092,0.096,0.094,0.095,0.095,0.095,0.098,0.1
[Soil].Physical.LL15 = 0.126,0.08,0.074,0.076,0.069,0.07,0.07,0.07,0.069,0.07,0.073,0.079,0.084,0.086,0.092,0.096,0.094,0.095,0.095,0.095,0.098,0.1
[ResetOnDate].Script.ResetDate = 2011-06-25
[ResetOnDate].Script.ResetWater = Yes
[ResetOnDate].Script.NewSW = 0.266,0.189,0.153,0.125,0.112,0.104,0.107,0.112,0.106,0.102,0.104,0.109,0.114,0.121,0.129,0.121,0.124,0.115,0.114,0.114,0.125,0.11
[Soil].Physical.SlurpSoil.KL[1:22] = 0.06
[SlurpSowingRule].Script.RFV = 12
[SlurpSowingRule].Script.KLReductionFactor = 0.005
[SlurpSowingRule].Script.MaxG = 0.008
[SlurpSowingRule].Script.R50 = 200
[SlurpSowingRule].Script.SummerU = 10
[SlurpSowingRule].Script.SummerCona = 5
[SlurpSowingRule].Script.WinterU = 4
[SlurpSowingRule].Script.WinterCona = 2
```

Figure 5.4 A snapshot of a configuration file for the APSIMX command to modify the simulation file.

Table 5.2 Description of parameters in customised APSIMX-Slurp

Model	ID	parameter	category	lower	upper	unit	layer
Slurp	3	KL	Soil water supply	0	0.5	$mm^3\ mm^{-3}$	TRUE
Slurp	4	RFV	Soil water supply	0	50	$mm\ day^{-1}$	FALSE
Slurp	5	KLR*	Soil water supply	0	0.01	NA	FALSE
Slurp	9	g_{smax}	Soil water demand	0	0.1	$m\ s^{-1}$	FALSE
Slurp	10	R50	Soil water demand	0	300	$W\ m^{-2}$	FALSE
Slurp	14	SummerU	Soil water demand	0	15	mm	FALSE
Slurp	15	WinterU	Soil water demand	0	15	mm	FALSE
Slurp	16	SummerCona	Soil water demand	0	8	$t^{1/2}$	FALSE
Slurp	17	WinterCona	Soil water demand	0	8	$t^{1/2}$	FALSE

**only valid when one assumed that the root distribution in soil profile decayed exponentially.*

5.2.3 Differential evolution algorithm

Storn and Price (1997) proposed the differential evolution (DE) algorithm for parameter optimisation in a system. The algorithm was developed to provide a solution for practitioners in fulfilling four requirements: 1) capable to compute nonlinear and non-differentiable cost functions; 2) efficient computation time, 3) self-organizing which contributes to user-friendly features, and 4) consistent convergence properties. The DE algorithm has been applied in many fields and the implementation in R became available in 2011 (Ardia et al. 2011). This study used the DEoptim R package as the optimisation tool. There are two reasons that the DE algorithm was adapted. Firstly, the DE algorithm used previous iteration results to guide the next parameter value sampling. This contrasts with blind search methods that try to exhaust all possible solutions, therefore the DE algorithm

should reach an optimal solution more quickly (Cortez 2014). The second reason was that the DE algorithm is a global search method (or global optimisation). A global search method initialises multiple solutions in different regions in the search space. Each solution is termed as a population. By having multiple populations potentially the situation that solutions were trapped in local minima can be avoided (Figure 5.5).

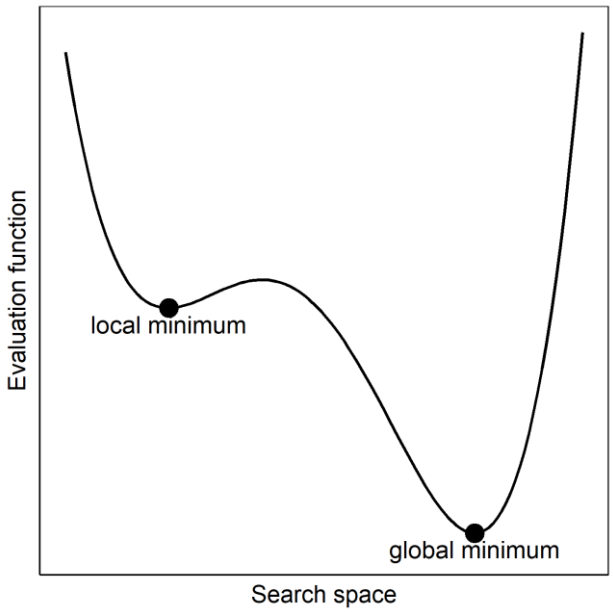

Figure 5.5 Example of local and global minimum in a non-convex function landscape. Adapted from Cortez (2014)

Table 5.3 lists arguments configured for this study in the R function "DEoptim". The essential arguments were "fn", "lower" and "upper". "fn" defines the function for optimising. In this study, a total sum of square (TSS_{SWC}) function was used to be the proxy of APSIMX-Slurp soil water content predictions (Table 5.3). TSS_{SWC} was calculated by subtracting predicted from observed values of profile SWC. Both lower and upper boundaries were determined by experts' knowledge and from the literature. The "control" argument allows users to declare the exact strategy for optimisation. For example, the default strategy in the "DEoptim" function was used, which consists of a mutation expression from previous populations (Storn and Price 1997). The number of populations for each iteration was 90 (9 parameters times 10). This recommended number of populations provides a relatively large pool of parameter values for selecting the next best values. The maximum iteration number was set at 1000 initially and later switched to 500

because early results of optimisation runs indicated convergence was generally reached between 200 and 300 iterations. Parallel computing was selected to be “on”, which meant that all available computer cores were used to do computing. The tolerance value was set to 1×10^{-6}. Feedback arguments, “storepopfrom” and “trace”, were used to store all the intermediate results and reported optimisation results every 200 iterations, respectively. Customised R functions that invoked and modified APSIMX files were passed via the “parVar” argument with the associated input requirements.

Table 5.3 Arguments used in the Deoptim function in R.

Arguments	Description	Value
fn	Function to optimise	$TSS_{SWC} = \sum_{i=1}^{n} (y_i - y)^2$
lower	The lower boundary of the parameter value	Table 5.2
upper	The upper boundary of the parameter value	Table 5.2
control	strategy	$v_{i,g} = old_{i,g} + (best_g - old_{i,g}) + x_{r0,g} + F \times (x_{r1,g} - x_{r2,g})$; $F = 0.8$
	np (number of population)	$np = number\ of\ parameters \times 10$
	itermax (maximum iterations)	Initially, 1000, reduced to 500 for SD 6 to 10
	parallelType	1
	reltol	0.000001
	storepopfrom	1
	trace	200
	packages	'RSQLite', 'here'
	parVar	"APSIMEditFun", "APSIMRun", obj_nms

5.2.4 Automated model optimisation

The current APSIM classic relies on third-party tools to do global optimisation. Two examples exist for the APSIM classic on the APSIM website. The examples used R language and Model-Independent Parameter Estimation and Uncertainty Analysis (PEST), respectively. However, no examples could be found to do automated parameterisation for APSIMX models.

Figure 5.6 shows an abstract level of the optimisation procedure. Domain experts and previous publications contributed to the table that consists of essential parameters with their sensible ranges. The table instructs function development to automatically generate

APSIMX-Slurp files based on the built-in sampling method in the optimisation algorithm. The combination of parameter values that produce the lowest cost will be presented for subsequent APSIMX-Lucerne model parametrisation and evaluation.

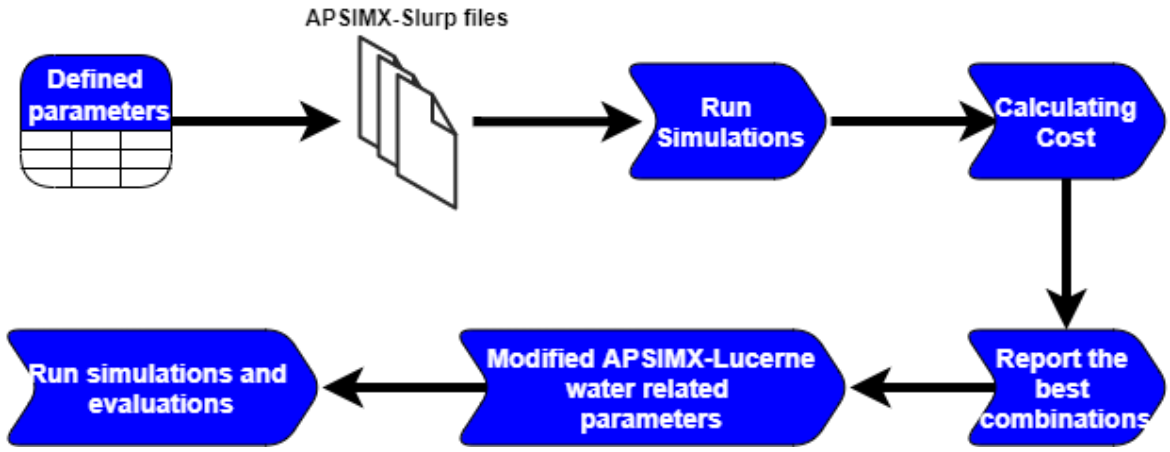

Figure 5.6 Abstract level flowchart for automating the optimisation processes. Defined parameters are prior knowledge that required information from literature review or experts. The parameter table instructed the design and implementation of the optimisation workflow.

A series of customised R functions were developed to implement the automatic workflow for applying the global optimisation method - DEoptim. The workflow manager in R, named "targets", was used extensively to orchestrate the input data, APSIMX-Slurp and configuration files, model output DB files, and communications between R and APSIMX-Slurp model. An environment control R package, named "renv", was also adapted into this study to ensure the reproducibility of the computing environment by capturing software dependences.

Figure 5.7 demonstrates the abstract workflow of the automated model optimisation procedure. First, a single simulation APSIMX file was copied to a designated directory, and modified in place based on the configuration file output from the data preparation (Section 5.2.1). Secondly, the modified APSIMX-Slurp file produced the baseline simulation with correct initial conditions and starting parameter values. Thirdly, the DEoptim function computed the TSS_{SWC}, and generated and selected 90 sets of parameter values according to the strategy set up in the "control" argument. Fourthly, these 90 parameter value

combinations were incorporated into 90 configuration files that instructed APSIMX to create 90 new simulation files. These steps ceased once the maximum iteration number was reached, and the best combination of parameter values was reported in R.

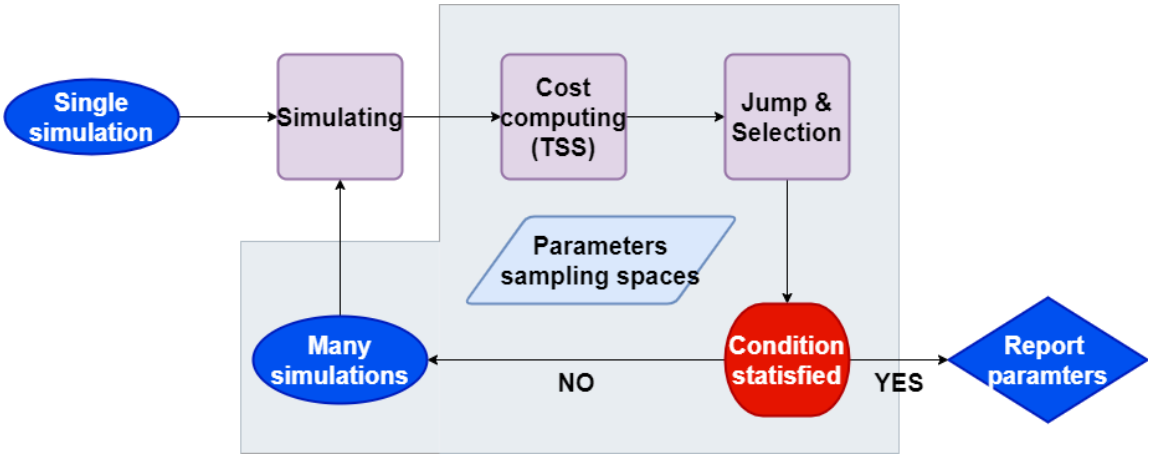

Figure 5.7 An abstract of automated optimisation workflow. Steps in the grey area indicated iterative procedures that were detailed in the DEoptim function.

5.2.5 Re-evaluate Lucerne model performance

Configuration files were saved in a designated directory and compressed into a single file. The configuration files contain the parameter values. The lucerne model was re-configured by the configuration file that produced the minimum TSS_{SWC} value. Statistical metrics, nRMSE, NSE and R^2, were reported to evaluate the model performance (Section 4.2.6). Comparisons were made between the original and re-configuration to quantify the differences between the two methods (manual and optimised configuration).

5.3 Results

5.3.1 Leaf area index interpolation

Daily-interpolated LAI values aligned with field observations (Figure 5.8). Daily LAI and k values were essential input data for APSIMX-Slurp with correct soil characteristics and climate data (Figure 5.1). Figure 5.8 shows the result from the step “Cover data*” in Figure 5.1. The black lines in the figure represent the daily LAI results interpolated from the observed data. The alignment between the lines and dots verified that the model used the correct input data source. As Bennett et al. (2013) and Brown et al. (2018) emphasised, such visual check is an essential tool to verify input data.

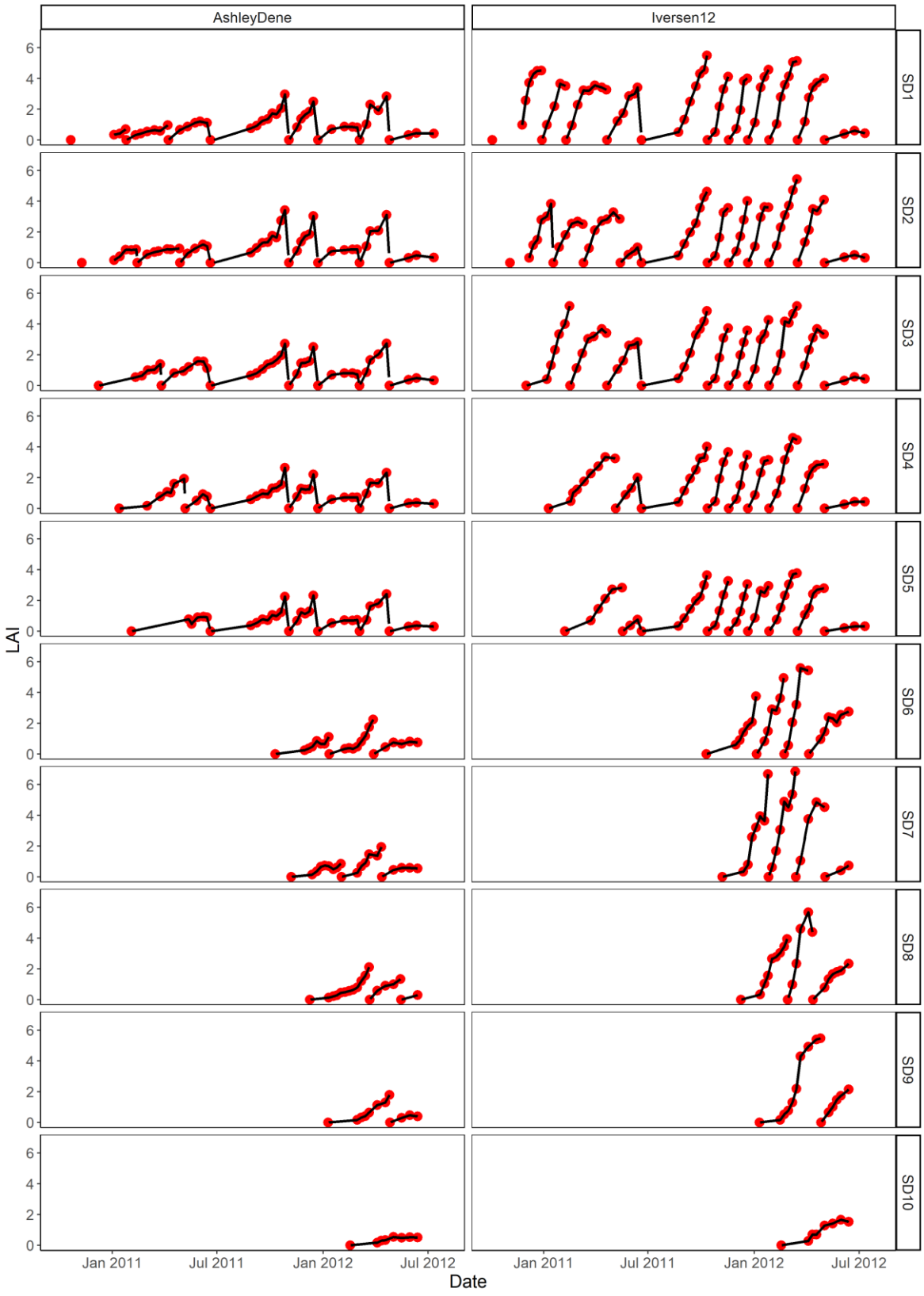

Figure 5.8 Linear interpolation of observed leaf area index for 10 sowing dates over two experiment sites. Observed data are shown as red dots (●) and black lines (—) indicate the daily-interpolated value.

5.3.2 Best values from APSIMX-Slurp optimisation

The objective of optimisation in this study was to minimise the TSS_{SWC} values. Hence, the parameter combination that contributed to minimum overall TSS_{SWC} was reported as the "best values". Figure 5.9 shows the optimisation history for the treatment ADSD1. In each iteration, APSIMX-Slurp simulations were created by 90 sets of parameter combinations (grey dots in Figure 5.9). TSS_{SWC} values were computed for all 90 simulations, and the combination of parameters produced the minimum TSS_{SWC} (red dot in Figure 5.9) which was stored in memory. For ADSD1, the overall best parameter combination was "g_{smax} = 0.064; KL[1:22] = 0.028; KLR = 0.000001; R50 = 291.557; RFV = 11.545; SummerCona = 1.545; SummerU = 0.0004; WinterCona =0.001 ; WinterU = 5.125" (Discussed further in Section *Making sense of the optimised values*).

With regard to canopy conductance parameters, g_{smax} and R50 failed to reach convergence (a large portion of grey dots) although the algorithm reported the best values possible. Additionally, both parameter values (0.064 m s^{-1} and 291 W m^{-2}) were much higher than the reported values (0.006 m s^{-1} and 175 W m^{-2} for g_{smax} and R50, respectively) in the past (Teixeira et al. 2018). In contrast, field observations of lucerne g_{smax} had a much larger value (12 mm s^{-1}) under optimal conditions (Kelliher et al. 1995). Further examination of the canopy conductance function may reveal the drivers of lack of convergence and differences from previous findings. For example, it is important to determine whether or not the parameter was stuck in a local minimum or a saddle point. Unfortunately, it is impossible to examine the true reasons in this study because optimisation only interacted with the TSS_{SWC} function, and had no access to the APSIMX internal functions.

Five parameters, RFV, SummerCona, SummerU, WinterCona and WinterU, started to show signs of convergences after 250 iterations. The optimised RFV value (11.6 mm/day) was within the measurements (11.2 to 14 mm/day) reported by (Meyers et al. 1996) and similar to Sim et al. (2017) field observations (15.1±2.45 mm/day) for seedling crops. Lower KL values with small KLR contributed to the best parameter combinations. In fact, KLR reached

the tolerant value, which was the lowest acceptable parameter value. Consequently, KL values were constant across the soil profile resulted in Equation 11.

For evaporation-related parameters, SummerU (first stage evaporation, Section 2.3.3.2) and WinterU (second stage evaporation) were close to zero. These optimised values indicated that first (direct evaporation from the soil surface) and second stage evaporation (evaporation limited by diffusion) were negligible in summer and winter, respectively for ADSD1 (Discussed further in Section *Making sense of the optimised values*).

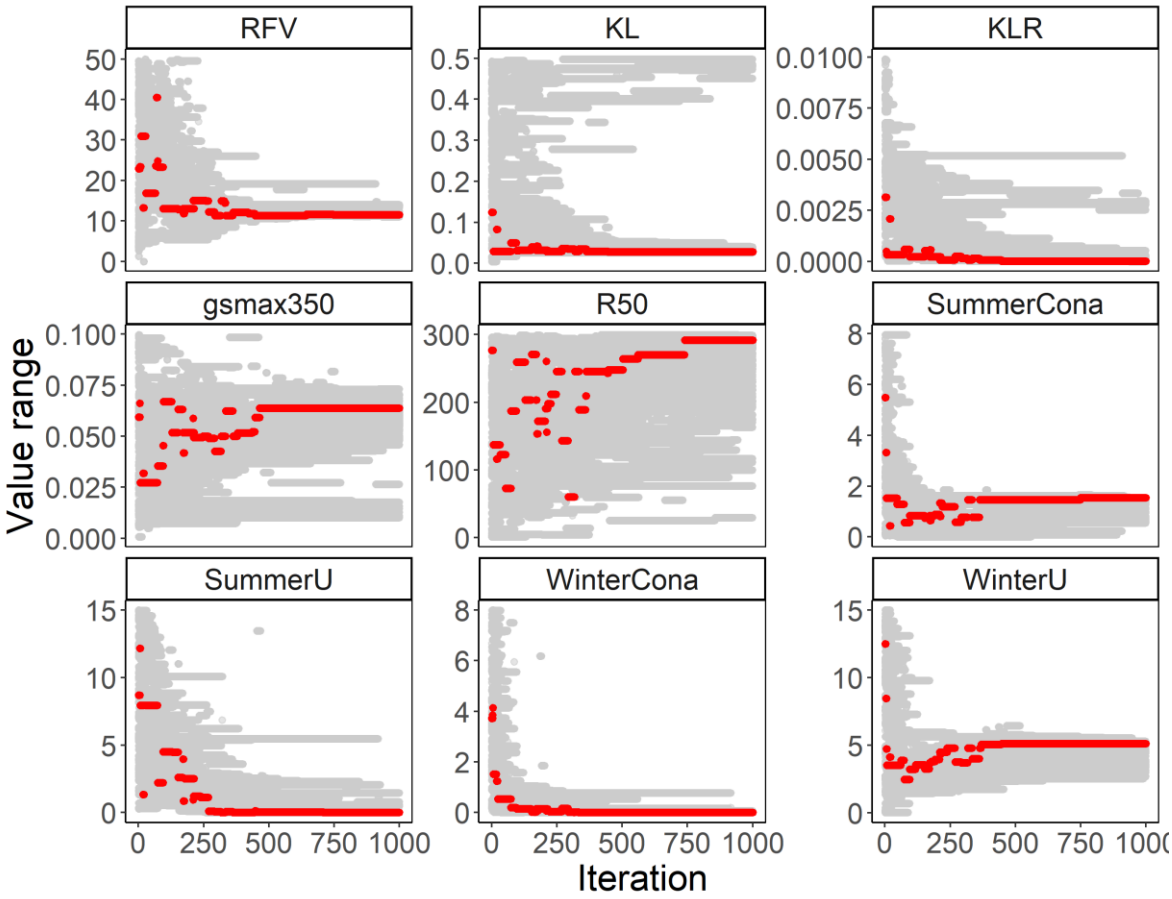

Figure 5.9 Optimisation results of nine parameters for ADSD1. Best parameter values contributing to soil water content minimisation in each iteration are labelled in red dots and searched parameter values are in grey. The X-axis is the number of iterations, and the y-axis represents the value range for each parameter.

The best parameter set contributed to a TSS_{SWC} value of 1032 for ADSD1 for the established crop. A reduction rate of 70% of TSS_{SWC} attributed to the optimisation exercise in

comparison to the initial parameter setting. Figure 5.10 shows the minimum TSS_{SWC} values in each iteration. The main reduction of TSS_{SWC} occurred in the first 100 iterations, where TSS_{SWC} decreased 64% (from 3500 to approximately 1250). The optimisation gain rapidly decreased from iteration number 100 to about 400, and flattened out around iteration 500. The DEoptim algorithm failed to gain more TSS_{SWC} reduction although it continuously explored the parameter spaces for g_{smax} 350, KL, KLR and R50. The results were similar for SD2-SD5 and over both sites; therefore, a maximum iteration number of 500 was used for optimising Sowing dates 6-10 in both experiments.

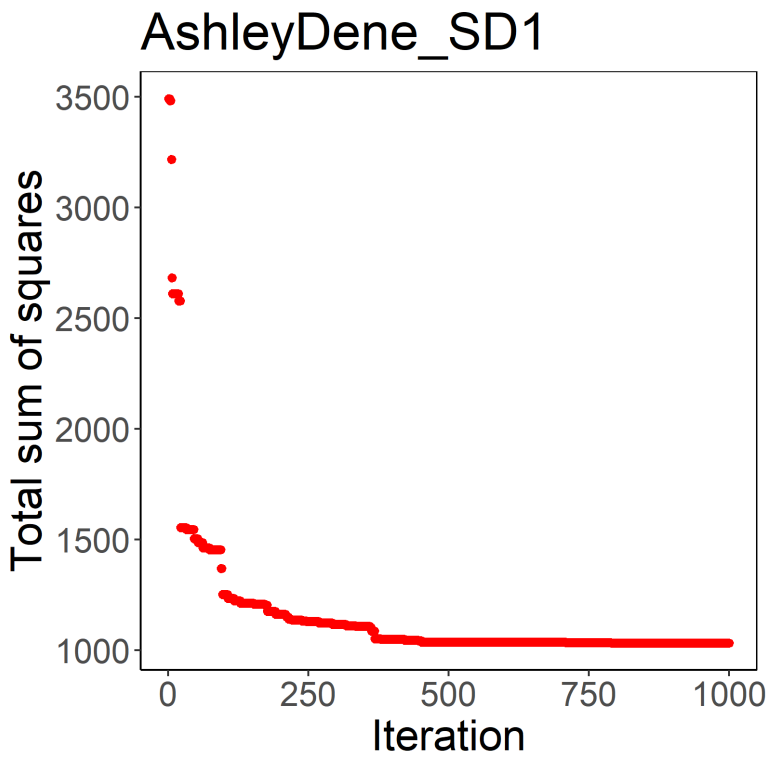

Figure 5.10 The total sum of squares for soil water content prediction after each iteration. The red dot represents the value of the total sum of squares calculated from subtracting profile SWC observations from predictions. Each iteration was one combination of parameter values.

The optimisation results over all treatments were a mixture (Figure 5.11). Lucerne root parameters, RFV, KL and KLR, reached biologically sensible values for ADSD 1 to 5. For example, RFV values started from 11.53 mm day^{-1} for ADSD1 and ended at 18.8 mm day^{-1} for ADSD5. The increases of RFV values with delayed sowing dates could be due to the

small PAW (~130 mm) in this stony soil and the high water demand from lucerne. More specifically, the demand was unsatisfied from ADSD1 to 5; therefore, delayed sowing contributed to accelerated water disappearance. In addition, the combination of KL and KLR values suggested that a constant KL value was acceptable in stony soil with relative low PAWC for established lucerne. However, the optimised values of RFV, KL and KLR for the other sowing dates showed no clear pattern or reasoning, and these are discussed further below.

Canopy conductance parameters in most sowing dates exceeded previously reported values. However, g_{smax} shows a weak seasonal pattern with ADSD1 excluded. Specifically, g_{smax} increased from 0.013 and 0.018 m s^{-1} in ADSD2 and I12SD2 (November sown) to 0.077 and 0.035 m s^{-1} in ADSD5 and I12SD5 (February sown). The pattern was not followed by seedling crops (SD6 to SD10). Moreover, R50 for all treatments diverged into lower or upper boundaries, which suggested that the parameter might be redundant or the parameter range might be too small.

There was consistency among the evaporation related parameters for ADSD1 to 5 except for ADSD2 that had a much higher SummerU (6.5 mm) and lower WinterU (0.28 mm). For example, the SummerCona and WinterU had a value of 4.90±0.430 $t^{1/2}$ and 1.350±0.188 $t^{1/2}$. Furthermore, SummerU and WinterCona were close to zero for ADSD1, SD3, SD4 and SD5. SummerCona ranged from 0.002 to 3.52 $t^{1/2}$ for ADSD6 to ADSD10. However, optimised SummerCona values remained constant (close to zero) for all sowing dates in Iversen12 which indicates that second stage evaporation could be ignored when configuring a lucerne model for deep soils. No clear pattern could be drawn for the rest of the sowing dates.

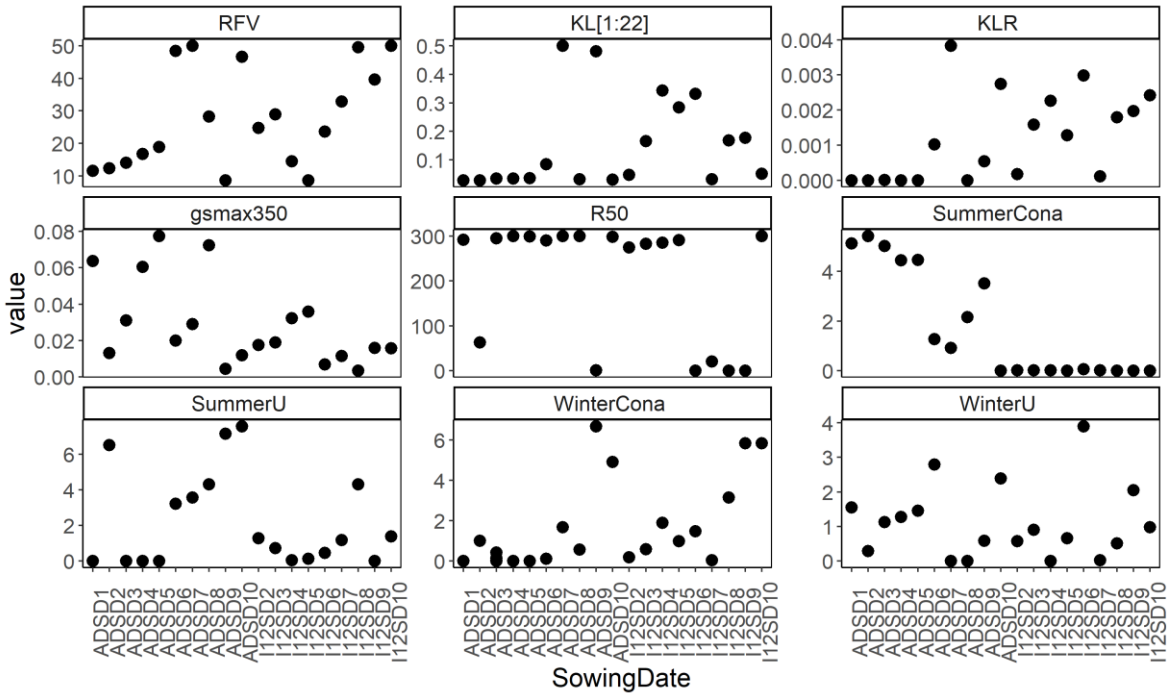

Figure 5.11 The best value combinations over 10 sowing dates over two sites. Sowing date one in Iversen12 was excluded due to the failure of the optimisation procedure for it.

5.3.3 Time expense of optimisation

The most important part of this study was to test whether automatic optimisation of APSIMX model parameters could improve the efficiency of model development. To the best of the author's knowledge, this study is the first that quantified the time cost of data preparation and optimisation processes by using state of the art data science tools. Figure 5.12 shows the overview of the time cost for configuring and optimising nine parameters in the APSIMX-Slurp model with 1000 and 500 iterations. The automatic workflow required 157±3 hours on average to complete 1000 iterations for simulating two years of lucerne crops. In contrast, optimisation time decreased to 31±7.2 hours when there were 500 iterations for simulating seedling crops. Furthermore, 86814±982 simulations were computed to complete 1000 iterations for SD1-5, which yielded approximately 6.5 seconds for each cycle of simulation, evaluation, parameter selection, and APSIMX file modification. Interestingly, a similar number of simulation files were generated for SD6-10 although the time expense was only one fifth compared to SD1-5. An average of 1.3 seconds was the cost for optimising SD6-10 with 500 iterations. This was probably due to the simulation period of SD6-10 being one year shorter than the first five sowing dates.

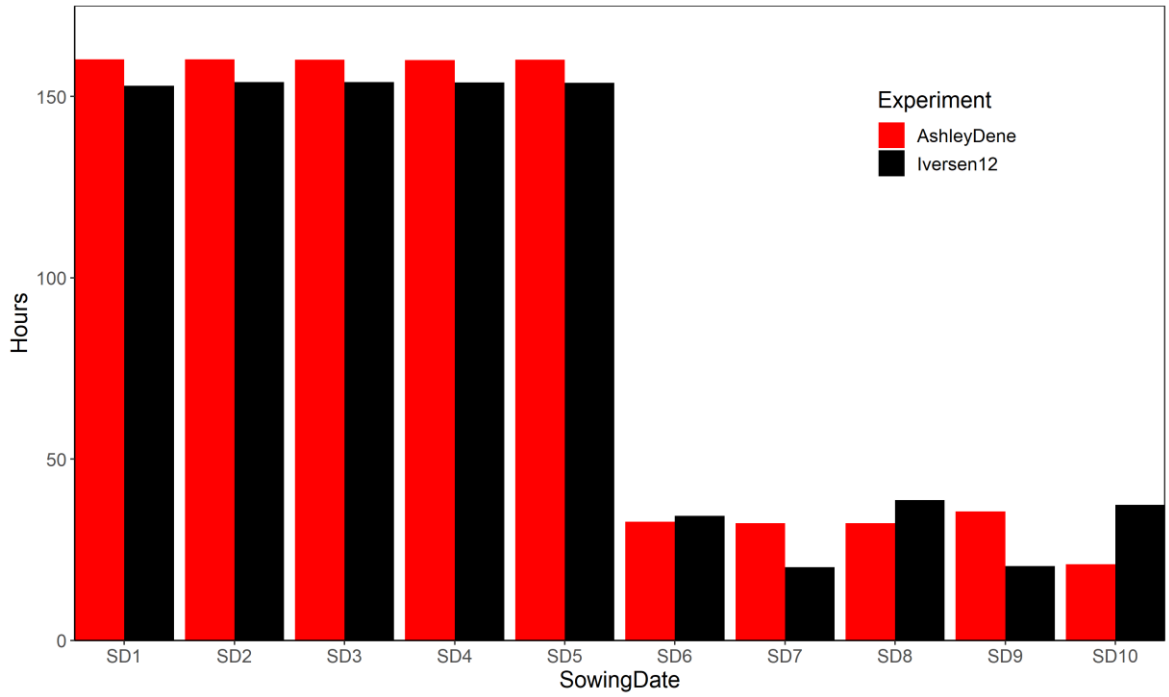

Figure 5.12 Time cost of the optimisation procedure when using R to optimise the APSIMX-Slurp model for nine parameters. Sowing dates 1 to 5 (two-year crops) in both experiment sites were optimised with 1000 iterations while sowing dates 6 to 10 (seedling crops) had 500 iterations.

5.3.4 The goodness of fit in APSIMX-Lucerne

The best parameter values from the optimisation process were incorporated into the APSIMX-Lucerne model to examine the model performance. This section documents the statistic metrics for the model re-evaluation.

5.3.4.1 Profile soil water content

Based on the assumptions that root biomass decayed exponentially across soil profile in APSIMX-Slurp, the optimised parameter values obtained from APSIMX-Slurp optimisation processed increased APSIMX-Lucerne model performance in the Ashley Dene site but decreased it for Iversen12 (Figure 5.13). The nRMSE of SWC gained an overall 1% of deduction for 10 sowing dates in Ashley Dene. The NSE and R^2 values increased from 0.81 to 0.89 and 0.83 to 0.89, respectively. However, the APSIMX-Lucerne model performed worse with optimised parameters than the manual parameterisation regarding SWC in Iversen12. For example, nRMSE increased from 10% to 12%, NSE value dropped from 0.7 to 0.53 and R^2 decreased 10%. The poor model performance in Iversen12 was possibly

attributed to the incorrect assumption of an exponential decay function to describe root biomass distribution across soil profiles.

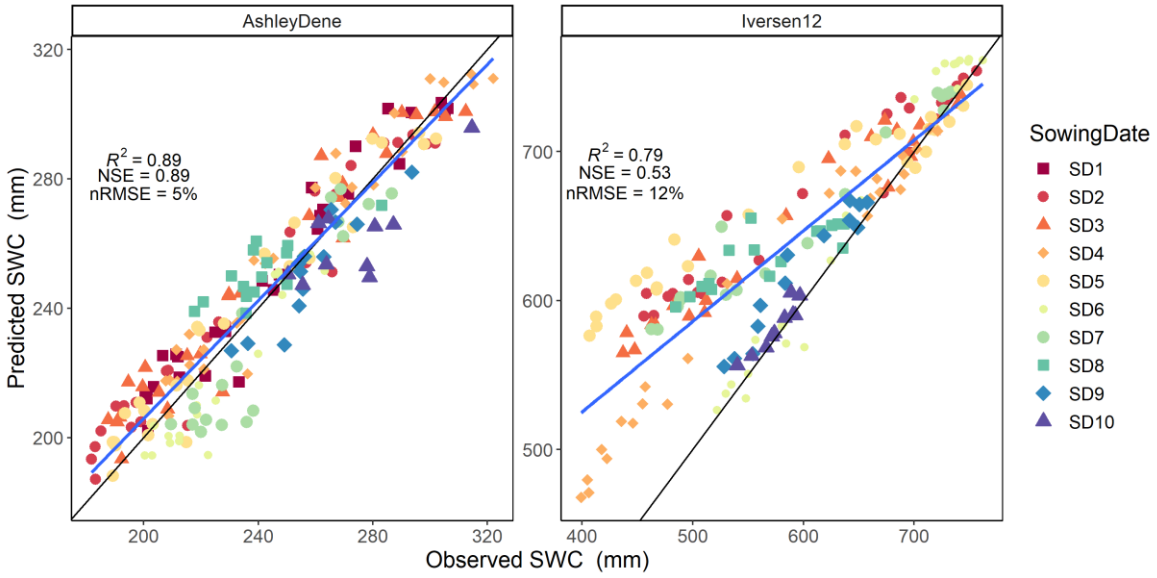

Figure 5.13 Predicted against observed soil water content (SWC) for all 10 sowing dates in AshleyDene and nine sowing dates (I12SD2 to 10) in Iversen12. The black diagonal line is the 1:1 line, the blue line is the regression line and black dots represent the predicted and observed data.

5.3.4.2 Leaf area index

Figure 5.14 shows the APSIMX-Lucerne model evaluation of LAI for two sites. The model performance improved in Ashley Dene while was slightly worse in Iversen12. For the experiment at Ashley Dene, nRMSE was reduced to 154% of mean observed LAI (was 183%; Section 4.3.3.2) after input of the optimised parameter values. R^2, however, decreased to 0.48 compared with the baseline value of 0.55. The NSE value was still negative, which suggests that the model prediction for LAI was no better than using a mean value of LAI. The main reason was that the water stress failed to constrain the canopy development for the first regrowth rotation, and the third rotation when lucerne experienced severe water stress in the field (Appendix 3). The incorrect levels of water stress effects were likely due to underestimated water demand.

In contrast, the experiment in Iversen12 had all three statistic metrics worsen. For example, nRMSE increased 2% from 41%, and NSE value decreased from 0.71 to 0.69 although still could be valid as good performance. R^2 dropped from x to 0.72. Under prediction of LAI

mainly happened in autumn for the seedling crops (I12SD6 to 9). This was likely due to the incorrect configuration of lucerne root parameters that control water extraction.

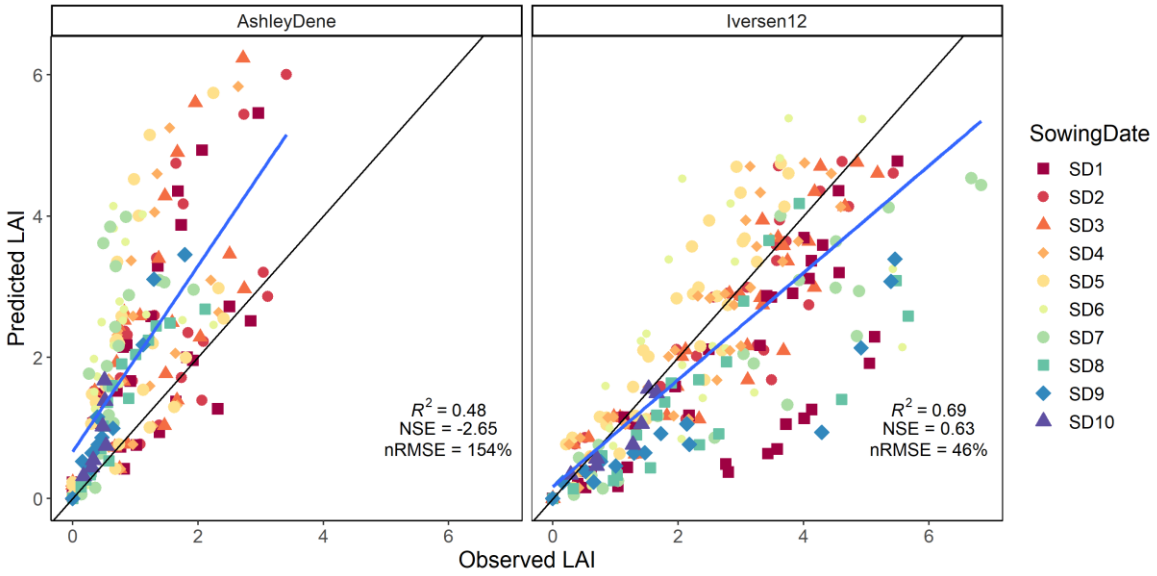

Figure 5.14 Predicted against observed leaf area index (LAI) for all 10 sowing dates in AshleyDene and nine sowing dates (I12SD2 to 10) in Iversen12. The black diagonal line is the 1:1 line, the blue line is the regression line and black dots represent the predicted and observed data.

5.3.4.3 Aboveground biomass

Predictions of shoot biomass were improved in Ashley Dene (Figure 5.15). The nRMSE value of ShootWt in AshleyDene decreased 26% even though the NSE value remained negative. The LeafWt nRMSE increased approximately 18% in comparison with the manually configured model. R^2 values decreased in Ashley Dene after the inclusion of the optimised parameters. For ShootWt, R^2 and NSE increased from 0.46 to 0.60 and -2.66 to -0.27, respectively. On the contrary, R^2 and NSE decreased from 0.61 to 0.48 and 0.56 to 0.37, respectively.

For the Iversen12 experiment, nRMSE values of ShootWt and LeafWt showed more than a 20% of reduction whereas apparent under estimation occurred in LeafWt. The relatively high R^2 value possibly indicates a systematic bias that resulted from a combination of poor predictions in SWC and LAI (Figure 5.13 and Figure 5.14). NSE values increased 43% from 0.46 and 112.5% from -0.48 for ShootWt and LeafWt, respectively. R^2 values remained identical.

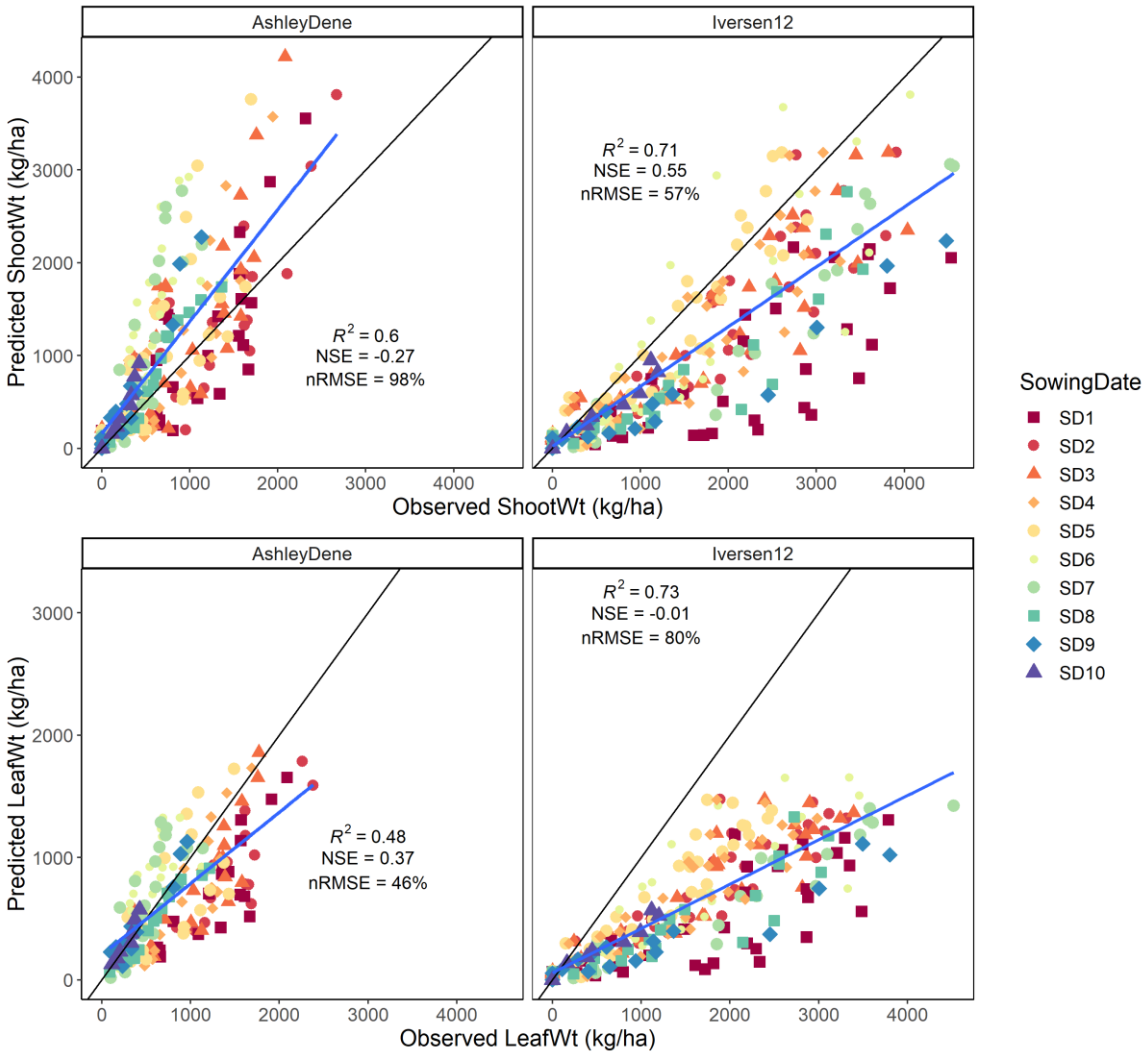

Figure 5.15 Predicted against observed values of aboveground biomass and its forming components including leaf and stem biomass. All available observations for two sites were included except for I12SD1. The black diagonal line is the 1:1 line, the blue line is the regression line and black dots represent the predicted and observed data.

5.3.4.4 Phenology

Simulated results of the main stem node number (MSNN) remained the same as in Chapter 4 (Figure 4.14). The overestimation of MSNN persisted for spring and autumn grew lucerne in Ashley Dene (Detailed in Section **Error! Reference source not found.**).

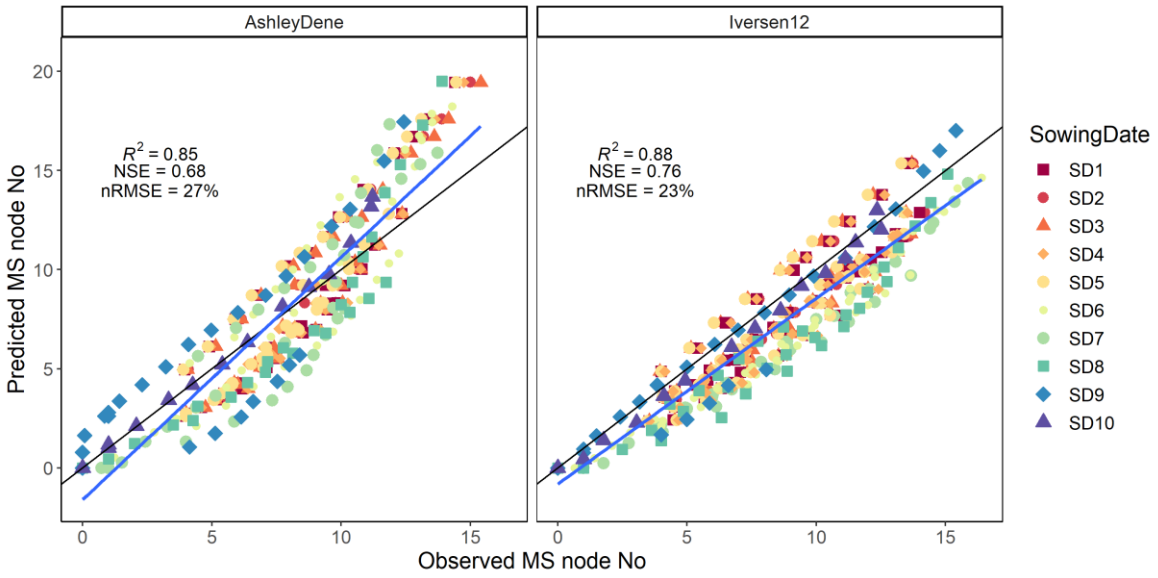

Figure 5.16 Predicted against observed values of main stem node number (MSNN). I12SD1 was excluded. The black diagonal line is the 1:1 line, the blue line is the regression line and black dots represent the predicted and observed data.

5.3.4.5 The ratio of water supply and demand

Figure 5.17 shows the modelled ratio of water supply and demand (Fw) for experiments at both sites. Optimised parameter values imposed water stress effects in early spring for the established crop, and longer autumn stress on both seedling and established crops at Ashley Dene. Longer and more severe water stress was also shown in Figure 5.17 compared with Figure 4.15. Specifically, water shortage in spring (1st September to 30th November) started as early as 18th September 2011 for established crops (SD1 to SD5) in Ashley Dene. Spring water stress on average lasted 24.8±6.8 days for the optimised model compared with 0 days for the baseline model. Furthermore, severe water stress (Fw ≤ 0.5) occurred for 46±13.6 days in the updated model while 28±5.9 days was simulated in the baseline model during summer (1st December to 28th February) for SD1 to SD8. Moreover, autumn water stresses lasted 27.4±8.1 and 18.2±5.8 days in the improved and baseline models, respectively.

In terms of Fw simulations in Iversen12, the result could be misleading due to the incorrect prediction of profile soil water content (Figure 5.13). More specifically, soil water demand parameters (g_{smax}, R50, U and Cona) could be higher in reality than the optimised values in the model. Although the modelled results aligned with empirical observations in Iversen12

(crop showed no sign of water stress under rain-fed conditions), this may be the wrong reason for the right answer.

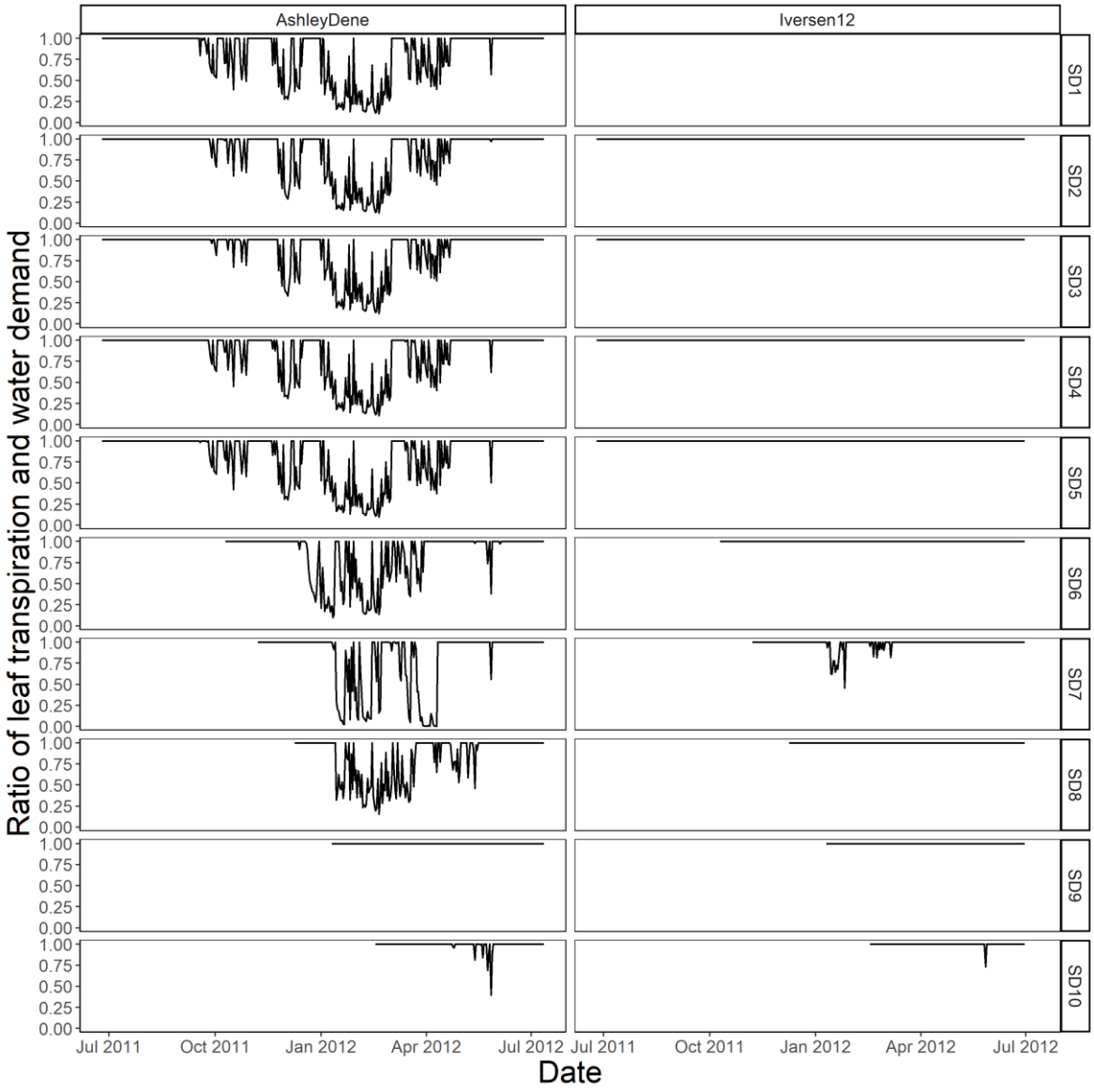

Figure 5.17 Modelled ratio of leaf transpiration and water demand (Fw). Fw ranges from 0 to 1 and is a multiplier to alter leaf growth. A value of 0 represents severe water stress that prevents any growth while 1 means no water stress effects. I12SD1 was excluded.

5.3.4.6 Comparison of statistical metrics

Optimisation marginally improved model performance for Ashley Dene experiments while model performance decreased for Iversen12 Table 5.4. More specifically, predictions for SWC, LAI and ShootWt improved in Ashley Dene via optimised parameter values although

none of the metrics had rating changes (Table 3.7). These negligible improvements and degradations may indicate two implications. First, it might be necessary to re-calibrate the relationships between water stress levels and their effects on different lucerne organs. Secondly, the soil-plant interaction mechanism requires more investigation. Potential pathways will be discussed in the next section.

Table 5.4 Comparison of statistical metrics from manual configured and optimised APSIMX-Lucerne model for five main variables in two experiment sites. R^2 and NSE values are unitless and between 0 and 1. nRMSE is calculated as RMSE concerning mean observation. Table 3.7 shows performance ratings.

Experiment	Varaible	Statistical metrics	Manual configured	Optimised
Ashley Dene	SWC	R^2	0.83	0.89
Ashley Dene	SWC	NSE	0.81	0.89
Ashley Dene	SWC	nRMSE	6%	5%
Ashley Dene	LAI	R^2	0.55	0.48
Ashley Dene	LAI	NSE	-4.14	-2.65
Ashley Dene	LAI	nRMSE	182%	154%
Ashley Dene	ShootWt	R^2	0.63	0.6
Ashley Dene	ShootWt	NSE	-1.29	-0.27
Ashley Dene	ShootWt	nRMSE	132%	98%
Ashley Dene	LeafWt	R^2	0.61	0.48
Ashley Dene	LeafWt	NSE	0.56	0.37
Ashley Dene	LeafWt	nRMSE	39%	46%
Ashley Dene	MSNN	R^2	0.85	0.85
Ashley Dene	MSNN	NSE	0.68	0.68
Ashley Dene	MSNN	nRMSE	27%	27%
Iversen12	SWC	R2	0.91	0.79
Iversen12	SWC	NSE	0.72	0.53
Iversen12	SWC	nRMSE	9%	12%
Iversen12	LAI	R2	0.75	0.69
Iversen12	LAI	NSE	0.71	0.63
Iversen12	LAI	nRMSE	41%	46%
Iversen12	ShootWt	R2	0.78	0.71
Iversen12	ShootWt	NSE	0.64	0.55
Iversen12	ShootWt	nRMSE	51%	57%
Iversen12	LeafWt	R2	0.8	0.73
Iversen12	LeafWt	NSE	0.05	-0.01
Iversen12	LeafWt	nRMSE	78%	80%
Iversen12	MSNN	R2	0.88	0.88
Iversen12	MSNN	NSE	0.76	0.76
Iversen12	MSNN	nRMSE	23%	23%

5.4 Discussion

Objective 2 was addressed in this chapter. An automated workflow in R provided the infrastructure to achieve automated parameterisation for APSIMX models. Water relevant parameters were first optimised via the APSIMX-Slurp model. The best combination parameter set reconfigured the APSIMX-Lucerne model. The updated APSIMX-lucerne model was then re-evaluated.

Automated parameterisation

Similar work was reported for APSIM classic by using the PEST software (Akponikpè et al. 2010; Chen et al. 2016; Harrison et al. 2019). Soil water parameters optimised by PEST were rejected by Akponikpè et al. (2010) due to insignificant improvement of model performance. In contrast, both Chen et al. (2016) and Harrison et al. (2019) highlighted the benefits of adopting an automated parameterisation strategy for crop model development. For example, PEST software increased time efficiency and reproducibility of model parameterisation. However, APSIMX and STICS development teams draw more and more attention to solutions in R, which validates the current study for making potential contributions to the process-based modelling community.

Furthermore, the majority of existing publications reported the improvement of statistical metrics for the goodness of fit (Seidel et al. 2018). Indeed, statistical metrics provide the quantifiable approach to evaluate model performance and make model comparison possible. Nevertheless, model development may fall into an engineering problem that Passioura (1996) criticised when modellers emphasise parameterising the model to best align with its observation data. Automated parameterisation could be a solution to avoid modellers failing to engineer their models unintentionally and gain underlying physiological mechanisms efficiently (Harrison et al. 2019).

This study established a holistic workflow that covers APSIMX model development from data preparation to automated parameterisation. It can be seen as one possible implementation of standardising model development procedures proposed by experienced modellers (Bennett et al. 2013, Brown et al. 2018). By leveraging the R software, advanced data science tools, such as the Bayesian framework, could be easily adapted into the workflow for capturing the extensive prior knowledge in the modelling

community (Sexton et al. 2016). On the contrary, the drawbacks are as apparent as the benefits. For example, modellers must be familiar with physiology, simulation models and are up-to-date about data science toolchains, which can be overwhelming.

Making sense of the optimised values

The soil module was calibrated based on the assumption of lucerne root decaying exponentially from top to bottom of the soil profile (Section 3.5.5). This assumption of root distribution in APSIMX-Slurp effectively predicted soil water changes in an Eyre shallow silt loam soil with nRMSE < 30% and NSE = 0.8 (Teixeira et al. 2018). Better statistical metrics were achieved in the study with the optimised soil water extraction parameters (RFV, KL, KLR) following the same assumption for Ashley Dene. The nRMSE and NSE were 5% and 0.89, respectively. Although the overall SWC predictions are satisfying in statistical terms, caution is needed due to the possibility of "getting the right answer with the wrong reason". Previous field experiments suggested that RFV is less likely to exceed 20 mm day^{-1} for lucerne seeding crops (Dolling et al. 2005, Sim et al. 2017), whereas 11 optimised RFV in this study have RFV values doubled (nine of them were seedling crops from both sites). Regarding KL and KLR, optimised values for ADSD1 to 5 aligned with previous in-field and –silico studies (Sim et al. 2017, Teixeira et al. 2018). By contrast, a KL value close to 0.5 (means that soil water is depleted in 2 days) is unrealistic. Therefore, ADSD7 and 9 are the case of "wrong reasons" (Figure 5.11).

The worsening model performance in SWC for Iversen12 indicates that the assumption of the exponential decaying root is probably incorrect (Figure 5.13). Sim et al. (2017) reported KL values that were greater (approximately 0.03) in the middle (0.8~1.7 m) than (approximately 0.02) in the top and bottom of the soil profile. However, Brown et al. (2009) used a model-fitting procedure to estimate KL layer by layer and found that the KL values were greater in the topsoil profile and gradually decreased with increased soil depth in similar soils. Furthermore, a constant KL value of 0.029 day^{-1} (0~2 m) was observed from two established lucerne cultivars in silt loam soil in Argentina (Dardanelli et al. 1997). Later, this constant KL value was adapted into the first APSIM-legume model for lucerne (Robertson et al. 2002). These conflicting results highlight the complexity of soil-root interactions, which desperately needs innovative approaches to investigate. Morandage et

al. (2021) published a hybrid approach (using both experiments and modelling) to explore the causal effects of stone contents and root architecture development using field rhizotron facilities. Although the idea of rhizotron is not new, it may shed light on the mechanism of root-soil water with new sensing technologies.

Canopy conductance parameters (g_{smax} and R50) are correlated (Equation 9; Snow et al. 2004). However, the majority of optimised value pairs (16 out of 20) show no sign of association (Figure 5.11). In addition, it may be unrealistic that R50 values separated into either below 50 or close to 300 W m^{-2}. These mixture results could be a signal that these two parameters became irrelevant for simulating water supply limited environments (Brown et al. 2012). Figure 5.17 shows 9 out of 10-regrowth lucerne crops experienced water stress in Ashley Dene. Nevertheless, efforts may be needed to understand the effects of water stress on g_{smax} because constant water stress may violate the assumption of the transpiration model in MicroClimate modules. The original equation developed by Kelliher et al. (1995) assumed that the plant was grown under optimal conditions (plentiful water and optimal temperature). It is unclear whether or not the hyperbolic function (Equation 9) still holds for lucerne under severe water stresses. Alternatively, the canopy conductance approach proposed by Brown et al. (2012) may be the appropriate approach for New Zealand conditions since it is independent of g_{smax} and R50.

In contrast, the assumption of the transpiration model is likely to be satisfied in Iversen12. This is because of the high PAWC (330 mm) in Iversen12 soils. Therefore, the undesired optimised values may be a result of incorrect water extraction parameterisation for Iversen12 experiments. Optimisation might yield sensible results once the water extraction parameters are reconfigured via a model-fitting approach (Brown et al. 2009).

Two-stage evaporation parameters (U and Cona) were reported to be sensitive to E_o that is highly influenced by soil water recharge in Australian dryland conditions (Yunusa & Sedgley 1994; Kodur 2017). U was negatively correlated with E_o while Cona operated inversely. To be specific, ADSD1 had a SummerU value of 0.0004 mm day^{-1} with the corresponding Cona value of 1.545 mm $day^{-1/2}$. Conversely, WinterU and WinterCona were 5.125 mm day^{-1} and 0.001 mm $day^{-1/2}$, respectively. These optimised values could be

explained by the evaporation mechanism described by Yunusa et al. (1994). Stage I evaporation tended to be short when E_o was high. This is because high E_o dries the waterfront in soil rapidly. Consequently, Stage II evaporation kicks in swiftly and compensates the E_o due to adequate soil water storage. In contrast, E_o is often low during winter, which contributes to continuously stage I evaporation (high U). As a result, soil water storage is largely depleted when stage II evaporation starts (low Cona). However, it has to be noted that Yunusa et al. (1994) summarised the mechanism from bare soil experiments with fine texture soils. Therefore, such an evaporation mechanism may be invalid for stony soils with lucerne grown. In Figure 5.11 it is evident that inversely correlated U and Cona values were inconsistent, such as ADSD2 and I12SD2 to 10.

Kodur (2017) addressed the limitations of the two-stage evaporation model, which assumed a persistent relationship between soil evaporation and atmosphere without considering crop performance influenced by seasonal variations. Stony soil may violate the underlying mechanism of Ritchie's equation. Furthermore, two sets of U and Cona with different values could provide similar soil evaporation (Kodur 2017). Such equifinality issues may be the cause of no clear pattern in I12 for soil evaporation parameters. However, Kodur 2017 demonstrated a modelling approach to examine the relationship between soil evaporation and choices of U and Cona in four soil types in Australian dryland conditions with wheat grown. Application of this approach in dryland lucerne with New Zealand soil type data may shed light on the understanding of soil evaporation mechanism.

Model performance

Negligible improvements were achieved from introducing the optimisation approach. This indicated the absence of a key biophysical mechanism. Plant height was the missing mechanism for parameterising APSIMX-lucerne correctly to response water limited conditions. Unfortunately, the current existing data was insufficient to derive or optimise a sensible relationship between water stress levels and plant height. Hence, further experiments may be necessary.

Modellers tend to invest the bulk of the effort in model performance improvement (Ojeda et al. 2016; Seidel et al. 2018). This tendency could lead to problems such as over

parameterisation and poor generalisation (Her & Chaubey 2015). In addition, Ojeda et al. (2021) analysed the error sources during model calibration based on previous publications, which highlighted the importance of rigorous data quality checks before model development. As Keating (2020) addressed that crop models demand a rigorous scientific approach to ensure the "right answers for the right reasons", model performance metrics should be only used as guidelines with caution. For example, SWC predictions for Iversen12 experiments were rated as "Good" for all three metrics (Figure 5.13), whereas the underlying soil water extraction mechanism was incorrect.

To ensure a rigorous scientific approach for model development, proper concepts and tools from other domains are necessary (Seidel et al. 2018; Keating 2020; Razavi et al. 2021), especially for junior modellers who have limited observations of possible processes. For example, Corral-Acero et al. (2020) proposed the concept of using statistical models to aid process-based model development for advancing cardiovascular research. Furthermore, sensitivity analysis has been addressed as a promising tool to facilitate data-driven system modelling (Razavi et al. 2021).

5.5 Conclusions

The current model with optimised parameter values is good for simulating soil water changes with regrowth lucerne in dryland conditions. Further investigation is needed to understand the root water extraction patterns in deep soils. Re-configured APSIMX-Lucerne model with optimised parameter values gained negligible improvements for Ashley Dene experiments while worsened performance for Iversen12 experiments. Despite this automated parameterisation provided an efficient and objective approach for APSIMX model parameterisation. Hence, the conclusion of this chapter is as follows:

- An exponential decay function might be inadequate to describe the soil water extraction pattern in the deep silt loam soil of Iversen 12.
- The water demand parameters failed to impose the correct level of water stress on lucerne variables at Ashley Dene and were unable to extract the correct amount of water from the soil in Iversen12.

- Only one season worth of data was used to calibrate the parameters with no independent data set to evaluate the model. Therefore, the data might be insufficient to describe the complexity of the dryland system and the overfitting problem still exists.

6 GENERAL DISCUSSION AND CONCLUSIONS

Lucerne is a promising pasture crop for New Zealand hill country farmers to cope with challenges imposed by climate change and nitrogen deficiency. APSIMX-Lucerne model has been actively developing in the last four years to facilitate researchers and farmers for informed decision-making. The available prototype APSIMX-Lucerne model was constrained by lacking water deficiency effects on the plant. Therefore, this study aimed to calibrate the APSIMX-Lucerne model to simulate lucerne growth and development responses to water stress by using historical datasets. However, conventional APSIMX model development is unstainable regarding time and resources expenses. State-of-art data science concepts and tools were implemented across this study to explore the possibilities of applying data science to process-based model development.

Chapter 1 briefly introduced the benefits of lucerne for New Zealand farmers and the rationale for applying process-based models to facilitate decision-making. Study objectives were addressed in Chapter 1. Three objectives were fulfilled by:

1. A literature review (Chapter 2) clarified the physiological processes of lucerne in the presence of water stress.
2. A dedicated chapter (Chapter 3) described datasets, model components and model development approaches.
3. Chapter 4 experimented with the conventional approach of model parameterisation, which extracted parameter values from existing publications.
4. Chapter 5 demonstrated the alternative approach for model parameterisation in a holistic fashion.

6.1 Lucerne responses to water stress (Chapter 2)

Water stress occurs for lucerne when crops are unable to extract the amount of water for satisfying the transpiration demand. To incorporate water stress effects in the APSIMX-Lucerne model developed with data collected under optimal conditions, the physiological processes of lucerne responses to water stress must be clarified. Chapter 2 delimited the major mechanisms of lucerne responses to water stress from the literature.

Effects of water stress on lucerne follow chronological orders. Generally, crop growth was affected prior to crop development. In the field, researchers observed morphological changes in lucerne leaves (Plate 2.1) as an immediate response to water stress. This change contributes to reduced leaf area, followed by suboptimal radiation interception. Hence, reduced dry matter accumulation eventually leads lucerne to prioritise resources to the root over the canopy. Stem elongation and leaf expansion are constrained due to suboptimal cell turgor pressure.

From a modelling perspective, water stress affects lucerne growth via the reduced canopy. Consequently, subsequent processes including radiation interception, carbon assimilation and node appearances could be affected. Previous studies have established the relationships between water stress level and LAER (Figure 2.2). An increase in phyllochron was reported when water supply was half of the water demand (Figure 2.6). Radiation use efficiency declined when soil water supply was 90% of the optimal conditions (Figure 2.8). These relationships of water stress effects on lucerne were incorporated into the APSIMX-Lucerne model. The actual implementation of physiological processes in APSIMX was documented in Chapter 3. Chapter 3 briefly introduced the field experiments (Section 3.1) and key methods for data analyses (Section 3.6) and model evaluation (Section 3.7).

6.2 APSIMX-Lucerne model performance with published parameter values (Chapter 4)

Manually configured the APSIMX-Lucerne model produced excellent statistical metrics for the overall profile SWC predictions in both sites overall 10 sowing dates (Section 4.3.3.1). However, the poor performance of aboveground variables suggested that the model did not capture the correct mechanism at the right levels. For example, profile SWC predictions in Ashely Dene aligned with seasonal observations while the implemented water stress effects failed to impose the correct level of reduction on LAI (Section 4.3.3.2). In contrast, seasonal SWC predictions in Iversen12 misaligned with observations despite the good statistical metrics. Interestingly, predictions of aboveground variables, such as LAI and biomass, performed better than for Ashley Dene (Section 4.3.3.2) although the profile SWC predictions indicated that less water was extracted (Section 4.3.1.2).

6.3 Optimisation for parameterisation (Chapter 5)

The optimisation procedure was set up in R to estimate the combination of nine water-related parameters that provided the minimum distances from profile SWC prediction to observation. The procedure was defined in a workflow management package to achieve automation (Section 5.2.4). Despite the mixture from optimisation results, automated parametrisation enabled data-driven parameter estimation in quantifiable time frames (Section 5.3.3). There were 19 out of 20 treatments that reached convergences after the optimisation processes. However, not all optimised parameter values aligned with current biophysical findings (Figure 5.11). Potential causes were discussed (Section 5.4).

6.4 Future work

New approaches and tools are necessary to sustain the development of mechanistic models. This study implemented the workflow manager to facilitate a global optimisation process for APSIMX model parameterisation. However, the number of parameters and optimisation iterations were limited to nine and 1000 maximum concerning the computation cost. These limitations will be easily eliminated by the application of a high-performance computing (HPC) system. New Zealand eScience Infrastructure (NeSI) has been used by researchers nationwide to study climate change, genetic information and ocean movements. The application of NeSI on crop modelling will be a bright avenue for future work.

During the optimisation processes, APSIMX-Lucerne was a “black box” and one could only use the output of the “black box” to signal the optimisation directions. Such behaviour concealed the driving factors that hindered optimisation convergences. Archontoulis et al. 2014 reconstructed the phenological equation in R based on the APSIM-Soybean model. Although the optimisation failed to converge, their approach provided an efficient way to marry modern data science with mechanistic model development. For example, global sensitivity analysis could be used to assess the importance of model parameters. Furthermore, statistical approaches, such as machine learning (ML), may help modellers to extract known parameters or identify hidden processes without having to consolidate dozens of literature when data are adequate. Corral-Acero et al. 2020 proposed an

interface between statistical and mechanistic models, which opens another avenue for crop modellers.

In terms of crop physiology, lucerne seedling crop is defined as a thermal time requirement in the APSIMX-Lucerne model. This is less likely appropriate for water-stressed lucerne as Sim 2014 pointed out that the lucerne crop may remain as a seedling crop until the root dry matter reaches a certain threshold. However, the current model structure was destabilised by the implementation of a dry matter defined crop development. Further investigation is needed to underpin the partitioning mechanism for lucerne grown under water deficit conditions. Especially, the mechanism of water stress effects on lucerne height was lacking, which requires height measurements under dryland conditions to quantify the relationship. Moreover, soil water extraction patterns are different in different soil types. An exponential decay function of root distribution across soil profile was applied to stony soil in Chapter 5. However, this assumption was inappropriate for deep soil. An improved workflow may be required to carry out layer by layer soil parameter estimation.

6.5 Conclusions

Alternative approaches for APSIMX model parameterisation are necessary to be explored and formalised into documentations due to the unsustainability of the conventional approach. Sound biological mechanism knowledge is indeed critical to ensure the model represents the real world appropriately. The governance of modelling data also has to be considered to accelerate model development. These points may only be achieved by applying modern data science.

REFERENCES

Akponikpè PBI, Gérard B, Michels K, Bielders C. 2010. Use of the APSIM model in long term simulation to support decision making regarding nitrogen management for pearl millet in the Sahel. *European Journal of Agronomy 32*: 144-154.

APSIMInitiative. *SoilWat*. Retrieved: https://www.apsim.info/documentation/model-documentation/soil-modules-documentation/soilwat/

APSIMInitiative. NA. *Construct a factorial simulation in the User Interface*. Retrieved 2021-11-08 https://www.apsim.info/support/apsim-training-manuals/construct-a-factorial-simulation-in-the-user-interface/.

Ardia D, Boudt K, Carl P, Mullen K, M., Peterson B, G. 2011. Differential Evolution with DEoptim. *The R Journal 3*: 27.

Arndt SK, Clifford SC, Wanek W, Jones HG, Popp M. 2001. Physiological and morphological adaptations of the fruit tree Ziziphus rotundifolia in response to progressive drought stress. *Tree Physiology 21*: 705-715.

Avery DT, Avery F, Ogle G, Wills BD, Moot DJ. Adapting farm systems to a drier future.

Avice JC, Lemaire G, Ourry A, Boucaud J. 1997. Effects of the previous shoot removal frequency on subsequent shoot regrowth in two Medicago sativa L. cultivars. *Plant and Soil 188*: 189-198.

Bai WM, Li LH. 2003. Effect of irrigation methods and quota on root water uptake and biomass of alfalfa in the Wulanbuhe sandy region of China. *Agricultural Water Management 62*: 139-148.

Bell LW, Williams AH, Ryan MH, Ewing MA. 2007. Water relations and adaptations to increasing water deficit in three perennial legumes, Medicago sativa, Dorycnium hirsutum and Dorycnium rectum. *Plant and Soil 290*: 231-243.

Bellocchi G, Rivington M, Donatelli M, Matthews K. 2010. Validation of biophysical models: issues and methodologies. A review. *Agronomy for Sustainable Development 30*: 109-130.

Black A, Anderson S, Dalgety S. 2017. Identification of pasture mixtures that maximise dry matter yield. *Journal of New Zealand Grasslands 79*: 103-109.

Bonhomme R. 2000. Bases and limits to using 'degree.day' units. *European Journal of Agronomy 13*: 1-10.

Bouton JH. 2012. An overview of the role of lucerne (Medicago sativa L.) in pastoral agriculture. *Crop and Pasture Science 63*: 734-738.

Boyer JS, Bowen B. 1970. Inhibition of oxygen evolution in chloroplasts isolated from leaves with low water potentials. *Plant physiology 45 5*: 612-615.

Brisson N. 1998. An analytical solution for the estimation of the critical available soil water fraction for a single layer water balance model under growing crops. *Hydrology and Earth System Sciences 2*: 221-231.

Brisson N, Gary C, Justes E, Roche R, Mary B, Ripoche D, Zimmer D, Sierra J, Bertuzzi P, Burger P, Bussière F, Cabidoche YM, Cellier P, Debaeke P, Gaudillère JP, Hénault C, Maraux F, Seguin B, Sinoquet H. 2003. An overview of the crop model STICS. *European Journal of Agronomy 18*: 309-332.

Brown DM. 1987. CERES-Maize: A simulation model of maize growth and development. *Agricultural and Forest Meteorology 41*: 339.

Brown H, Moot D. Leaf appearance in seedling lucerne crops.

Brown H, Huth N, Holzworth D. 2018. Crop model improvement in APSIM: Using wheat as a case study. *European Journal of Agronomy 100*: 141-150.
Brown HE. 2004. Understanding yield and water use of dryland forage crops in New Zealand. 288.
Brown HE, Moot DJ, Pollock KM. 2005a. Herbage production, persistence, nutritive characteristics and water use of perennial forages grown over 6 years on a wakanui silt loam. *New Zealand Journal of Agricultural Research 48*: 423-439.
Brown HE, Moot DJ, Teixeira EI. 2005b. The components of lucerne (Medicago sativa) leaf area index respond to temperature and photoperiod in a temperate environment. *European Journal of Agronomy 23*: 348-358.
Brown HE, Moot DJ, Teixeira EI. 2006. Radiation use efficiency and biomass partitioning of lucerne (Medicago sativa) in a temperate climate. *European Journal of Agronomy 25*: 319-327.
Brown HE, Moot DJ, Fletcher AL, Jamieson PD. 2009. A framework for quantifying water extraction and water stress responses of perennial lucerne. *Crop and Pasture Science 60*: 785-794.
Brown HE, Jamieson PD, Moot DJ. 2012. Predicting the transpiration of lucerne. *European Journal of Agronomy 43*: 9-17.
Brown HE, Huth NI, Holzworth DP, Teixeira EI, Zyskowski RF, Hargreaves JNG, Moot DJ. 2014. Plant Modelling Framework: Software for building and running crop models on the APSIM platform. *Environmental Modelling & Software 62*: 385-398.
Brown PW, Tanner CB. 1983. Alfalfa Stem and Leaf Growth during Water Stress 1 *Agronomy Journal 75*: 799-805.
Carter PR, Sheaffer CC. 1983. Alfalfa Response to Soil Water Deficits. I. Growth, Forage Quality, Yield, Water Use, and Water‐Use Efficiency 1 *Crop Science 23*: 669-675.
Chacon S, Straub B. 2014. *Pro git*: Springer Nature.
Chen C, Lawes R, Fletcher A, Oliver Y, Robertson M, Bell M, Wang E. 2016. How well can APSIM simulate nitrogen uptake and nitrogen fixation of legume crops? *Field Crops Research 187*: 35-48.
Collino DJ, Dardanelli JL, De Luca MJ, Racca RW. 2005. Temperature and water availability effects on radiation and water use efficiencies in alfalfa (Medicago sativa L.). *Australian Journal of Experimental Agriculture 45*: 383-390.
Corral-Acero J, Margara F, Marciniak M, Rodero C, Loncaric F, Feng Y, Gilbert A, Fernandes JF, Bukhari HA, Wajdan A, Martinez MV, Santos MS, Shamohammdi M, Luo H, Westphal P, Leeson P, DiAchille P, Gurev V, Mayr M, Geris L, Pathmanathan P, Morrison T, Cornelussen R, Prinzen F, Delhaas T, Doltra A, Sitges M, Vigmond EJ, Zacur E, Grau V, Rodriguez B, Remme EW, Niederer S, Mortier P, McLeod K, Potse M, Pueyo E, Bueno-Orovio A, Lamata P. 2020. The 'Digital Twin' to enable the vision of precision cardiology. *European Heart Journal 41*: 4556-4564B.
Cortez P. 2014. *Modern Optimization with R*. Cham: Springer International Publishing.
Dalgliesh N, Foale M. 1998. *Soil Matters—Monitoring Soil Water and Nutrients in Dryland Farming Systems*.
Dardanelli JL, Bachmeier OA, Sereno R, Gil R. 1997. Rooting depth and soil water extraction patterns of different crops in a silty loam Haplustoll. *Field Crops Research 54*: 29-38.
Dardanelli JL, Ritchie JT, Calmon M, Andriani JM, Collino DJ. 2004. An empirical model for root water uptake. *Field Crops Research 87*: 59-71.

Dolling PJ, Latta RA, Ward PR, Robertson MJ, Asseng S. 2005. Soil water extraction and biomass production by lucerne in the south of Western Australia. *Australian Journal of Agricultural Research 56*: 389.

Douglas JA. 1986. The production and utilization of lucerne in New Zealand. *Grass and Forage Science 41*: 81-128.

Ministry for the Environment. 2018. *Climate Change Projections for New Zealand: Atmosphere Projections Based on Simulations from the IPCC Fifth Assessment, 2nd Edition*.

Erice G, Louahlia S, Irigoyen JJ, Sanchez-Diaz M, Avice JC. 2010. Biomass partitioning, morphology and water status of four alfalfa genotypes submitted to progressive drought and subsequent recovery. *Journal of Plant Physiology 167*: 114-120.

Fick GW, Holt DA, Lugg DG. 1988. Environmental Physiology and Crop Growth. *Alfalfa and Alfalfa Improvement*, pp. 163-194.

Foley J, Fainges J. 2014. *Soil evaporation – how much water is lost from northern crop systems and do agronomic models accurately represent this loss?*

Hanson B, Putnam D, Snyder R. 2007. Deficit irrigation of alfalfa as a strategy for providing water for water-short areas. *Agricultural Water Management 93*: 73-80.

Harrison MT, Roggero PP, Zavattaro L. 2019. Simple, efficient and robust techniques for automatic multi-objective function parameterisation: Case studies of local and global optimisation using APSIM. *Environmental Modelling and Software 117*: 109-133.

Hay RKM, Porter JR. 2006a. Limiting factors and the achievement of high yield. *The Physiology of Crop Yield*, pp. 180-202.

Hay RKM, Porter JR. 2006b. Interception of solar radiation by the canopy. *The Physiology of Crop Yield*, pp. 36-72.

He D, Wang E, Wang J, Robertson MJ. 2017. Data requirement for effective calibration of process-based crop models. *Agricultural and Forest Meteorology 234-235*: 136-148.

Her Y, Chaubey I. 2015. Impact of the numbers of observations and calibration parameters on equifinality, model performance, and output and parameter uncertainty. *Hydrological Processes 29*: 4220-4237.

Hewitt AE. 2010. *New Zealand soil classification*: Manaaki Whenua Press.

Holzworth D, Huth NI, Fainges J, Brown H, Zurcher E, Cichota R, Verrall S, Herrmann NI, Zheng B, Snow V. 2018. APSIM Next Generation: Overcoming challenges in modernising a farming systems model. *Environmental Modelling & Software 103*: 43-51.

Holzworth DP, Snow V, Janssen S, Athanasiadis IN, Donatelli M, Hoogenboom G, White JW, Thorburn P. 2015. Agricultural production systems modelling and software: Current status and future prospects. *Environmental Modelling & Software 72*: 276-286.

Huth NI, Bristow KL, Verburg K. 2012. SWIM3: Model use, calibration, and validation. *Transactions of the ASABE 55*: 1303-1313.

Jamieson PD, Porter JR, Wilson DR. 1991. A test of the computer simulation model ARCWHEAT1 on wheat crops grown in New Zealand. *Field Crops Research 27*: 337-350.

Jamieson PD, Francis GS, Wilson DR, Martin RJ. 1995. Effects of water deficits on evapotranspiration from barley. *Agricultural and Forest Meteorology 76*: 41-58.

Jing Q, Qian B, Bélanger G, VanderZaag A, Jégo G, Smith W, Grant B, Shang J, Liu J, He W, Boote K, Hoogenboom G. 2020. Simulating alfalfa regrowth and biomass in eastern Canada using the CSM-CROPGRO-perennial forage model. *European Journal of Agronomy 113*.

Jones JW, Antle JM, Basso B, Boote KJ, Conant RT, Foster I, Godfray HCJ, Herrero M, Howitt RE, Janssen S, Keating BA, Munoz-Carpena R, Porter CH, Rosenzweig C, Wheeler TR. 2017. Brief history of agricultural systems modeling. *Agricultural Systems 155*: 240-254.

Keating B, Carberry PS, Hammer G, Probert ME, Robertson MJ, Holzworth D, Huth NI, Hargreaves J, Meinke H, Hochman Z, McLean G, Verburg K, Snow V, Dimes J, Silburn D, Wang E, Brown S, Bristow K, Asseng S, Smith C. 2003. An overview of APSIM, a model designed for farming systems simulation. *European Journal of Agronomy 18*: 267-288.

Keating BA. 2020. Crop, soil and farm systems models – science, engineering or snake oil revisited. *Agricultural Systems 184*: 102903.

Kelliher FM, Leuning R, Raupach MR, Schulze ED. 1995. Maximum conductances for evaporation from global vegetation types. *Agricultural and Forest Meteorology 73*: 1-16.

Kirkham MB. 2005. Field Capacity, Wilting Point, Available Water, and the Non-Limiting Water Range. *Principles of Soil and Plant Water Relations*, pp. 101-115.

Kodur S. 2017. Improving the prediction of soil evaporation for different soil types under dryland cropping. *Agricultural Water Management 193*: 131-141.

Landau WM. 2021. The targets R package: A dynamic Make-like function-oriented pipeline toolkit for reproducibility and high-performance computing. *Journal of Open Source Software 6*: 2959.

Lehmann P, Assouline S, Or D. 2008. Characteristic lengths affecting evaporative drying of porous media. *Physical Review E 77*: 056309.

Littleboy M, Silburn D, Freebairn D, Woodruff D, Hammer G, Leslie J. 1992. Impact of soil erosion on production in cropping systems .I. Development and validation of a simulation model. *Soil Research 30*: 757-774.

Lucas RJ, Gow NG, Nicol AM, Lincoln U. 2012. *Ashley Dene : Lincoln University farm : the first 100 years*. Lincoln, N.Z.]: Lincoln, N.Z. : Lincoln University.

Luo Y, Meyerhoff PA, Loomis RS. 1995. Seasonal patterns and vertical distributions of fine roots of alfalfa (Medicago sativa L.). *Field Crops Research 40*: 119-127.

Luo YZ, Li G, Yan G, Liu H, Turner NC. 2020. Morphological features and biomass partitioning of lucerne plants (medicago sativa l.) subjected to water stress. *Agronomy 10*.

McCallum MH. 1998. The water and nitrogen dynamics of a lucerne-based farming system in the Victorian Wimmera.

McIntyre BD, Riha SJ, Flower DJ. 1995. Water uptake by pearl millet in a semiarid environment. *Field Crops Research 43*: 67-76.

McLaren RG, Cameron KC. 1996. *Soil Science: Sustainable Production and Environmental Protection*: Oxford University Press.

Meyers LL, Russelle MP, Lamb JAFS. 1996. Fluridone reveals root elongation differences among alfalfa germplasms. *Agronomy Journal 88*: 67-72.

Mills A, Moot DJ, Mckenzie B. Cocksfoot pasture production in relation to environmental variables.

Mills A, Lucas RJ, Moot DJ. 2015a. 'MaxClover' grazing experiment: I. Annual yields, botanical composition and growth rates of six dryland pastures over nine years. *Grass and Forage Science 70*: 557-570.
Mills A, Lucas RJ, Moot DJ. 2015b. 'MaxClover' grazing experiment II: Sheep liveweight production from six grazed dryland pastures over 8 years. *New Zealand Journal of Agricultural Research 58*: 57-77.
Mills A, Smith MC, Moot DJ. 2016. Relationships between dry matter yield and height of rotationally grazed dryland lucerne. *Journal of New Zealand Grasslands 78*: 185-196.
Mohanty P, Boyer JS. 1976. Chloroplast Response to Low Leaf Water Potentials: IV. Quantum Yield Is Reduced 1. *Plant Physiology 57*: 704-709.
Molloy L. 1998. *Soils in the New Zealand landscape : the living mantle*. 2nd ed. / with revised appendix by Allan Hewitt.. ed. Lincoln, N.Z.]: Lincoln, N.Z. : New Zealand Society of Soil Science.
Monteith JL, Greenwood DJ, Penman HL, Pereira SC, Hamlin MJ, Mansell-Moullin M. 1986. How do crops manipulate water supply and demand? *Philosophical Transactions of the Royal Society of London. Series A, Mathematical and Physical Sciences 316*: 245-259.
Moore AD, Holzworth DP, Herrmann NI, Brown HE, de Voil PG, Snow VO, Zurcher EJ, Huth NI. 2014. Modelling the manager: Representing rule-based management in farming systems simulation models. *Environmental Modelling and Software 62*: 399-410.
Moot D, Robertson MJ, Pollock K. 2001. Validation of the APSIM-Lucerne model for phenological development in a cool-temperate climate. 10th Australian Agronomy Conference, Hobart. *Tasmania*: 1-5.
Moot D, Brown HE, Teixeira E, Pollock K. 2003. *Crop growth and development affect seasonal priorities for lucerne management*: Citeseer, 18-19 p.
Moot DJ, Scott WR, Roy AM, Nicholls AC. 2000. Base temperature and thermal time requirements for germination and emergence of temperate pasture species. *New Zealand Journal of Agricultural Research 43*: 15-25.
Moot DJ, Brown HE, Pollock KM, Mills A. Yield and water use of temperate pastures in summer dry environments.
Moot DJ. 2012. An overview of dryland legume research in New Zealand. *Crop and Pasture Science 63*: 726-733.
Moot DJ. A review of recent research and extension on dryland lucerne in New ZealandNew Zealand Society of Animal Production.
Moot DJ, Hargreaves J, Brown HE, Teixeira EI. 2015. Calibration of the APSIM-Lucerne model for 'Grasslands Kaituna' lucerne crops grown in New Zealand. *New Zealand Journal of Agricultural Research 58*: 190-202.
Moot DJ, Bennett SM, Mills A, Smith MC. 2016. Optimal grazing management to achieve high yields and utilisation of dryland lucerne. *NZ Grassland Association 78*: 27-34.
Moot DJ, Anderson PVA, Anderson LJ, Anderson DK. 2019. Animal performance changes over 11 years after implementing a lucerne grazing system on Bog Roy Station. *Journal of New Zealand Grasslands*.
Moot DJ. 2003. *Legumes for dryland pastures : proceedings of a New Zealand Grassland Association*. Lincoln University: New Zealand Grassland Association.

Morandage S, Vanderborght J, Zörner M, Cai G, Leitner D, Vereecken H, Schnepf A. 2021. Root architecture development in stony soils. *Vadose Zone Journal 20*: e20133.
Moriasi DN, Arnold JG, Van Liew MW, Bingner RL, Harmel RD, Veith TL. 2007. Model evaluation guidelines for systematic quantification of accuracy in watershed simulations. *Transactions of the ASABE 50*: 885-900.
Mortenson MC, Schuman* GE, Ingram LJ. 2004. Carbon Sequestration in Rangelands Interseeded with Yellow-Flowering Alfalfa (Medicago sativa ssp. falcata). *Environmental Management 33*: S475-S481.
Mouradi M, Bouizgaren A, Farissi M, Ghoulam C. 2018. Assessment of Deficit Irrigation Responses of Moroccan Alfalfa (Medicago Sativa L.) Landraces Grown Under Field Conditions. *Irrigation and Drainage 67*: 179-190.
Neal JS, Fulkerson WJ, Lawrie R, Barchia IM. 2009. Difference in yield and persistence among perennial forages used by the dairy industry under optimum and deficit irrigation. *Crop and Pasture Science 60*: 1071-1087.
Ojeda JJ, Pembleton KG, Islam MR, Agnusdei MG, Garcia SC. 2016. Evaluation of the agricultural production systems simulator simulating Lucerne and annual ryegrass dry matter yield in the Argentine Pampas and south-eastern Australia. *Agricultural Systems 143*: 61-75.
Or D, Lehmann P, Shahraeeni E, Shokri N. 2013. Advances in Soil Evaporation Physics—A Review. *Vadose Zone Journal 12*: vzj2012.0163.
Orloff S, Putnam D, Bali K. 2015. *Drought Tip: Drought Strategies for Alfalfa*.
Pang J, Yang J, Ward P, Siddique KHM, Lambers H, Tibbett M, Ryan M. 2011. Contrasting responses to drought stress in herbaceous perennial legumes. *Plant and Soil 348*: 299.
Passioura JB. 1983. Roots and drought resistance. *Agricultural Water Management 7*: 265-280.
Passioura JB. 1996. Simulation Models: Science, Snake Oil, Education, or Engineering? *Agronomy Journal 88*: 690-694.
Pearson CJ, Hunt lA. 1972. Effects of temperature on primary growth and regrowths of alfalfa. *Canadian Journal of Plant Science 52*: 1017-1027.
Pecetti L, Annicchiarico P, Scotti C, Paolini M, Nanni V, Palmonari A. 2017. Effects of plant architecture and drought stress level on lucerne forage quality. *Grass and Forage Science 72*: 714-722.
Ratliff LF, Ritchie JT, Cassel DK. 1983. Field-Measured Limits of Soil Water Availability as Related to Laboratory-Measured Properties. *Soil Science Society of America Journal 47*: 770-775.
Razavi S, Jakeman A, Saltelli A, Prieur C, Iooss B, Borgonovo E, Plischke E, Lo Piano S, Iwanaga T, Becker W, Tarantola S, Guillaume JHA, Jakeman J, Gupta H, Melillo N, Rabitti G, Chabridon V, Duan Q, Sun X, Smith S, Sheikholeslami R, Hosseini N, Asadzadeh M, Puy A, Kucherenko S, Maier HR. 2021. The Future of Sensitivity Analysis: An essential discipline for systems modeling and policy support. *Environmental Modelling and Software 137*.
Ridley AM, Christy B, Dunin FX, Haines PJ, Wilson KF, Ellington A. 2001. Lucerne in crop rotations on the Riverine Plains 1. The soil water balance. *Australian Journal of Agricultural Research 52*: 263-277.

Rimi F, Macolino S, Leinauer B, Lauriault LM, Ziliotto U. 2012. Fall dormancy and harvest stage effects on alfalfa nutritive value in a subtropical climate. *Agronomy Journal 104*: 415-422.

Ritchie JT. 1972. Model for predicting evaporation from a row crop with incomplete cover. *Water Resources Research 8*: 1204-1213.

Ritter A, Muñoz-Carpena R. 2013. Performance evaluation of hydrological models: Statistical significance for reducing subjectivity in goodness-of-fit assessments. *Journal of Hydrology 480*: 33-45.

Robertson MJ, Carberry PS, Huth NI, Turpin JE, Probert ME, Poulton PL, Bell M, Wright GC, Yeates SJ, Brinsmead RB. 2002. Simulation of growth and development of diverse legume species in APSIM. *Australian Journal of Agricultural Research 53*: 429-446.

Russelle MP, Lamb JFS, Turyk NB, Shaw BH, Pearson B. 2007. Managing Nitrogen Contaminated Soils:Benefits of N2–Fixing Alfalfa. *Agronomy Journal 99*: 738-746.

Seidel SJ, Palosuo T, Thorburn P, Wallach D. 2018. Towards improved calibration of crop models – Where are we now and where should we go? *European Journal of Agronomy 94*: 25-35.

Sexton J, Everingham Y, Inman-Bamber G. 2016. A theoretical and real world evaluation of two Bayesian techniques for the calibration of variety parameters in a sugarcane crop model. *Environmental Modelling & Software 83*: 126-142.

Sim. 2014. *Water extraction and use of seedling and established dryland lucerne crops*. Unpublished Digital thesis, Lincoln University.

Sim RE, Brown HE, Teixeira EI, Moot DJ. 2017. Soil water extraction patterns of lucerne grown on stony soils. *Plant and Soil 414*: 95-112.

Snow V, Huth N, Huth N. 2004. *The APSIM – MICROMET module*.

Storn R, Price K. 1997. Differential Evolution - A Simple and Efficient Heuristic for Global Optimization over Continuous Spaces. *Journal of Global Optimization 11*: 341-359.

Tanner CB, Sinclair TR. 1983. Efficient Water Use in Crop Production: Research or Re-Search? *Limitations to Efficient Water Use in Crop Production*, pp. 1-27.

R Core Team. 2013. R: A language and environment for statistical computing.

Teixeira E, Kersebaum KC, Ausseil A-G, Cichota R, Guo J, Johnstone P, George M, Liu J, Malcolm B, Khaembah E, Meiyalaghan S, Richards K, Zyskowski R, Michel A, Sood A, Tait A, Ewert F. 2021. Understanding spatial and temporal variability of N leaching reduction by winter cover crops under climate change. *Science of The Total Environment 771*: 144770.

Teixeira EI. 2006. *Understanding growth and development of lucerne crops (Medicago sativa L.) with contrasting levels of perennial reserves*. Unpublished thesis.

Teixeira EI, Moot DJ, Brown HE, Pollock KM. 2007. How does defoliation management impact on yield, canopy forming processes and light interception of lucerne (Medicago sativa L.) crops? *European Journal of Agronomy 27*: 154-164.

Teixeira EI, Moot DJ, Brown HE. 2008. Defoliation frequency and season affected radiation use efficiency and dry matter partitioning to roots of lucerne (Medicago sativa L.) crops. *European Journal of Agronomy 28*: 103-111.

Teixeira EI, Moot DJ, Brown HE. 2009. Modelling seasonality of dry matter partitioning and root maintenance respiration in lucerne (Medicago sativa L.) crops. *Crop and Pasture Science 60*: 778-784.

Teixeira EI, Brown HE, Meenken ED, Moot DJ. 2011. Growth and phenological development patterns differ between seedling and regrowth lucerne crops (Medicago sativa L.). *European Journal of Agronomy 35*: 47-55.

Teixeira EI, Brown HE, Michel A, Meenken E, Hu W, Thomas S, Huth NI, Holzworth DP. 2018. Field estimation of water extraction coefficients with APSIM-Slurp for water uptake assessments in perennial forages. *Field Crops Research 222*: 26-38.

Xu W, Cui K, Xu A, Nie L, Huang J, Peng S. 2015. Drought stress condition increases root to shoot ratio via alteration of carbohydrate partitioning and enzymatic activity in rice seedlings. *Acta physiologiae plantarum 37*: 9.

Yang X, Ta TH, Brown HE, Teixeira EI, Jauregui JM, Moot DJ. Modelling Phenological Development of Regrowth Lucerne (Medicago sativa L.) using APSIMX.

Yang X. 2020. Modelling phenological development, yield and quality of lucerne (Medicago sativa L.) using APSIMX.

Yang X, Brown HE, Teixeira EI, Moot DJ. 2021. Development of a lucerne model in APSIM next generation: 1 phenology and morphology of genotypes with different fall dormancies. *European Journal of Agronomy 130*: 126372.

Yunusa IAM, Sedgley RH. 1994. Evaporation from bare soil in south-western australia: A test of two models using lysimetry. *Australian Journal of Soil Research*.

Zahid MS. 2009. *Lucerne performance on duplex soil under Mediterranean climate : field measurement and simulation modelling*. Unpublished thesis, The University of Adelaide.

Zeileis A, Grothendieck G. 2005. zoo: S3 Infrastructure for Regular and Irregular Time Series. *Journal of Statistical Software; Vol 1, Issue 6 (2005)*

Zhang C, Shi S, Wang B, Zhao J. 2018. Physiological and biochemical changes in different drought-tolerant alfalfa (Medicago sativa L.) varieties under PEG-induced drought stress. *Acta Physiologiae Plantarum 40*: 1-15.

APPENDICES

Appendix 1 Cutting dates for removing all above-ground biomass in the APSIMX-Lucerne model for Ashley Dene and Iversen12. The dates differed due to the defoliation method. The "Mown" method had the cutting date one day after the actual mown date occurred in experiments while the "Grazed" method had one day after the grazing period was completed. This table was derived from Sim 2014 raw data and appendix 4 and 6.

Season	SowingDate	Rotation	Ashley Dene	Iversen12
2010/11	SD1	1	2011-01-25	2010-12-29
2010/11	SD1	2	2011-04-08	2011-02-09
2010/11	SD1	3	2011-06-15	2011-04-21
2010/11	SD1	4	-	2011-06-14
2010/11	SD2	1	2011-02-12	2011-01-15
2010/11	SD2	2	2011-04-28	2011-03-11
2010/11	SD2	3	2011-06-15	2011-05-14
2010/11	SD2	4	-	2011-06-14
2010/11	SD3	1	2011-03-26	2011-02-16
2010/11	SD3	2	2011-06-15	2011-04-21
2010/11	SD3	3	-	2011-06-14
2010/11	SD4	1	2011-05-06	2011-05-06
2010/11	SD4	2	2011-06-15	2011-06-14
2010/11	SD5	1	2011-06-15	2011-05-18
2010/11	SD5	2	-	2011-06-14
2011/12	SD1	1	2011-10-28	2011-10-12
2011/12	SD1	2	2011-12-16	2011-11-18
2011/12	SD1	2	2011-12-24	-
2011/12	SD1	3	2012-03-01	2011-12-21
2011/12	SD1	4	2012-04-21	2012-01-27
2011/12	SD1	5	2012-07-12	2012-03-16
2011/12	SD1	6	-	2012-05-02
2011/12	SD1	7	-	2012-07-12
2011/12	SD2	1	2011-10-28	2011-10-12
2011/12	SD2	2	2011-12-16	2011-11-18
2011/12	SD2	2	2011-12-24	-
2011/12	SD2	3	2012-03-01	2011-12-21
2011/12	SD2	4	2012-04-21	2012-01-27
2011/12	SD2	5	2012-07-12	2012-03-16
2011/12	SD2	6	-	2012-05-02
2011/12	SD2	7	-	2012-07-12
2011/12	SD3	1	2011-10-28	2011-10-12
2011/12	SD3	2	2011-12-16	2011-11-18
2011/12	SD3	2	2011-12-24	-
2011/12	SD3	3	2012-03-01	2011-12-21
2011/12	SD3	4	2012-04-21	2012-01-27
2011/12	SD3	5	2012-07-12	2012-03-16
2011/12	SD3	6	-	2012-05-02
2011/12	SD3	7	-	2012-07-12
2011/12	SD4	1	2011-10-28	2011-10-12
2011/12	SD4	2	2011-12-16	2011-11-18

Season	SowingDate	Rotation	Ashley Dene	Iversen12
2011/12	SD4	2	2011-12-24	-
2011/12	SD4	3	2012-03-01	2011-12-21
2011/12	SD4	4	2012-04-21	2012-01-27
2011/12	SD4	5	2012-07-12	2012-03-16
2011/12	SD4	6	-	2012-05-02
2011/12	SD4	7	-	2012-07-12
2011/12	SD5	1	2011-10-28	2011-10-12
2011/12	SD5	2	2011-12-16	2011-11-18
2011/12	SD5	2	2011-12-24	-
2011/12	SD5	3	2012-03-01	2011-12-21
2011/12	SD5	4	2012-04-21	2012-01-27
2011/12	SD5	5	2012-07-12	2012-03-16
2011/12	SD5	6	-	2012-05-02
2011/12	SD5	7	-	2012-07-12
2011/12	SD6	1	2012-01-12	2012-01-05
2011/12	SD6	2	2012-03-29	2012-02-22
2011/12	SD6	3	2012-06-14	2012-04-05
2011/12	SD6	4	-	2012-06-14
2011/12	SD7	1	2012-02-02	2012-01-26
2011/12	SD7	2	2012-04-12	2012-03-13
2011/12	SD7	3	2012-06-14	2012-05-03
2011/12	SD7	4	-	2012-06-14
2011/12	SD8	1	2012-03-22	2012-02-28
2011/12	SD8	2	2012-05-15	2012-04-12
2011/12	SD8	3	2012-06-14	2012-06-14
2011/12	SD9	1	2012-04-26	2012-04-26
2011/12	SD9	2	2012-06-14	2012-06-14
2011/12	SD10	1	2012-06-14	2012-06-14

Appendix 2 Additional output variables for inspecting model performance in APSIMX.

Module	Variable Name	Unit	Description
Control	SimulationID	-	Simulation index
Control	CheckpointID	-	Checkpoint index. Check point allows users to save multiple versions of simulation results in one SQLite db
Control	CheckpointName	-	Checkpoint Name
Control	Clock.Today	Date	Timestamp of the simulation.
Control	Experiment	-	Experiment name
Control	FolderName	-	Folder Name
Control	SowingDate	-	Sowing Date
Control	Zone	-	
Climate	Weather.DaysSinceWinterSolstice	Day	Weather Solstice
Plant + Soil	ET	mm	Predectied evaporation and transipiration
Plant	Lucerne.Leaf.Area		Predicted lucerne leaf area
Plant	Lucerne.Leaf.Area.LeafArea.DeltaLAI	m2 m-2	Predicted daily changes of leaf area index
Plant	Lucerne.Leaf.Area.LeafArea.FrostDeath		Predicted leaf area damaged by frost
Plant	Lucerne.Leaf.Area.LeafArea.Senescence		Predicted lucerne leaf senescence
Plant	Lucerne.Leaf.BasalBuds.LAI	m2 m-2	Predicted LAI from basal bud
Plant	Lucerne.Leaf.BasalBuds.NodeNumber	Count	Predicted node numbers in the basal bud
Plant	Lucerne.Leaf.CoverDead	0-1	Predicted percentage of lucerne light interception reduced by death
Plant	Lucerne.Leaf.CoverTotal	0-1	Predicted percentage of lucerne light interception
Plant	Lucerne.Leaf.Dead.Wt	g m-2	Predicted dead leaf dry weight
Plant	Lucerne.Leaf.Fw	0-1	Predicted water stress effects on leaf
Plant	Lucerne.Leaf.Photosynthesis		Predicted Lucerne Photosynthesis
Plant	Lucerne.Leaf.SenescenceRate	0-1	Predicted Lucerne leaf Senescence Rate
Plant	Lucerne.Leaf.WaterDemand	mm	Predicted Lucerne leaf water Demand
Plant	Lucerne.Nodule.FixationRate		Predicted Lucerne nodule fixation Rate of nitrogen
Plant	Lucerne.Root.Depth	mm	Predicted Lucerne Rooting Depth
Plant	Lucerne.Root.MaintenanceRespiration	g m-2	Predicted Lucerne fine root maintenance Respiration
Plant	Lucerne.Root.WaterUptake	mm	Predicted Lucerne root water Uptake
Plant	Lucerne.Stem.Live.Wt	g m-2	Predicted Lucerne live stem dry weight

Plant	MS.node.No	Count	Predicted lucerne main stem node number
Plant	Phenology.CurrentPhase.Name	-	Predicted Phenological phase Name
Plant	Phenology.CurrentStageName	-	Predicted Phenological growth stage Name
Plant	Phenology.DaysAfterCutting	Day	Days after cutting
Plant	Phenology.DeltaPhotoperiod	-	Predicted Photoperiod daily changes
Plant	Photoperiod	-	Predicted Photoperiod
Plant	RootTotal	g m-2	Predicted Root Total dry weight including dead material
Plant	StemLiveWt	g m-2	Predicted live Stem dry weight
Plant	TapRoot	kg ha-1	Predicted live Root dry weight
Plant	ThermalTimeAfterCutting	Cd	Thermal time accumulation after Cutting
Soil	Soil.SoilWater.Eo	mm	Predicted transpiration demand in soil-plant system
Soil	Soil.SoilWater.Es	mm	Predicted water evaporation from the soil surface
Soil	Soil.SoilWater.WaterTable	mm	Predicted water Table in soils
Soil	SWmm(1) to (22)	mm	Predicted soil water in mm for layer 1 to 22

Appendix 3 Temporal comparison of simulated (—) and observed (●) leaf area index in two sites. SD1 in Iversen12 was excluded.